Adenine Base Editing *in vivo* with a Single Adeno-Associated Virus Vector

Han Zhang[a], Nathan Bamidele[a], Pengpeng Liu[b], Ogooluwa Ojelabi[a, 1], Xin D. Gao[a,2], Tomás Rodriguez[a], Haoyang Cheng[a], Scot A. Wolfe[b,d], Wen Xue[a,b,c,d], and Erik J. Sontheimer[a,c,d,e]

[a]RNA Therapeutics Institute, University of Massachusetts Medical School, Worcester, Massachusetts, 01605, USA

[b]Department of Molecular, Cell and Cancer Biology, University of Massachusetts Medical School, Worcester, Massachusetts, 01605, USA

[c]Program in Molecular Medicine, University of Massachusetts Medical School, Worcester, Massachusetts, 01605, USA

[d]Li Weibo Institute for Rare Diseases Research, University of Massachusetts Medical School, Worcester, Massachusetts, 01605, USA

[1]Present address: LogicBio Therapeutics, Lexington, Massachusetts, 02421, USA

[2]Present address: Merkin Institute of Transformative Technologies in Healthcare, Broad Institute of Harvard and MIT, Cambridge, Massachusetts, 02142, USA

[e]Correspondence: erik.sontheimer@umassmed.edu

Abstract

Base editors (BEs) have opened new avenues for the treatment of genetic diseases. However, advances in delivery approaches are needed to enable disease targeting of a broad range of tissues and cell types. Adeno-associated virus (AAV) vectors remain one of the most promising delivery vehicles for gene therapies. Currently, most BE/guide combinations and their promoters exceed the packaging limit (~5 kb) of AAVs. Dual-AAV delivery strategies often require high viral doses that impose safety concerns. In this study, we engineered an adenine base editor using a compact Cas9 from *Neisseria meningitidis* (Nme2Cas9). Compared to the well-characterized *Streptococcus pyogenes* Cas9-containing ABEs, Nme2-ABE possesses a distinct PAM (N_4CC) and editing window, exhibits fewer off-target effects, and can efficiently install therapeutically relevant mutations in both human and mouse genomes. Importantly, we show that *in vivo* delivery of Nme2-ABE and its guide RNA by a single-AAV vector can efficiently edit mouse genomic loci and revert the disease mutation and phenotype in an adult mouse model of tyrosinemia. We anticipate that Nme2-ABE, by virtue of its compact size and broad targeting range, will enable a range of therapeutic applications with improved safety and efficacy due in part to packaging in a single-vector system.

Key words: AAV, base editing, genome editing, CRISPR, sgRNA, deaminase

Introduction

Point mutations represent the largest class of known human pathogenic genetic variants [1,2]. Base editors (BEs), which comprise a single-guide RNA (sgRNA) loaded onto a Cas9 (nuclease-inactivated or nickase form) fused to a deaminase enzyme, enable precise installation of A•T to G•C (in the case of adenine base editors (ABEs) [3]) or C•G to T•A (in the case of cytidine base editors (CBEs) [4]) substitutions. In contrast to traditional nuclease-dependent genome editing approaches, base editors do not generate double-stranded DNA breaks (DSBs), do not require a DNA donor template, and are more efficient in editing non-dividing cells, making them attractive agents for *in vivo* therapeutic genome editing.

While robust editing has been achieved in many cultured mammalian cell systems, safe and effective *in vivo* delivery of base editors remains a major challenge. To date, both non-viral and viral delivery methods have shown great promise for delivering base editors for *in vivo* therapeutic purposes in rodents and primates [5,6]. For example, *in vivo* delivery via AAVs has achieved efficient editing in a wide range of tissue and cell types including liver [5–10], heart [11], muscle [12,13], retina [14,15], inner ear [16], and central nervous system (CNS) [17,18]. However, the large coding size (5.2 kb) of the best-characterized *Streptococcus pyogenes* Cas9 (SpyCas9)-containing BEs exceed the packaging limit of AAV (5 kb) [19,20]. Currently, *in vivo* delivery of base editors by AAV has been approached by splitting the SpyCas9 base editor between two AAVs and relying on the use of intein trans-splicing for the assembly of the full-length effector [13,16–18,21,22]. Although effective, this approach requires transduction of the target cell by both AAVs and successful *in trans* splicing of the two intein halves. The requirement to deliver two AAV vectors also increases the viral dosage needed for a treatment, which raises safety concerns and adds burdens to AAV manufacturing [23–25].

Compact Cas9 orthologs are ideal candidates for engineering base editors suitable for single-AAV delivery [26–28]. For example, single-AAV delivery of a domain-inlaid *Staphylococcus aureus* Cas9 (SauCas9) ABE has been reported in cultured HEK293 cells [29]. Previously, we developed a *Neisseria meningitidis* Cas9 (Nme2Cas9) as an *in vivo* genome editing platform [27,30]. Nme2Cas9 is a compact, naturally accurate genome editor with a distinct N_4CC PAM specificity. Recently, two other groups have successfully implemented Nme2-CBEs in cultured mammalian cells and in rabbits [31], as well as Nme2-ABEs in rice [32]. Here, we develop ABEs using Nme2Cas9 (Nme2-ABEs) and define their editing efficiencies, editing windows, and off-target activities in comparison to those of the widely applied Spy-ABEs in cultured mammalian cells. Next, we show that Nme2-ABE can edit multiple therapeutically significant loci, including one of the most common mutations occurring in Rett syndrome patients that cannot be targeted by other compact ABEs (e.g. ABEs derived from SauCas9 and SauCas9-KKH [33–36]) due to PAM restrictions. Lastly, by optimizing the promoter and the nuclear localization signals, we show that Nme2-ABE and its guide can be packaged into a single-AAV vector genome for *in vivo* delivery. One systematic administration of the single-AAV vector encoding both Nme2-ABE and sgRNA readily corrects the disease-causing mutation and phenotype in an adult mouse model of hereditary tyrosinemia type 1 (HT1).

Results

Development of Nme2-ABE and comparison of editing windows and off-target effects to those of Spy-ABE

First, to evaluate base editing efficiency in a streamlined manner, we developed an ABE reporter cell line in which a G-to-A mutation in the mCherry coding sequence generates a nonsense mutation. Adenine base editing can reverse the mutation and recover red fluorescence, and the editing efficiency can be readily measured by fluorescence-activated cell sorting (FACS) (**Figure 1a, Supplementary Figure 1**). Initially, we constructed Nme2-ABE7.10 by linking a TadA-TadA7.10 dimer from the Spy-ABE7.10 to the N-terminus of the Nme2Cas9 HNH nickase [3]. However, by plasmid transient transfection, Nme2-ABE7.10 showed poor activity in the ABE reporter cell line. Because the evolved TadA8e is highly active and compatible with a wide range of Cas9s [35], we next engineered Nme2-ABE8e by linking TadA8e monomer to the N-terminus of the Nme2Cas9 HNH nickase (**Figure 1b**). We found that Nme2-ABE8e supports robust editing activity in the ABE reporter cell line (**Figure 1c**). Next, to define the editing window and editing efficiency of Nme2-ABE8e, and to compare them to those parameters of Spy-ABE7.10 and Spy-ABE8e, we transfected HEK293T cells with plasmids expressing each ABE along with sgRNAs targeting 12 human genomic loci for Nme2-ABE8e [including eight dual-target sites (target sites followed by NGGNCC PAMs for both SpyCas9 and Nme2Cas9) [30] and four Nme2Cas9-specific target sites]. We found that this first-generation Nme2-ABE8e has a broad but shallow editing window that, due to modest activity, was difficult to define clearly (**Figure 1d**).

We next sought to understand the potential extent of off-target editing by Nme2-ABE8e. It has been shown that the major source of DNA off-target base editing is Cas9-dependent [37,38], caused by Cas9 binding and unwinding at near-cognate sequences. Because Nme2Cas9 is highly accurate during nuclease-driven editing in cells and *in vivo* [27,30,39], we hypothesized that Nme2-ABE8e would exhibit similar accuracy advantages relative to Spy-ABE8e. As an initial test, we systematically investigated the tolerance for nucleotide mismatches between the guide and the target sequence for the two effectors. We designed a panel of guides targeting the ABE reporter with single- and di-nucleotide mismatches with the target sequence for both Nme2-ABE8e and Spy-ABE8e and measured their activities by plasmid transfection and FACS (**Figure 1e**). Considering the differences in on-target efficiencies between the two effectors, we further normalized the activities of the mismatched guides to those of the perfectly complementary guides for each effector. We found that Nme2-ABE8e exhibited significantly lower off-target editing propensity than Spy-ABE8e: while single-nucleotide mismatches in the seed region (guide nucleotide positions 17-24 for Nme2Cas9, and 10-20 for SpCas9) and the majority of dinucleotide mismatches significantly compromised the editing efficiency of Nme2-ABE8e, these near-cognate sequences were mostly efficiently edited by Spy-ABE8e (**Figure 1e**).

Inhibition of base editing by anti-CRISPR proteins that limit DNA binding activity

The development of Nme2Cas9 base editing platforms raises the possibility that regulation strategies developed for nuclease-based editing could be similarly implemented in the case of base editing. One such strategy is the use of anti-CRISPR (Acr) proteins that limit Cas9 DNA-binding activity [40–43], which have been deployed to reduce both off-target [44] and off-tissue editing [45]. AcrIIC3 and AcrIIC4 have been reported to reduce Nme2Cas9 DNA binding activity [41,43,46] but have no effect on SpyCas9 [41,43]. To test whether such Acr proteins can

function as off-switches for Nme2-ABE8e base editing, we co-transfected the ABE reporter cell line described above with plasmids expressing Nme2-ABE8e, sgRNA, and Acr proteins. Spy-ABE7.10 and AcrIIA4 (an anti-CRISPR that prevents SpyCas9 DNA binding [40], nuclease editing [40,44], and base editing [47]) was used as a positive control. Conversely, AcrE2, which is a Type I-E Acr [43] that has no effect on SpyCas9 or Nme2Cas9 activity, was used as a negative control. As expected, Spy-ABE7.10 base editing was reduced to background levels by AcrIIA4, but AcrE2, AcrIIC3, and AcrIIC4 had no effect (**Supplementary Figure 3a**). By contrast, Nme2-ABE8e editing was strongly inhibited by AcrIIC3 and AcrIIC4, but AcrE2 and AcrIIA4 had no effect. These results confirm that these anti-CRISPRs can be effective off-switches for Nme2-ABE8e editing.

Tissue-specific miRNAs, in combination with miRNA response elements [MREs] in the 3'UTR of an Acr construct, have been used to restrict editing to cell types that express such miRNAs, both in cultured cells [41,48] and *in vivo* [45]. To determine whether such a strategy could be used to control Nme2-ABE8e, we inserted miR-122 MREs into the 3'UTRs of our AcrIIC3 and AcrIIC4 constructs. Mir-122 is a hepatocyte-specific miRNA that is expressed in Huh7 cells but not HEK293 cells, and has been used to validate this strategy for nuclease-based editing. Again, AcrIIC3 and AcrIIC4 inhibited Nme2-ABE8e activity at an endogenous site in HEK293T cells, and inhibition largely persisted even with the MREs (**Supplementary Figure 3b**), as expected since miR-122 is not present to silence Acr expression. In Huh7 cells, which are transfected with lower efficiencies, AcrIIC3 and AcrIIC4 again inhibited Nme2-ABE8e, but this inhibition of editing activity was largely relieved by the insertion of the MRE122 sites. These results indicate that miRNA-repressible anti-CRISPRs can be used to enforce the cell-type specificity of base editing, as it can for nuclease editing.

Installation of therapeutically relevant edits with Nme2-ABE8e

We next tested the potential of Nme2-ABE8e to correct pathogenic mutations or to introduce disease-suppressing mutations. One of the most common mutations that cause Rett syndrome is a C•G to T•A base transition that produces a nonsense mutation in the human *MeCP2* gene (c.502 C>T; p.R168X) [49–51]. Because the target adenine is within a cytidine-rich region, this mutation is not readily accessible for ABEs based on other compact Cas9s such as SauCas9 and SauCas9-KKH [33–36]. To test whether Nme2-ABE8e can correct this pathogenic mutation, we electroporated Nme2-ABE8e mRNA with a synthetic sgRNA into a Rett syndrome patient-derived fibroblast cell line that possesses this mutation. By amplicon deep sequencing, we found that Nme2-ABE8e successfully edited the target adenine (A10) (**Figure 2a, 2b**). A bystander edit at an upstream adenine (A16) causes a missense mutation (c.496 T>C; p.S166P), although this occurs with only one-fourth the frequency of intended edit at A10. Because S166 has been shown to be subject to phosphorylation in mice and is conserved from *X. laevis* to humans [52], further investigation will be needed to determine whether bystander editing at A16 impairs functional rescue of edited cells. However, as with other base editors [3,29,53–58], future protein engineering efforts adjusting the editing window promise to provide greater control over Nme2-ABE editing outcomes.

Next, we sought to generate a disease-suppressing mutation that has been shown to reverse phenotypes of a validated Duchenne muscular dystrophy (DMD) mouse model (ΔEx51) [59]. The ΔEx51 mouse model was generated by deletion of the exon 51 in the *Dmd* gene, resulting in a downstream premature stop codon in exon 52, causing the production of a nonfunctional

truncated dystrophin protein. Previously, it has been shown that the *Dmd* reading frame can be restored by skipping exon 50 by adenine base editing (**Figure 2c**) [13]. However, *in vivo* base editing using ABE_{max}-SpCas9-NG delivered by dual-AAV vectors was limited to local muscle injection due to the high viral dosage required to achieve therapeutic benefit. We identified a guide design for Nme2-ABE8e to target the adenine (A7) within the splice donor site downstream of exon 50 (**Figure 2c**). By plasmid transfection in the mouse N2a cell line and amplicon deep sequencing, we found that Nme2-ABE8e can generate 17.67 ± 4.57% editing at A7 (**Figure 2d**). The efficient editing at multiple bystander adenines is not a concern in this case as those adenines are within the skipped exon 50 or the intron.

Optimization of an Nme2-ABE8e construct for single AAV delivery

Previously, we showed that Nme2Cas9 with one or two sgRNAs can be packaged into a single AAV vector and support efficient editing *in vivo* [27,30]. We reasoned, based upon the compact sizes of Nme2Cas9 and TadA8e, that Nme2-ABE8e with a sgRNA could be packaged into a single AAV for *in vivo* delivery. To achieve this, we first replaced NmeCas9 with Nme2-ABE8e in the minimized all-in-one AAV vector reported previously [27]. We attached one cMyc NLS sequence on each terminus of Nme2-ABE8e while retaining the original promoters for effector and sgRNA expression (**Figure 3a,** 2x cMyc). By transient transfection of vector backbone plasmids, the single-AAV construct successfully edited the ABE reporter cell line. To further improve Nme2-ABE editing efficiency, we then tested three different NLS configurations: 1) one cMyc NLS on the N-terminus and two cMyc NLSs on the C-terminus (3x cMyc); 2) one Ty1 NLS, which derived from the yeast Ty1 retrotransposon that supports robust nuclear localization in dPspCas13b fusion proteins, on the N-terminus (Ty1) [60]; and 3) one bipartite SV40 NLS (BP_SV40) on each terminus (2x BP_SV40) (**Figure 3a**) [61]. When transfecting the vector plasmid into the ABE reporter cell line, the 2x BP_SV40 construct showed the highest editing efficiency (**Figure 3b**).

The total length of the vector constructed with the 2xBP_SV40 NLS, hereafter Nme2-ABE8e-U6, is 4998 bp, very close to the packaging limit of AAV. To test whether we could further reduce the vector size without significantly compromising editing efficiency, we turned to a recently reported "miniU6" promoter that has been shown to support sgRNA expression and achieve comparable editing efficiencies as with the complete U6 promoter [62]. Upon replacement of the U6 promoter with miniU6 promoter, the vector, hereafter Nme2-ABE8e-miniU6, was shortened to 4860 bp, within the packaging limit of AAV (**Figure 3c**). Both constructs induced robust editing in the ABE reporter cell line via transient transfection of the vector plasmids (**Figure 3c**).

To avoid potential ABE reporter-specific effects, we further tested both single-AAV vector backbone plasmids at two endogenous target sites: 1) one of the human dual-target sites, DS12, and 2) a previously reported Nme2Cas9 target site in the mouse *Rosa26* gene [45]. By plasmid transfection in human HEK293T or mouse N2a cells, we observed significant editing at these loci by both vectors, although the Nme2-ABE8e-miniU6 vector was somewhat less efficient (**Figure 3c**). We thus chose both vector designs for the subsequent *in vivo* study.

Hydrodynamic injection of single-AAV vector plasmids corrects the disease mutation and phenotype in an adult mouse model of HT1

233 To test the *in vivo* editing efficiency and therapeutic potential of the single-AAV constructs, we
234 chose to target a pathogenic mutation associated with the liver disease HT1. HT1 is caused by
235 mutations in fumarylacetoacetate hydrolase (FAH), which catalyzes one step of the tyrosine
236 catabolic pathway. FAH deficiency leads to accumulations of toxic fumarylacetoacetate and
237 succinyl acetoacetate, causing liver, kidney, and CNS damage [63]. The *Fah*$^{PM/PM}$ mouse model
238 possesses a G•C to A•T point mutation in the last nucleotide of exon 8, which causes skipping of
239 exon 8 and FAH deficiency (**Figure 4a**). Without treatment, FAH deficient mice will rapidly
240 lose weight and eventually die. The *Fah*$^{PM/PM}$ mouse can be treated with 2-(2-nitro-4-
241 trifluoromethylbenzoyl)-1,3-cyclohexanedione (NTBC), an inhibitor of an enzyme upstream
242 within the tyrosine degradation pathway, which prevents toxin accumulation [64]. Previously, we
243 and others have tested various *in vivo* gene-editing tools to treat the *Fah*$^{PM/PM}$ mouse model,
244 including Cas9-directed HDR [27,65,66], base editing [67,68], microhomology-directed end
245 joining [69], and prime editing [70]. Among these, multiple approaches including AAV, lipid
246 nanoparticle (LNP), and plasmid hydrodynamic tail-vein injection have been used to deliver the
247 gene-editing agents into this mouse model. However, caveats should be considered when
248 comparing the efficiencies of different gene-editing strategies: only the initial editing efficiency
249 (measured before NTBC withdrawal) reflects the activity of the gene-editing agents, because after
250 NTBC withdraw, the hepatocytes in which *Fah* has been repaired will show clonal expansion
251 over time due to their survival advantage.
252
253 We first validated a guide targeting the point mutation by electroporation of the single-AAV
254 vector plasmids, either Nme2-ABE8e-U6 or Nme2-ABE8e-miniU6, into mouse embryonic
255 fibroblasts (MEFs) isolated from a *Fah*$^{PM/PM}$ mouse (**Figure 4b**). We detected modest but
256 significant editing by both vectors at the target adenine at position 13 (A13), despite low (~12%)
257 plasmid electroporation efficiencies. We also observed higher levels of bystander editing at A16
258 with both vectors, and a lower level of bystander editing at A10 for Nme2-ABE8e-U6. Bystander
259 editing at A10 (which changes an active-site-proximal serine into an alanine) has been observed
260 previously with Spy-ABE as well [67]. The effect (if any) of the intronic A16 edit on intron 8
261 splice donor activity has not been defined (**Figure 4c**).
262
263 To test our single-AAV vectors of Nme2-ABE8e *in vivo*, we first performed hydrodynamic tail-
264 vein injections of the AAV-vector plasmids into 10-week-old HT1 mice, or PBS injection as a
265 negative control group [71]. We also injected plasmids expressing Spy-RA6.3, which is a codon-
266 optimized Spy-ABE, as a positive control [67]. Seven days post-injection, we sacrificed 2 mice
267 from each experimental group, and 1 mouse from each control group, to measure the editing
268 efficiency before hepatocyte expansion. We then withdrew NTBC for the rest of the mice for
269 long-term phenotypic study**.** Before NTBC withdrawal, anti-FAH immunohistochemistry (IHC)
270 staining showed 4.58 ± 1.1% FAH$^+$ hepatocytes from the group that was injected with the
271 Nme2-ABE8e-U6 plasmid, and 1.71 ± 0.49% from the group injected with the Nme2-ABE8e-
272 miniU6 plasmid (**Figure 4d**). The mouse injected with Spy-RA6.3 plasmid showed 4.5% FAH$^+$
273 hepatocytes, consistent with previously reported data [67] (**Figure 4d**). After NTBC withdrawal,
274 we monitored body weight changes. The PBS injected mice rapidly lost body weight after NTBC
275 withdrawal and were euthanized. By contrast, mice injected with either the Nme2-ABE8e-U6 or
276 Nme2-ABE8e-miniU6 plasmid gradually gained body weight, suggesting rescue of the
277 pathological phenotype (**Figure 4e)**. Forty days after NTBC withdrawal, we sacrificed mice
278 from all surviving groups. To determine whether Nme2-ABE8e successfully corrects the *Fah*
279 splicing defect, we extracted total RNA from the livers and performed reverse transcription PCR

280 (RT-PCR) using primers that spanned exons 5 and 9. By contrast to the PBS-injected mice,
281 which only showed a 305 bp PCR product corresponding to the truncated mRNA lacking exon
282 8, we observed that the 405 bp PCR product (containing exon 8) predominated in the Nme2-
283 ABE treated mice (**Figure 4f**). Sanger sequencing of the 405 bp bands further confirmed the
284 presence of the corrected G residue at the end of exon 8 (**Figure 4g**). When performing anti-
285 FAH IHC staining, we observed expansion of FAH^+ hepatocytes in the groups that were injected
286 with either of the single-AAV vector plasmids (**Figure 4h**). Amplicon deep sequencing of
287 genomic DNA from the livers of treated mice again provided evidence for Nme2-ABE activity
288 (**Figure 4i**). By contrast to the efficiencies achieved in the MEF cells, we observed a lower
289 editing at A16 and no significant editing at A10, likely due to partial (A16) or complete (A10)
290 selection against mice harboring bystander edits at those positions. These data indicate that our
291 Nme2-ABE8e single-AAV vector plasmids can correct the disease genotype and phenotype of the
292 *Fah*$^{PM/PM}$ mice *in vivo*.
293
294 ***In vivo* base editing by single AAV delivered Nme2-ABE8e in the *Fah*$^{PM/PM}$ mice**
295 Encouraged by the initial results, we packaged AAV9 with the Nme2-ABE8e-U6 construct, as
296 well as the Nme2-ABE8e-miniU6 construct, considering that the relatively smaller size of the
297 latter may potentially benefit packaging efficiency (**Figure 5a**). However, both constructs
298 yielded similar vector titers. Next, to confirm the AAV genome integrity, we performed AAV
299 genomic DNA extraction and alkaline gel electrophoresis. We did not observe any sign of
300 genome truncation (**Supplemental Figure 4**). We then tail-vein injected 8-week-old *Fah*$^{PM/PM}$
301 mice at a dosage of 4×10^{11} vg per mouse. We kept the mice on NTBC for one month before
302 analyzing the editing efficiency. One month after AAV injection and before NTBC withdrawal,
303 we sacrificed the mice and performed IHC staining using an anti-FAH antibody. The negative
304 control groups injected with AAV9 expressing Nme2-ABE and a sgRNA targeting the *Rosa26*
305 gene did not show any FAH^+ hepatocytes. In contrast, we observed 6.49 ± 2.08% FAH^+
306 hepatocytes in the AAV9-Nme2-ABE8e-U6-*Fah* treated group, and 1.62 ± 0.49% FAH^+
307 hepatocytes in AAV9-Nme2-ABE8e-miniU6-*Fah* treated group (**Figure 5b**). Because repair of
308 1/100,000 hepatocytes was reported to rescue the phenotype, both AAV constructs achieved
309 efficiencies that were well above the therapeutic threshold [72]. Moreover, the percentage of
310 edited hepatocytes by AAV9-Nme2-ABE8e-U6-*Fah* was higher than what has been reported
311 previously by other genome editing strategies [65–67,70]. By targeted deep sequencing, the
312 editing efficiency at the target adenine (A13) in the AAV9-Nme2-ABE8e-U6 treated group is
313 0.34 ± 0.14%, while no significant editing was observed in the AAV9-Nme2-ABE8e-miniU6
314 treated group, possibly due to low efficiency that was below the detection limit of amplicon deep
315 sequencing (**Figure 5c**). The reason for the higher frequency of FAH^+ hepatocytes than the
316 frequency of editing at the DNA level is likely due to hepatocyte polyploidy [73], as well as the
317 presence of genomic DNA from nonparenchymal cells. Similar distinctions in FAH^+ frequencies
318 and genomic readouts were also observed in previous studies using this mouse model [67,70]. We
319 also measured the editing efficiency at the *Rosa26* locus and observed ~5% editing efficiency at
320 the target site, indicating that the efficiency of AAV9-delivered Nme2-ABE8e is target site
321 dependent, and higher-efficiency sites can be identified (**Figure 5d**). We did not detect any
322 above-background level of indel, indicating that single-AAV delivered Nme2-ABE8e can install
323 precise editing *in vivo* without generating unwanted indels (**Figure 5c, d**).
324
325 Nme2Cas9 is known to be highly accurate in nuclease based editing in cells [27,30,39], and our
326 mismatch scanning experiments (**Figure 1e**) strongly suggest that the same will be true *in vivo*.

To evaluate potential Cas9-dependent off-target effects in the AAV9-injected mice, we searched for genome-wide off-target sites for Nme2Cas9 using Cas-OFFinder [74], allowing for up to 6 mismatches. We then performed amplicon deep sequencing in the AAV9 treated livers at the two top-ranking potential off-target sites, each including 5 mismatches. We did not detect any above-background A•T-to-G•C editing at these sites (**Supplementary Figure 5**).

Optimizing effector and sgRNA arrangement improves editing efficiency by AAV delivery

Previous studies have shown that effector and sgRNA placement and orientation within the AAV genome can affect transgene expression levels and editing efficiencies [18, 26, 85]. To test if different arrangements of sgRNA and effector cassettes in the Nme2-ABE8e all-in-one AAV construct can further increase *in vivo* editing efficiency, we moved the U6-sgRNA cassette to the 3' end of the AAV genome and reversed its orientation, similar to the optimal arrangement reported by Fry *et al.* [85] (**Figure 6a**). Using the same *Rosa26* guide described above (**Figure 5d**), we packaged the rearranged construct in AAV9 capsids and performed tail-vein injections in 8-week-old mice. We observed significantly improved editing efficiency (34 ± 11.6%) with the optimized construct (**Figure 6b**), which is significantly greater than the 4.7 ± 0.94% efficiency with the original configuration, and comparable to the editing efficiency achieved previously by dual-AAV delivered split-intein SpyCas9-ABEmax targeting the *Dnmt1* gene in adult mouse liver (38 ± 2.9%) [18]. We conclude that efficient adenine base editing can be achieved *in vivo* via single-AAV delivery of the Nme2-ABE8e system.

Discussion

Rapidly evolving and precise genome editing tools such as base editors and prime editors possess great potential to address the root causes of human genetic diseases [2,75,76]. However, the safe and effective delivery of genome editors remains a major challenge. Viral delivery using AAV, which is the only FDA-approved *in vivo* gene therapy vector to date, has a limited packaging capacity. Previous studies using AAV to deliver base editors or prime editors have been reported to be effective in rodents [7,8,10–13,15–18,21], but all of them required multiple vectors and most of them required high viral dosage [7,10–13,17,18]. To date, AAV administered at high dose has been reported to relate to severe toxicity or even death in nonhuman primates, piglets, and humans [23,24,77–79]. Engineering single-AAV deliverable genome editing tools has the potential to achieve therapeutic benefits at lower dosage, which would not only ease manufacturing burdens but also reduce likelihoods of serious adverse events [80,81].

Engineering new genome editors based on compact Cas9s is an alternative approach to address this issue. Previously, single-AAV delivery of Cas9 nucleases has been reported to generate NHEJ-based editing *in vivo* [26,30,82]. Precision editing via HDR has also been achieved with single-AAV systems, albeit with low efficiencies [27,83]. The only single-AAV BE system reported previously (which was not tested *in vivo*) was based on SauCas9, which has limited targeting range due to its PAM constraints. In this study, we constructed and characterized a compact, accurate adenine base editor, Nme2-ABE8e, which can target many sites that are inaccessible to SauCas9 base editors due to their distinct PAMs. We showed that Nme2-ABE8e with a sgRNA can be packaged into a single AAV vector, and a single intravenous injection in an adult disease mouse model of tyrosinemia reversed both the disease mutation and phenotypes. Furthermore, the dosage used in this study (4×10^{11} per mouse or 2×10^{13} vg/kg) is well below the 1×10^{14} vg/kg systemic doses that have been tolerated in clinical trials [77,78].

Although the editing efficiency was modest at the *Fah* disease locus, we reached therapeutic thresholds for HT1, and the initial editing efficiency of the AAV9-delivered Nme2-ABE8e-U6 construct exceeded that reported previously at this locus using other precision genome editing tools and delivery approaches [65–67,70]. Moreover, by optimizing transgene orientation in the AAV construct, we achieved significantly improved editing efficiency (~5-fold increase) by AAV9-delivered Nme2-ABE8e targeting the *Rosa26* gene, comparable to that achieved previously by dual-AAV delivered split-intein SpyCas9-ABEmax in adult mouse liver targeting another genomic site [18]. Future optimization of this system promises to further improve efficiency. There are multiple potential explanations for the inconsistent editing efficiencies we achieved with our first-generation Nme2Cas9 ABE that suggest directions for future improvement. First, structural analyses of Nme2Cas9 [84] indicate that the position of the N-terminally fused TadA8e domain relative to the predicted path of the displaced strand is not optimal. With other effectors, domain-inlaid deaminase fusions have proven to be advantageous in some contexts [29,54], and the same is likely to be true with Nme2-ABEs. Second, the current Nme2-ABE8e has a wide editing window that could result in increased bystander editing. For example, we observed higher editing at a bystander adenine (A16) at the *Fah* locus compared to the on-target adenine at A13. Optimizations of linker composition and length [3,53], as well as domain-inlaid systems [29,54–58], may confer greater control over the editing window and improved efficiency in editing the intended position.

396 Our studies also suggest factors that must be considered for optimal guide expression. In contrast
397 to a previous study that showed no significant difference between the U6 and miniU6 promoters
398 in supporting Cas9 editing efficiency [62], we found that the construct with the miniU6 promoter
399 was consistently less efficient than that with the U6 promoter, including via AAV delivery.
400 Because the previous study compared these promoters in T cells by lentivirus transduction, our
401 observations may only apply to certain delivery strategies and cellular contexts.
402
403 In summary, we have engineered and characterized Nme2-ABE8e editing in mammalian cell
404 culture and achieved efficient *in vivo* editing by delivery of a single AAV vector. To our
405 knowledge, this is the first single-AAV-delivered *in vivo* base editing reported to date [29]. We
406 anticipate that Nme2-ABE8e, with its distinct PAM specificity, editing window, and high
407 accuracy, will provide additional targetability, safety, and therapeutic potential for genome
408 engineering applications.
409

410 **Methods**
411
412 **Cell culture.** HEK293T cells (ATCC CRL-3216), ABE reporter cells, MEF cells, and mouse
413 N2a cells (ATCC CCL-131) were cultured in in Dulbecco's Modified Eagle Media (DMEM,
414 Genesee Scientific Cat. #: 25-500) supplemented with 10% Fetal Bovine Serum (Gibco Cat. #:
415 26140079). Rett syndrome human patient-derived fibroblasts (hPDFs) were obtained from the
416 Rett Syndrome Research Trust and cultured with DMEM supplemented with 15% FBS and 1x
417 non-essential amino acids (Gibco Cat. #: 11140050). All cells were incubated in a 37°C
418 incubator with 5% CO_2.
419
420 **Molecular cloning.** To generate the CMV-Nme2-ABE8e and the CMV-Nme2-ABE7.10
421 plasmids used in **Figure 1**, the Nme2-ABE8e, Nme2-ABE7.10, Spy-ABE8e, and Spy-ABE7.10
422 constructs were cloned into the pCMV-PE2 vector backbone (Addgene #132775) by Gibson
423 assembly. Briefly, the pCMV-PE2 plasmid was digested with NotI and PmeI restriction enzymes,
424 and the plasmid backbone was then Gibson-assembled with five fragments: N-terminal NLS,
425 TadA8e (for Nme2-ABE8e or Spy-ABE8e), or TadA-TadA*7.10 (for Nme2-ABE7.10 or Spy-
426 ABE7.10), the linker, Nme2Cas9-D16A or SpCas9-D10A nickase, and the C-terminal NLS. The
427 ABE reporter construct was cloned by site-directed mutagenesis to change the 47th amino acid
428 (Glutamine, CAG) of the mCherry coding sequence to a stop codon (TAG). The ABE reporter
429 was further cloned into a lentiviral transfer vector backbone (Addgene #99373) by Gibson
430 assembly. The sgRNA expression plasmids used in **Figure 1** were cloned from pBluescriptSKII
431 (Addene #74705) in two steps. First, pBluescriptSKII was digested by NotI and XbaI, and a gene
432 fragment that contains a U6 promoter, a type-IIS restriction cloning site (BfuAI), and a
433 tracrRNA was assembled into the backbone by Gibson assembly. The plasmids were further
434 digested with BfuAI and ligated to the annealed oligos to insert the guide sequences. The single-
435 AAV vector plasmids in **Figure 3a** were cloned from the Addgene #119924 plasmid by
436 replacing the Nme2Cas9 sequence with the Nme2-ABE8e sequence, and then subsequently re-
437 cloned to encode different NLS configurations and the miniU6 promoter by restriction enzyme
438 digestion and Gibson assembly. The NLS configuration of Nme2-ABE8e mRNA used in **Figure**
439 **2b** was 2x_BPSV40, and the plasmid used in **Figure 2d** was the single-AAV Nme2-ABE8e-U6
440 plasmid shown in **Figure 3a** (2xBP_SV40). To clone the AAV-Nme2-ABE8e_V2 plasmid in
441 **Figure 6**, first, the 2xBP_SV40 plasmid from **Figure 3a** was digested by PmeI and NotI, the
442 AAV backbone fragment was then Gibson-assembled with the fragment containing U1a-Nme2-
443 ABE8e, and the fragment containing U6-sgRNA with homology sequences by overhang PCR.
444 Most of the plasmids used in **Supplementary Figure 3a** were previously deposited in
445 Addgene (AcrIIC3, Addgene #85713; AcrIIC4, Addgene #113434; Acr-E2, Addgene #85677).
446 To clone the plasmid expressing AcrIIA4, Addgene #85713 plasmid was digested with XhoI and
447 BamHI and Gibson-assembled with a gene fragment containing AcrIIA4 coding sequence [46].
448 In **Supplementary Figure 3b**, the AcrIIC3-MRE122 plasmid was cloned from Addgene
449 plasmid #129531 by replacing the *Rosa26*-targeting guide with the DS12-targeting guide through
450 restriction enzyme cloning. Subsequent replacement of the coding sequence of AcrIIC3 with
451 AcrIIC4 generated the AcrIIC4-MRE122 plasmid. Sequences of plasmids first described in this
452 paper can be found in the **Supplementary note** and will be made available from Addgene.
453
454 **ABE reporter HEK293T cell line.** Lentivirus was produced following instructions from
455 Addgene (https://www.addgene.org/protocols/lentivirus-production/). Briefly, HEK293T cells
456 were transfected with the transfer vector and the packaging plasmids psPAX2 (Addgene #12260)

457 and pMD2.G (Addgene #12259), using Lipofectamine 3000 (ThermoFisher Cat. #: L3000015).
458 Two days later, the medium was collected and filtered through a 0.45 µm filter (Cytiva Cat. #:
459 6780-25040) to remove cell debris. The viral titer was determined using Lenti-X™GoStix™
460 (Takara Bio Cat. #: 631280). HEK293T cells were transduced with lentivirus encoding the ABE
461 reporter at varying dilutions (1:10, 1:100, 1:500, and 1:1000) in the presence of 8 µg/ml
462 polybrene (Millipore Sigma Cat. #: TR-1003-G). Three days after transduction, the media was
463 removed, and fresh media was supplemented with 2 µg/ml Puromycin to select cells expressing
464 the full-length reporter construct. Seven days after selection, the puromycin-resistant cells were
465 collected. Single-cell clones were established by serial dilution in 96-well plates.
466
467 **Fluorescent reporter assay.** Forty-eight hours after transfection, cells were trypsinized and
468 harvested into microcentrifuge tubes. After centrifuging at 300 x g for 3 mins, cells were
469 resuspended into 150ul 1xPBS for flow cytometry analysis (MACSQuant VYB). For each
470 sample, 10,000 events were counted for FACS analysis. Data was analyzed using Flowjo v10.
471 Representative gating strategy can be found in **Supplementary Figure 2**.
472
473 ***In vitro* transcription of Nme2-ABE8e mRNA.** Nme2-ABE8e mRNA was *in vitro*
474 transcribed using the NEB HiScribe T7 RNA synthesis kit, from 500ng of a linearized template.
475 Uridine was fully substituted with 1-methylpseudouridine, and mRNA was capped co-
476 transcriptionally using CleanCap AG analog (TriLink Biotechnologies Cat. #N-1081 and N-
477 7113, respectively). All enzymes were purchased from New England Biolabs. Transcription was
478 conducted according to the manufacturer's protocol with the following amendments:
479 transcriptions were completed in 1× NEB HiScribe transcription buffer, and 4 mM CleanCap
480 AG was used during transcription. Transcription reactions were incubated at 37 °C for 2 hours
481 then treated with 0.4 U/µl DNase I (final concentration) for 15 min at 37 °C. mRNAs were
482 purified with NEB Monarch RNA purification columns and treated with pyrophosphatase for 1
483 hour with 0.25 U/µg Antarctic phosphatase (final concentration) in 1X Antarctic phosphatase
484 buffer. The final product was further purified with a NEB Monarch RNA column and eluted in
485 water.
486
487 **Transfection and electroporation**. For plasmid transfection, cells were seeded in 24-well
488 plates at 80,000 cells per well in culture media and incubated overnight. Briefly, plasmids were
489 transfected at 400ng per well when targeting the ABE reporter, and 1ug per well for the
490 endogenous target sites. Specifically, in **Figure 1c**, **1e**, **2d**, **3b**, **3c**, and **Supplementary**
491 **Figure 3**, plasmids were transfected using Lipofectamine3000 (ThermoFisher Cat #L3000001),
492 while in **Figure 1d** and **Supplementary Figure 2**, plasmids were transfected using
493 Lipofectamine2000 (ThermoFisher Cat #11668030), following the manufacturer's protocols.
494 Electroporation was performed using Neon TransfectionSystem 10 ul kit (ThermoFisher Cat #:
495 MPK 1096), with the following electroporation parameters: Pulse voltage (1650 v), Pulse width
496 (20 ms), Pulse number (1). Specifically, in **Figure 2a**, 264 ng Nme2-ABE8e mRNA and 100
497 pmole of sgRNA were electroporated into 50,000 Rett Syndrome hPDFs, while in **Figure 4c**, 1
498 ug plasmid DNA was electroporated into 100,000 MEF cells.
499
500 **AAV production**. AAV vector packaging was done at the Viral Vector Core of the Horae Gene
501 Therapy Center at the UMass Chan Medical School as previously described [86]. Constructs
502 were packaged in AAV9 capsids and viral titers were determined by digital droplet PCR and gel
503 electrophoresis followed by silver staining.

504
505 **AAV genomic DNA extraction and alkaline agarose gel electrophoresis.** Genomic
506 DNAs were extracted from 10^{11} vg AAV by incubating with 20 units of DNase I (ThermoFisher
507 Cat. #: EN0521) at 37 °C for 30 minutes and then with an equal volume of 2 x Pronase solution
508 (Sigma-Aldrich, Cat. # 10165921001) for 4 hours. The genomic DNA was subsequently purified
509 by phenol-chloroform (ThermoFisher Cat. #:15593-049) extraction and ethanol precipitation.
510 DNA pellets were resuspended in water and analyzed by alkaline agarose gel electrophoresis and
511 SYBR Gold staining.
512
513 **Mouse experiments.** All animal study protocols were approved by the Institutional Animal
514 Care and Use Committee (IACUC) at UMass Chan Medical School. The *Fah*$^{PM/PM}$ mice were
515 kept on water supplemented with 10 mg/L 2-(2-nitro-4-trifluoromethylbenzoyl)-1,3-
516 cyclohexanedione (NTBC; Sigma-Aldrich, Cat. #: PHR1731-1G). Mice with more than 20%
517 weight loss were humanely euthanized according to IACUC guidelines. For hydrodynamic tail
518 vein injections, plasmids were prepared by EndoFree Plasmid Maxi Kit (Qiagen Cat. #12362).
519 Briefly, 30 ug SpCas8-RA6.3 and 30 ug sgRNA plasmids, or 60 ug Nme2-ABE8e single AAV
520 plasmids were suspended in 2 ml saline and injected via tail vein within 5-7 seconds into 10-
521 week-old *Fah*$^{PM/PM}$ mice. Mice were euthanized 7 days after injection and livers were collected
522 for analysis. For AAV injection, a dosage of 4 x 10^{11} vg per mouse (in 200 ul saline) was tail-vein
523 injected into 8-week-old *Fah*$^{PM/PM}$ mice.
524
525 **Genomic DNA extraction from cultured cells and mouse liver.** For cultured cells,
526 genomic DNAs were extracted 72 hours after plasmid transfection, or 48 hours after mRNA and
527 sgRNA electroporation. Briefly, cell culture media were aspirated, and cells were washed with 1x
528 PBS. Genomic DNAs were prepared using QuickExtract DNA Extraction Solution (Lucigen)
529 following the manufacturer's protocols. To extract genomic DNA from mouse livers, all 5 lobes
530 of mouse liver were combined and pulverized in liquid nitrogen, and 15 mg of the tissue from
531 each mouse liver was used for genomic DNA extraction using GenElute Mammalian Genomic
532 DNA Miniprep Kit (Millipore Sigma Cat. #: G1N350).
533
534 **Amplicon deep sequencing and data analysis**. Genomic DNA was amplified by PCR
535 using Q5 High-Fidelity 2X Master Mix (NEB Cat. #: M0492) for 20 cycles. One microliter of
536 the unpurified PCR product was used as a template for 20 cycles of barcoding PCR. The
537 barcoding PCR reactions were further pooled and gel-extracted using Zymo gel extraction kit
538 and DNA clean & concentrator (Zymo research Cat. #: 11-301 and 11-303) and quantified by
539 Qubit 1x dsDNA HS assay kits (Thermo Fisher Scientific, Cat #: Q32851). Sequencing of the
540 pooled amplicons was performed using an Illumina MiniSeq system (300-cycles, FC-420-1004)
541 following the manufacturer's protocol. The raw MiniSeq output was de-multiplexed using
542 bcl2fastq2 (Illumina, version 2.20.0) with the flag --barcode-mismatches 0. To align the
543 generated fastq files and to quantify editing efficiency, CRISPResso2 [87] (version 2.0.40) was
544 used in batch mode with base editor output and the following flags: -w 15, -q 30. Indel frequency
545 = (insertions reads + deletions reads)/all aligned reads x 100%.
546
547 **Immunohistochemistry (IHC).** Mice were euthanized by CO_2 asphyxiation and livers were
548 fixed with 10% neutral buffered formalin (Epredia Cat. #: 5735), sectioned at 10um, and stained
549 with hematoxylin and eosin for pathology analysis. For IHC, liver sections were dewaxed,

550 rehydrated, and stained using an anti-FAH antibody (Abcam Cat. #: ab83770) at 1:400 dilution
551 as described previously [67].
552
553 **Reverse transcription PCR**. All 5 lobes of each mouse liver were combined and pulverized in
554 liquid nitrogen. Total RNA was extracted from 50 mg of liver tissue using TRIzol reagent
555 (ThermoFisher Cat. #: 15596026) and reverse-transcribed using SuperScript III First-Strand
556 Synthesis System (ThermoFisher Cat. #:18080051). PCR was performed using primers
557 previously described [67].
558
559 **Author contributions**
560
561 H.Z., X.D.G., and E.J.S conceived the study. H.Z. designed, performed, and analyzed the *in vivo*
562 experiments. H.Z., N.B., O.O., P.L., and X.D.G., designed, performed, and analyzed the *in vitro*
563 experiments. T.R. and H.C. analyzed the deep sequencing data. E.J.S., W.X., and S.A.W.
564 supervised research. H.Z. and E.J.S. wrote the manuscript with contributions from N.B., P.L.,
565 and H.C. All authors edited the manuscript.
566
567 **Acknowledgements**
568
569 We thank Yueying Cao and Greg Cottle for their assistance with the mouse colony maintenance
570 and tail vein injections. We thank Zexiang Chen for his help with the *in vitro* mRNA
571 transcription, Nadia Amrani for providing the AcrIIA4 plasmid, Tingting Jiang for providing
572 *Fah*$^{PM/PM}$ MEF cells and Spy-RA6.3 plasmid, and NamKung Suk for his assistance with the
573 alkaline gel electrophoresis. We also thank the UMMS Viral Vector Core for AAV packaging
574 service, the UMMS Morphology Core for tissue sectioning and IHC staining, and the Rett
575 Syndrome Research Trust for patient-derived fibroblasts. We are grateful to all members of the
576 Wolfe, Xue and Sontheimer labs for their valuable discussions, advice, and helpful feedback.
577
578 **Funding**
579
580 This work was supported by the National Institutes of Health [grant numbers R01GM125797 to
581 E.J.S., F31GM143879 to N.B., and R01HL150669 to S.A.W.; the Rett Syndrome Research
582 Trust [to S.A.W. and E.J.S.]; and the Leducq Foundation [grant number 20CVD04 to E.J.S.].
583 W.X. was supported by grants from the National Institutes of Health (DP2HL137167,
584 P01HL131471 and UH3HL147367), American Cancer Society (129056-RSG-16-093), and the
585 Cystic Fibrosis Foundation.
586
587 **Declaration of Competing Interests**
588
589 H.Z., N.B., P.L., X.D.G., S.A.W., W.X., and E.J.S. are co-inventors on patent filings related to
590 this work. E.J.S. is a co-founder and Scientific Advisor Board member of Intellia Therapeutics.
591

592 **References**

593 [1] M.J. Landrum, J.M. Lee, M. Benson, G. Brown, C. Chao, S. Chitipiralla, B. Gu, J. Hart,
594 D. Hoffman, J. Hoover, W. Jang, K. Katz, M. Ovetsky, G. Riley, A. Sethi, R. Tully, R.
595 Villamarin-Salomon, W. Rubinstein, D.R. Maglott, ClinVar: public archive of interpretations of
596 clinically relevant variants, Nucleic Acids Res. 44 (2016) D862–8.
597 [2] H.A. Rees, D.R. Liu, Base editing: precision chemistry on the genome and transcriptome
598 of living cells, Nat. Rev. Genet. 19 (2018) 770–788.
599 [3] N.M. Gaudelli, A.C. Komor, H.A. Rees, M.S. Packer, A.H. Badran, D.I. Bryson, D.R.
600 Liu, Programmable base editing of A•T to G•C in genomic DNA without DNA cleavage,
601 Nature. 551 (2017) 464–471.
602 [4] A.C. Komor, Y.B. Kim, M.S. Packer, J.A. Zuris, D.R. Liu, Programmable editing of a
603 target base in genomic DNA without double-stranded DNA cleavage, Nature. 533 (2016) 420–
604 424.
605 [5] T. Rothgangl, M.K. Dennis, P.J.C. Lin, R. Oka, D. Witzigmann, L. Villiger, W. Qi, M.
606 Hruzova, L. Kissling, D. Lenggenhager, C. Borrelli, S. Egli, N. Frey, N. Bakker, J.A. Walker
607 2nd, A.P. Kadina, D.V. Victorov, M. Pacesa, S. Kreutzer, Z. Kontarakis, A. Moor, M. Jinek, D.
608 Weissman, M. Stoffel, R. van Boxtel, K. Holden, N. Pardi, B. Thöny, J. Häberle, Y.K. Tam,
609 S.C. Semple, G. Schwank, In vivo adenine base editing of PCSK9 in macaques reduces LDL
610 cholesterol levels, Nat. Biotechnol. 39 (2021) 949–957.
611 [6] K. Musunuru, A.C. Chadwick, T. Mizoguchi, S.P. Garcia, J.E. DeNizio, C.W. Reiss, K.
612 Wang, S. Iyer, C. Dutta, V. Clendaniel, M. Amaonye, A. Beach, K. Berth, S. Biswas, M.C.
613 Braun, H.-M. Chen, T.V. Colace, J.D. Ganey, S.A. Gangopadhyay, R. Garrity, L.N. Kasiewicz,
614 J. Lavoie, J.A. Madsen, Y. Matsumoto, A.M. Mazzola, Y.S. Nasrullah, J. Nneji, H. Ren, A.
615 Sanjeev, M. Shay, M.R. Stahley, S.H.Y. Fan, Y.K. Tam, N.M. Gaudelli, G. Ciaramella, L.E.
616 Stolz, P. Malyala, C.J. Cheng, K.G. Rajeev, E. Rohde, A.M. Bellinger, S. Kathiresan, In vivo
617 CRISPR base editing of PCSK9 durably lowers cholesterol in primates, Nature. 593 (2021) 429–
618 434.
619 [7] L. Wang, W. Xue, H. Zhang, R. Gao, H. Qiu, J. Wei, L. Zhou, Y.-N. Lei, X. Wu, X. Li,
620 C. Liu, J. Wu, Q. Chen, H. Ma, X. Huang, C. Cai, Y. Zhang, B. Yang, H. Yin, L. Yang, J.
621 Chen, Eliminating base-editor-induced genome-wide and transcriptome-wide off-target
622 mutations, Nat. Cell Biol. 23 (2021) 552–563.
623 [8] P. Liu, S.-Q. Liang, C. Zheng, E. Mintzer, Y.G. Zhao, K. Ponnienselvan, A. Mir, E.J.
624 Sontheimer, G. Gao, T.R. Flotte, S.A. Wolfe, W. Xue, Improved prime editors enable
625 pathogenic allele correction and cancer modelling in adult mice, Nat. Commun. 12 (2021).
626 https://doi.org/10.1038/s41467-021-22295-w.
627 [9] L. Villiger, T. Rothgangl, D. Witzigmann, R. Oka, P.J.C. Lin, W. Qi, S. Janjuha, C.
628 Berk, F. Ringnalda, M.B. Beattie, M. Stoffel, B. Thöny, J. Hall, H. Rehrauer, R. van Boxtel,
629 Y.K. Tam, G. Schwank, In vivo cytidine base editing of hepatocytes without detectable off-target
630 mutations in RNA and DNA, Nat Biomed Eng. 5 (2021) 179–189.
631 [10] D. Böck, T. Rothgangl, L. Villiger, L. Schmidheini, N. Mathis, E. Ioannidi, S. Kreutzer,
632 Z. Kontarakis, N. Rimann, H.M. Grisch-Chan, B. Thöny, G. Schwank, Treatment of a
633 metabolic liver disease by in vivo prime editing in mice, bioRxiv. (2021) 2021.08.17.456632.
634 https://doi.org/10.1101/2021.08.17.456632.
635 [11] L.W. Koblan, M.R. Erdos, C. Wilson, W.A. Cabral, J.M. Levy, Z.-M. Xiong, U.L.
636 Tavarez, L.M. Davison, Y.G. Gete, X. Mao, G.A. Newby, S.P. Doherty, N. Narisu, Q. Sheng,
637 C. Krilow, C.Y. Lin, L.B. Gordon, K. Cao, F.S. Collins, J.D. Brown, D.R. Liu, In vivo base

638 editing rescues Hutchinson-Gilford progeria syndrome in mice, Nature. 589 (2021) 608–614.
639 [12] S.-M. Ryu, T. Koo, K. Kim, K. Lim, G. Baek, S.-T. Kim, H.S. Kim, D.-E. Kim, H. Lee,
640 E. Chung, J.-S. Kim, Adenine base editing in mouse embryos and an adult mouse model of
641 Duchenne muscular dystrophy, (n.d.). https://doi.org/10.1038/nbt.xxxx.
642 [13] F. Chemello, A.C. Chai, H. Li, C. Rodriguez-Caycedo, E. Sanchez-Ortiz, A. Atmanli,
643 A.A. Mireault, N. Liu, R. Bassel-Duby, E.N. Olson, Precise correction of Duchenne muscular
644 dystrophy exon deletion mutations by base and prime editing, Sci Adv. 7 (2021).
645 https://doi.org/10.1126/sciadv.abg4910.
646 [14] S. Suh, E.H. Choi, H. Leinonen, A.T. Foik, G.A. Newby, W.-H. Yeh, Z. Dong, P.D.
647 Kiser, D.C. Lyon, D.R. Liu, K. Palczewski, Restoration of visual function in adult mice with an
648 inherited retinal disease via adenine base editing, Nat Biomed Eng. 5 (2021) 169–178.
649 [15] S. Zhi, Y. Chen, G. Wu, J. Wen, J. Wu, Q. Liu, Y. Li, R. Kang, S. Hu, J. Wang, P.
650 Liang, J. Huang, Dual-AAV delivering split prime editor system for in vivo genome editing, Mol.
651 Ther. (2021). https://doi.org/10.1016/j.ymthe.2021.07.011.
652 [16] W.-H. Yeh, O. Shubina-Oleinik, J.M. Levy, B. Pan, G.A. Newby, M. Wornow, R. Burt,
653 J.C. Chen, J.R. Holt, D.R. Liu, In vivo base editing restores sensory transduction and transiently
654 improves auditory function in a mouse model of recessive deafness, Sci. Transl. Med. 12 (2020).
655 https://doi.org/10.1126/scitranslmed.aay9101.
656 [17] C.K.W. Lim, M. Gapinske, A.K. Brooks, W.S. Woods, J.E. Powell, M.A. Zeballos C, J.
657 Winter, P. Perez-Pinera, T. Gaj, Treatment of a Mouse Model of ALS by In Vivo Base Editing,
658 Mol. Ther. 28 (2020) 1177–1189.
659 [18] J.M. Levy, W.-H. Yeh, N. Pendse, J.R. Davis, E. Hennessey, R. Butcher, L.W. Koblan, J.
660 Comander, Q. Liu, D.R. Liu, Cytosine and adenine base editing of the brain, liver, retina, heart
661 and skeletal muscle of mice via adeno-associated viruses, Nat Biomed Eng. 4 (2020) 97–110.
662 [19] Z. Wu, H. Yang, P. Colosi, Effect of genome size on AAV vector packaging, Mol. Ther.
663 18 (2010) 80–86.
664 [20] J.Y. Dong, P.D. Fan, R.A. Frizzell, Quantitative analysis of the packaging capacity of
665 recombinant adeno-associated virus, Hum. Gene Ther. 7 (1996) 2101–2112.
666 [21] L. Villiger, H.M. Grisch-Chan, H. Lindsay, F. Ringnalda, C.B. Pogliano, G. Allegri, R.
667 Fingerhut, J. Häberle, J. Matos, M.D. Robinson, B. Thöny, G. Schwank, Treatment of a
668 metabolic liver disease by in vivo genome base editing in adult mice, Nat. Med. 24 (2018) 1519–
669 1525.
670 [22] J. Winter, A. Luu, M. Gapinske, S. Manandhar, S. Shirguppe, W.S. Woods, J.S. Song, P.
671 Perez-Pinera, Targeted exon skipping with AAV-mediated split adenine base editors, Cell
672 Discov. 5 (2019) 41.
673 [23] C. Hinderer, N. Katz, E.L. Buza, C. Dyer, T. Goode, P. Bell, L.K. Richman, J.M.
674 Wilson, Severe Toxicity in Nonhuman Primates and Piglets Following High-Dose Intravenous
675 Administration of an Adeno-Associated Virus Vector Expressing Human SMN, Hum. Gene
676 Ther. 29 (2018) 285–298.
677 [24] J.M. Wilson, T.R. Flotte, Moving Forward After Two Deaths in a Gene Therapy Trial of
678 Myotubular Myopathy, Human Gene Therapy. 31 (2020) 695–696.
679 https://doi.org/10.1089/hum.2020.182.
680 [25] L. Wang, J. Smith, C. Breton, P. Clark, J. Zhang, L. Ying, Y. Che, J. Lape, P. Bell, R.
681 Calcedo, E.L. Buza, A. Saveliev, V.V. Bartsevich, Z. He, J. White, M. Li, D. Jantz, J.M. Wilson,
682 Meganuclease targeting of PCSK9 in macaque liver leads to stable reduction in serum
683 cholesterol, Nat. Biotechnol. 36 (2018) 717–725.
684 [26] F.A. Ran, L. Cong, W.X. Yan, D.A. Scott, J.S. Gootenberg, A.J. Kriz, B. Zetsche, O.

685 Shalem, X. Wu, K.S. Makarova, E.V. Koonin, P.A. Sharp, F. Zhang, In vivo genome editing
686 using Staphylococcus aureus Cas9, Nature. 520 (2015) 186–191.
687 [27] R. Ibraheim, P.W.L. Tai, A. Mir, N. Javeed, J. Wang, T.C. Rodríguez, S. Namkung, S.
688 Nelson, E.S. Khokhar, E. Mintzer, S. Maitland, Z. Chen, Y. Cao, E. Tsagkaraki, S.A. Wolfe, D.
689 Wang, A.A. Pai, W. Xue, G. Gao, E.J. Sontheimer, Self-inactivating, all-in-one AAV vectors for
690 precision Cas9 genome editing via homology-directed repair in vivo, Nat. Commun. 12 (2021)
691 6267.
692 [28] M.L. Maeder, M. Stefanidakis, C.J. Wilson, R. Baral, L.A. Barrera, G.S. Bounoutas, D.
693 Bumcrot, H. Chao, D.M. Ciulla, J.A. DaSilva, A. Dass, V. Dhanapal, T.J. Fennell, A.E.
694 Friedland, G. Giannoukos, S.W. Gloskowski, A. Glucksmann, G.M. Gotta, H. Jayaram, S.J.
695 Haskett, B. Hopkins, J.E. Horng, S. Joshi, E. Marco, R. Mepani, D. Reyon, T. Ta, D.G.
696 Tabbaa, S.J. Samuelsson, S. Shen, M.N. Skor, P. Stetkiewicz, T. Wang, C. Yudkoff, V.E. Myer,
697 C.F. Albright, H. Jiang, Development of a gene-editing approach to restore vision loss in Leber
698 congenital amaurosis type 10, Nat. Med. 25 (2019) 229–233.
699 [29] M.T. Nguyen Tran, M.K.N. Mohd Khalid, Q. Wang, J.K.R. Walker, G.E. Lidgerwood,
700 K.L. Dilworth, L. Lisowski, A. Pébay, A.W. Hewitt, Engineering domain-inlaid SaCas9 adenine
701 base editors with reduced RNA off-targets and increased on-target DNA editing, Nat. Commun.
702 11 (2020) 4871.
703 [30] A. Edraki, A. Mir, R. Ibraheim, I. Gainetdinov, Y. Yoon, C.-Q. Song, Y. Cao, J. Gallant,
704 W. Xue, J.A. Rivera-Pérez, E.J. Sontheimer, A Compact, High-Accuracy Cas9 with a
705 Dinucleotide PAM for In Vivo Genome Editing, Mol. Cell. 73 (2019) 714–726.e4.
706 [31] Z. Liu, S. Chen, Y. Jia, H. Shan, M. Chen, Y. Song, L. Lai, Z. Li, Efficient and high-
707 fidelity base editor with expanded PAM compatibility for cytidine dinucleotide, Sci. China Life
708 Sci. 64 (2021) 1355–1367.
709 [32] R. Xu, R. Qin, H. Xie, J. Li, X. Liu, M. Zhu, Y. Sun, Y. Yu, P. Lu, P. Wei, Genome
710 editing with type II-C CRISPR-Cas9 systems from Neisseria meningitidis in rice, Plant
711 Biotechnol. J. (2021). https://doi.org/10.1111/pbi.13716.
712 [33] K. Hua, X. Tao, J.-K. Zhu, Expanding the base editing scope in rice by using Cas9
713 variants, Plant Biotechnol. J. 17 (2019) 499–504.
714 [34] L. Yang, X. Zhang, L. Wang, S. Yin, B. Zhu, L. Xie, Q. Duan, H. Hu, R. Zheng, Y.
715 Wei, L. Peng, H. Han, J. Zhang, W. Qiu, H. Geng, S. Siwko, X. Zhang, M. Liu, D. Li,
716 Correction to: Increasing targeting scope of adenosine base editors in mouse and rat embryos
717 through fusion of TadA deaminase with Cas9 variants, Protein Cell. 10 (2019) 700.
718 [35] M.F. Richter, K.T. Zhao, E. Eton, A. Lapinaite, G.A. Newby, B.W. Thuronyi, C.
719 Wilson, L.W. Koblan, J. Zeng, D.E. Bauer, J.A. Doudna, D.R. Liu, Phage-assisted evolution of
720 an adenine base editor with improved Cas domain compatibility and activity, Nat. Biotechnol.
721 38 (2020) 883–891.
722 [36] N.M. Gaudelli, D.K. Lam, H.A. Rees, N.M. Solá-Esteves, L.A. Barrera, D.A. Born, A.
723 Edwards, J.M. Gehrke, S.-J. Lee, A.J. Liquori, R. Murray, M.S. Packer, C. Rinaldi, I.M.
724 Slaymaker, J. Yen, L.E. Young, G. Ciaramella, Directed evolution of adenine base editors with
725 increased activity and therapeutic application, Nat. Biotechnol. 38 (2020) 892–900.
726 [37] H.A. Rees, A.C. Komor, W.-H. Yeh, J. Caetano-Lopes, M. Warman, A.S.B. Edge, D.R.
727 Liu, Improving the DNA specificity and applicability of base editing through protein engineering
728 and protein delivery, Nat. Commun. 8 (2017) 15790.
729 [38] D. Kim, K. Lim, S.-T. Kim, S.-H. Yoon, K. Kim, S.-M. Ryu, J.-S. Kim, Genome-wide
730 target specificities of CRISPR RNA-guided programmable deaminases, Nat. Biotechnol. 35
731 (2017) 475–480.

732 [39] J. Wen, T. Cao, J. Wu, Y. Chen, S. Zhi, Y. Huang, P. Zhen, G. Wu, L. Aagaard, J.
733 Zhong, P. Liang, J. Huang, Single AAV-mediated CRISPR-Nme2Cas9 efficiently reduces
734 mutant hTTR expression in a transgenic mouse model of transthyretin amyloidosis, Mol. Ther.
735 (2021). https://doi.org/10.1016/j.ymthe.2021.05.010.
736 [40] B.J. Rauch, M.R. Silvis, J.F. Hultquist, C.S. Waters, M.J. McGregor, N.J. Krogan, J.
737 Bondy-Denomy, Inhibition of CRISPR-Cas9 with Bacteriophage Proteins, Cell. 168 (2017) 150–
738 158.e10.
739 [41] J. Lee, A. Mir, A. Edraki, B. Garcia, N. Amrani, H.E. Lou, I. Gainetdinov, A. Pawluk, R.
740 Ibraheim, X.D. Gao, P. Liu, A.R. Davidson, K.L. Maxwell, E.J. Sontheimer, Potent Cas9
741 Inhibition in Bacterial and Human Cells by AcrIIC4 and AcrIIC5 Anti-CRISPR Proteins,
742 MBio. 9 (2018). https://doi.org/10.1128/mBio.02321-18.
743 [42] S. Hwang, K.L. Maxwell, Meet the Anti-CRISPRs: Widespread Protein Inhibitors of
744 CRISPR-Cas Systems, CRISPR J. 2 (2019) 23–30.
745 [43] A. Pawluk, N. Amrani, Y. Zhang, B. Garcia, Y. Hidalgo-Reyes, J. Lee, A. Edraki, M.
746 Shah, E.J. Sontheimer, K.L. Maxwell, A.R. Davidson, Naturally Occurring Off-Switches for
747 CRISPR-Cas9, Cell. 167 (2016) 1829–1838.e9.
748 [44] J. Shin, F. Jiang, J.-J. Liu, N.L. Bray, B.J. Rauch, S.H. Baik, E. Nogales, J. Bondy-
749 Denomy, J.E. Corn, J.A. Doudna, Disabling Cas9 by an anti-CRISPR DNA mimic, Sci Adv. 3
750 (2017) e1701620.
751 [45] J. Lee, H. Mou, R. Ibraheim, S.-Q. Liang, P. Liu, W. Xue, E.J. Sontheimer, Tissue-
752 restricted genome editing in vivo specified by microRNA-repressible anti-CRISPR proteins,
753 RNA. 25 (2019) 1421–1431.
754 [46] L.B. Harrington, K.W. Doxzen, E. Ma, J.-J. Liu, G.J. Knott, A. Edraki, B. Garcia, N.
755 Amrani, J.S. Chen, J.C. Cofsky, P.J. Kranzusch, E.J. Sontheimer, A.R. Davidson, K.L. Maxwell,
756 J.A. Doudna, A Broad-Spectrum Inhibitor of CRISPR-Cas9, Cell. 170 (2017) 1224–1233.e15.
757 [47] M. Liang, T. Sui, Z. Liu, M. Chen, H. Liu, H. Shan, L. Lai, Z. Li, AcrIIA5 Suppresses
758 Base Editors and Reduces Their Off-Target Effects, Cells. 9 (2020).
759 https://doi.org/10.3390/cells9081786.
760 [48] M.D. Hoffmann, S. Aschenbrenner, S. Grosse, K. Rapti, C. Domenger, J. Fakhiri, M.
761 Mastel, K. Börner, R. Eils, D. Grimm, D. Niopek, Cell-specific CRISPR–Cas9 activation by
762 microRNA-dependent expression of anti-CRISPR proteins, Nucleic Acids Res. 47 (2019) e75–
763 e75.
764 [49] T. Bienvenu, A. Carrié, N. de Roux, M.C. Vinet, P. Jonveaux, P. Couvert, L. Villard, A.
765 Arzimanoglou, C. Beldjord, M. Fontes, M. Tardieu, J. Chelly, MECP2 mutations account for
766 most cases of typical forms of Rett syndrome, Hum. Mol. Genet. 9 (2000) 1377–1384.
767 [50] M.J. Lyst, A. Bird, Rett syndrome: a complex disorder with simple roots, Nat. Rev.
768 Genet. 16 (2015) 261–275.
769 [51] R. Krishnaraj, G. Ho, J. Christodoulou, RettBASE: Rett syndrome database update,
770 Hum. Mutat. 38 (2017) 922–931.
771 [52] G. Stefanelli, A. Gandaglia, M. Costa, M.S. Cheema, D. Di Marino, I. Barbiero, C.
772 Kilstrup-Nielsen, J. Ausió, N. Landsberger, Brain phosphorylation of MeCP2 at serine 164 is
773 developmentally regulated and globally alters its chromatin association, Sci. Rep. 6 (2016) 28295.
774 [53] J. Tan, F. Zhang, D. Karcher, R. Bock, Engineering of high-precision base editors for
775 site-specific single nucleotide replacement, Nature Communications. 10 (2019).
776 https://doi.org/10.1038/s41467-018-08034-8.
777 [54] S.H. Chu, M. Packer, H. Rees, D. Lam, Y. Yu, J. Marshall, L.-I. Cheng, D. Lam, J.
778 Olins, F.A. Ran, A. Liquori, B. Gantzer, J. Decker, D. Born, L. Barrera, A. Hartigan, N.

779 Gaudelli, G. Ciaramella, I.M. Slaymaker, Rationally Designed Base Editors for Precise Editing
780 of the Sickle Cell Disease Mutation, CRISPR J. 4 (2021) 169–177.
781 [55] T.P. Huang, K.T. Zhao, S.M. Miller, N.M. Gaudelli, B.L. Oakes, C. Fellmann, D.F.
782 Savage, D.R. Liu, Circularly permuted and PAM-modified Cas9 variants broaden the targeting
783 scope of base editors, Nat. Biotechnol. 37 (2019) 626–631.
784 [56] Y. Wang, L. Zhou, N. Liu, S. Yao, BE-PIGS: a base-editing tool with deaminases inlaid
785 into Cas9 PI domain significantly expanded the editing scope, Signal Transduct Target Ther. 4
786 (2019) 36.
787 [57] S. Li, B. Yuan, J. Cao, J. Chen, J. Chen, J. Qiu, X.-M. Zhao, X. Wang, Z. Qiu, T.-L.
788 Cheng, Docking sites inside Cas9 for adenine base editing diversification and RNA off-target
789 elimination, Nat. Commun. 11 (2020) 5827.
790 [58] Y. Liu, C. Zhou, S. Huang, L. Dang, Y. Wei, J. He, Y. Zhou, S. Mao, W. Tao, Y.
791 Zhang, H. Yang, X. Huang, T. Chi, A Cas-embedding strategy for minimizing off-target effects
792 of DNA base editors, Nat. Commun. 11 (2020) 6073.
793 [59] F. Chemello, Z. Wang, H. Li, J.R. McAnally, N. Liu, R. Bassel-Duby, E.N. Olson,
794 Degenerative and regenerative pathways underlying Duchenne muscular dystrophy revealed by
795 single-nucleus RNA sequencing, Proc. Natl. Acad. Sci. U. S. A. 117 (2020) 29691–29701.
796 [60] K.M. Anderson, P. Poosala, S.R. Lindley, D.M. Anderson, Targeted Cleavage and
797 Polyadenylation of RNA by CRISPR-Cas13, bioRxiv. (2019) 531111.
798 https://doi.org/10.1101/531111.
799 [61] L.W. Koblan, J.L. Doman, C. Wilson, J.M. Levy, T. Tay, G.A. Newby, J.P. Maianti, A.
800 Raguram, D.R. Liu, Improving cytidine and adenine base editors by expression optimization
801 and ancestral reconstruction, Nat. Biotechnol. 36 (2018) 843–846.
802 [62] R. Preece, C. Georgiadis, S.A. Gkazi, A. Etuk, A. Christi, W. Qasim, "Mini" U6 Pol III
803 promoter exhibits nucleosome redundancy and supports multiplexed coupling of CRISPR/Cas9
804 effects, Gene Ther. 27 (2020) 451–458.
805 [63] J.L. Aponte, G.A. Sega, L.J. Hauser, M.S. Dhar, C.M. Withrow, D.A. Carpenter, E.M.
806 Rinchik, C.T. Culiat, D.K. Johnson, Point mutations in the murine fumarylacetoacetate
807 hydrolase gene: Animal models for the human genetic disorder hereditary tyrosinemia type 1,
808 Proc. Natl. Acad. Sci. U. S. A. 98 (2001) 641–645.
809 [64] S. Lindstedt, Treatment of hereditary tyrosinaemia type I by inhibition of 4-
810 hydroxyphenylpyruvate dioxygenase, The Lancet. 340 (1992) 813–817.
811 https://doi.org/10.1016/0140-6736(92)92685-9.
812 [65] H. Yin, W. Xue, S. Chen, R.L. Bogorad, E. Benedetti, M. Grompe, V. Koteliansky, P.A.
813 Sharp, T. Jacks, D.G. Anderson, Genome editing with Cas9 in adult mice corrects a disease
814 mutation and phenotype, Nat. Biotechnol. 32 (2014) 551–553.
815 [66] H. Yin, C.-Q. Song, J.R. Dorkin, L.J. Zhu, Y. Li, Q. Wu, A. Park, J. Yang, S. Suresh, A.
816 Bizhanova, A. Gupta, M.F. Bolukbasi, S. Walsh, R.L. Bogorad, G. Gao, Z. Weng, Y. Dong, V.
817 Koteliansky, S.A. Wolfe, R. Langer, W. Xue, D.G. Anderson, Therapeutic genome editing by
818 combined viral and non-viral delivery of CRISPR system components in vivo, Nat. Biotechnol.
819 34 (2016) 328–333.
820 [67] C.-Q. Song, T. Jiang, M. Richter, L.H. Rhym, L.W. Koblan, M.P. Zafra, E.M. Schatoff,
821 J.L. Doman, Y. Cao, L.E. Dow, L.J. Zhu, D.G. Anderson, D.R. Liu, H. Yin, W. Xue, Adenine
822 base editing in an adult mouse model of tyrosinaemia, Nat Biomed Eng. 4 (2020) 125–130.
823 [68] T. Jiang, J.M. Henderson, K. Coote, Y. Cheng, H.C. Valley, X.-O. Zhang, Q. Wang,
824 L.H. Rhym, Y. Cao, G.A. Newby, H. Bihler, M. Mense, Z. Weng, D.G. Anderson, A.P.
825 McCaffrey, D.R. Liu, W. Xue, Chemical modifications of adenine base editor mRNA and guide

826 RNA expand its application scope, Nat. Commun. 11 (2020) 1979.
827 [69] J.H. Shin, S. Jung, S. Ramakrishna, H.H. Kim, J. Lee, In vivo gene correction with
828 targeted sequence substitution through microhomology-mediated end joining, Biochem. Biophys.
829 Res. Commun. 502 (2018) 116–122.
830 [70] H. Jang, D.H. Jo, C.S. Cho, J.H. Shin, J.H. Seo, G. Yu, R. Gopalappa, D. Kim, S.-R.
831 Cho, J.H. Kim, H.H. Kim, Application of prime editing to the correction of mutations and
832 phenotypes in adult mice with liver and eye diseases, Nat Biomed Eng. (2021).
833 https://doi.org/10.1038/s41551-021-00788-9.
834 [71] G. Zhang, V. Budker, J.A. Wolff, High levels of foreign gene expression in hepatocytes
835 after tail vein injections of naked plasmid DNA, Hum. Gene Ther. 10 (1999) 1735–1737.
836 [72] N.K. Paulk, K. Wursthorn, Z. Wang, M.J. Finegold, M.A. Kay, M. Grompe, Adeno-
837 associated virus gene repair corrects a mouse model of hereditary tyrosinemia in vivo,
838 Hepatology. 51 (2010) 1200–1208. https://doi.org/10.1002/hep.23481.
839 [73] M.-J. Wang, F. Chen, J.T.Y. Lau, Y.-P. Hu, Hepatocyte polyploidization and its
840 association with pathophysiological processes, Cell Death Dis. 8 (2017) e2805.
841 [74] S. Bae, J. Park, J.-S. Kim, Cas-OFFinder: a fast and versatile algorithm that searches for
842 potential off-target sites of Cas9 RNA-guided endonucleases, Bioinformatics. 30 (2014) 1473–
843 1475.
844 [75] A.V. Anzalone, L.W. Koblan, D.R. Liu, Genome editing with CRISPR-Cas nucleases,
845 base editors, transposases and prime editors, Nat. Biotechnol. 38 (2020) 824–844.
846 [76] G.A. Newby, D.R. Liu, In vivo somatic cell base editing and prime editing, Mol. Ther.
847 (2021). https://doi.org/10.1016/j.ymthe.2021.09.002.
848 [77] High-dose AAV gene therapy deaths, Nat. Biotechnol. 38 (2020) 910.
849 [78] L. Morales, Y. Gambhir, J. Bennett, H.H. Stedman, Broader Implications of Progressive
850 Liver Dysfunction and Lethal Sepsis in Two Boys following Systemic High-Dose AAV, Mol.
851 Ther. 28 (2020) 1753–1755.
852 [79] T.R. Flotte, Revisiting the "New" Inflammatory Toxicities of Adeno-Associated Virus
853 Vectors, Hum. Gene Ther. 31 (2020) 398–399.
854 [80] D. Wang, P.W.L. Tai, G. Gao, Adeno-associated virus vector as a platform for gene
855 therapy delivery, Nat. Rev. Drug Discov. 18 (2019) 358–378.
856 [81] D. Wang, F. Zhang, G. Gao, CRISPR-Based Therapeutic Genome Editing: Strategies
857 and In Vivo Delivery by AAV Vectors, Cell. 181 (2020) 136–150.
858 [82] R. Ibraheim, C.-Q. Song, A. Mir, N. Amrani, W. Xue, E.J. Sontheimer, All-in-one
859 adeno-associated virus delivery and genome editing by Neisseria meningitidis Cas9 in vivo,
860 Genome Biol. 19 (2018) 137.
861 [83] S.A. Krooss, Z. Dai, F. Schmidt, A. Rovai, J. Fakhiri, A. Dhingra, Q. Yuan, T. Yang, A.
862 Balakrishnan, L. Steinbrück, S. Srivaratharajan, M.P. Manns, A. Schambach, D. Grimm, J.
863 Bohne, A.D. Sharma, H. Büning, M. Ott, Ex Vivo/In vivo Gene Editing in Hepatocytes Using
864 "All-in-One" CRISPR-Adeno-Associated Virus Vectors with a Self-Linearizing Repair
865 Template, iScience. 23 (2020) 100764. https://doi.org/10.1016/j.isci.2019.100764.
866 [84] W. Sun, J. Yang, Z. Cheng, N. Amrani, C. Liu, K. Wang, R. Ibraheim, A. Edraki, X.
867 Huang, M. Wang, J. Wang, L. Liu, G. Sheng, Y. Yang, J. Lou, E.J. Sontheimer, Y. Wang,
868 Structures of Neisseria meningitidis Cas9 Complexes in Catalytically Poised and Anti-CRISPR-
869 Inhibited States, Mol. Cell. 76 (2019) 938–952.e5.
870 [85] L.E. Fry, C.F. Peddle, M. Stevanovic, A.R. Barnard, M.E. McClements, R.E. MacLaren,
871 Promoter Orientation within an AAV-CRISPR Vector Affects Cas9 Expression and Gene
872 Editing Efficiency, CRISPR J. 3 (2020) 276–283.

873 [86] M. Sena-Esteves, G. Gao, Introducing Genes into Mammalian Cells: Viral Vectors, Cold
874 Spring Harb. Protoc. 2020 (2020) 095513.
875 [87] K. Clement, H. Rees, M.C. Canver, J.M. Gehrke, R. Farouni, J.Y. Hsu, M.A. Cole, D.R.
876 Liu, J.K. Joung, D.E. Bauer, L. Pinello, CRISPResso2 provides accurate and rapid genome
877 editing sequence analysis, Nat. Biotechnol. 37 (2019) 224–226.

878

Figures

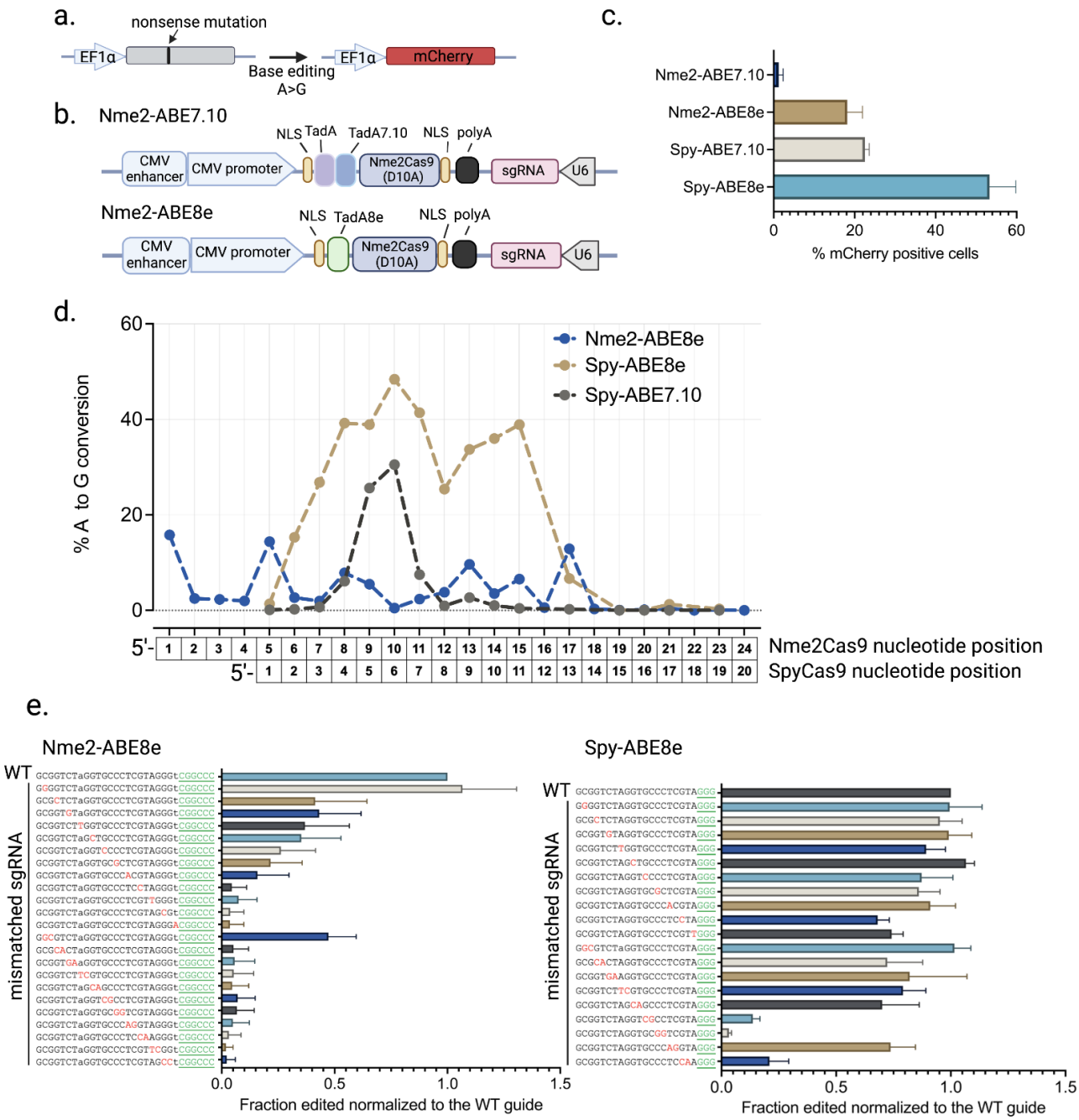

Figure 1

a). Schematic representation of the ABE reporter HEK293T cell line. **b).** Schematic representation of the Nme2-ABE constructs. **c).** Comparison of editing efficiencies of Nme2-ABEs to those of Spy-ABEs in the ABE reporter cell line by plasmid transient transfection (n = 3 biological replicates). **d).** Summary of editing windows and comparison of editing efficiencies for the ABEs at endogenous genomic loci. Each data point represents the mean A-to-G editing efficiency at the indicated position of the spacer across 12 Nme2Cas9 target sites and 8 SpyCas9 target sites, respectively (n = 3 biological replicates). Summary of the individual A-to-G conversion and indel efficiencies at each target site can be found in **Supplementary Figure 2**. **e).** Comparison of Nme2-ABE8e mismatch tolerance to that of Spy-ABE8e in the ABE reporter cell line. The activities of the effectors with the mismatched guides are normalized to that of the perfectly complementary (WT) guide. Red, mismatched nucleotides; green, PAM sequence (n = 3 biological replicates).

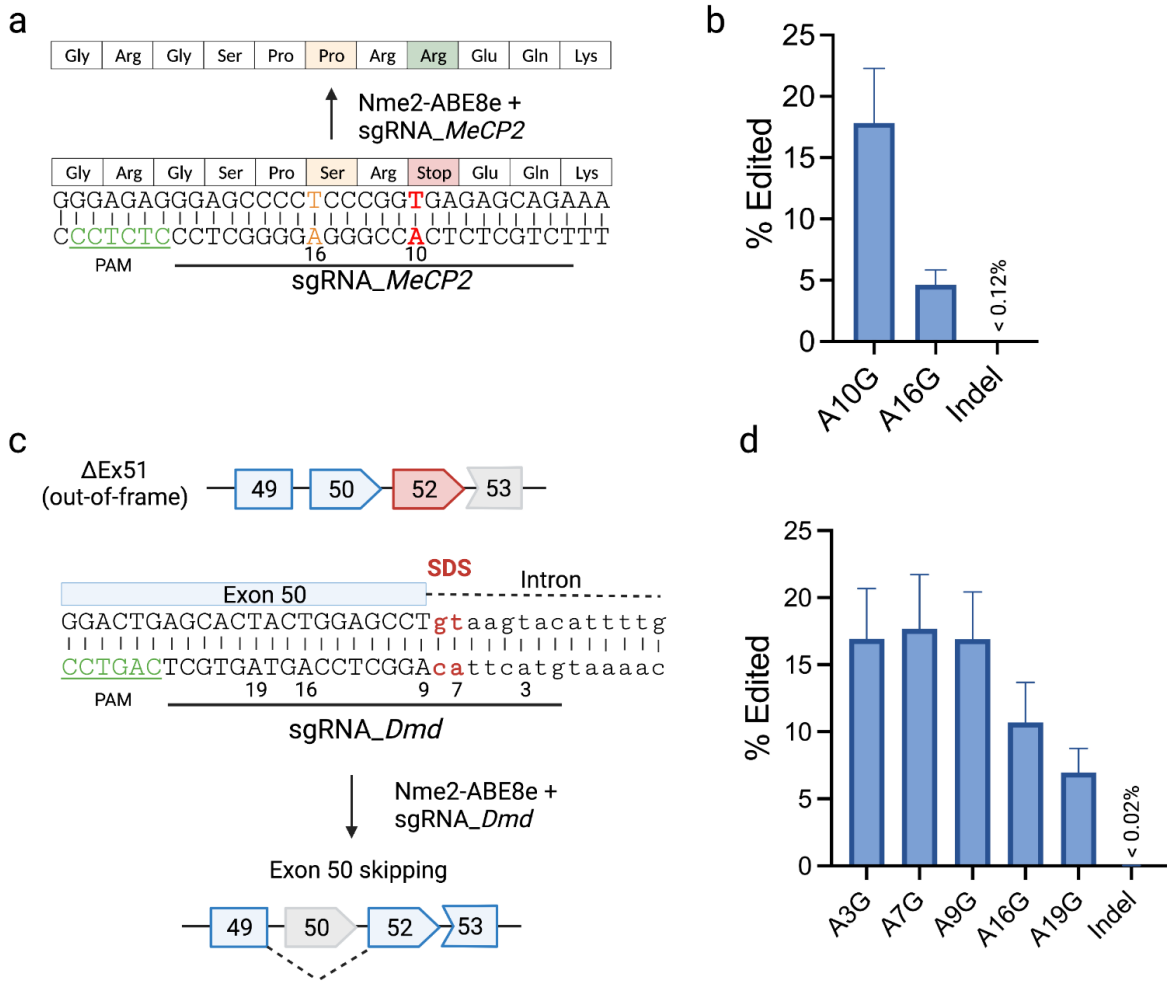

Figure 2

a). Schematic representation of a nonsense mutation in the human *MeCP2* gene (c.502 C>T; p.R168X) that causes Rett Syndrome. The black underline denotes the target sequence of an Nme2-ABE8e guide for reverting the mutant A to G (wildtype) at position 10 (red, bold). The PAM region is underlined in green. A bystander edit at position 16 (orange) can generate a missense mutation (c.496 T>C; p.S166P). **b).** Amplicon deep sequencing quantifying the editing efficiency in Rett patient-derived fibroblasts transfected with the Nme2-ABE8e mRNA and the synthetic sgRNA_*MeCP2* noted in **a** (n = 3 biological replicates). **c).** Schematic representation of the exon skipping strategy that restores the reading frame of the mouse *Dmd* transcript. Deletion of exon 51 (ΔEx51) can alter the reading frame and generate a premature stop codon in exon 52 (red). Adenine base editing at the splice site of exon 50 (red) by Nme2-ABE8e can cause exon 50 skipping (gray) and restore the *Dmd* reading frame. The PAM region is underlined in green. **d).** Amplicon deep sequencing quantifies the editing efficiency at the target site in mouse N2a cells transfected with the Nme2-ABE8e and sgRNA_*Dmd* expression plasmid (n = 3 biological replicates).

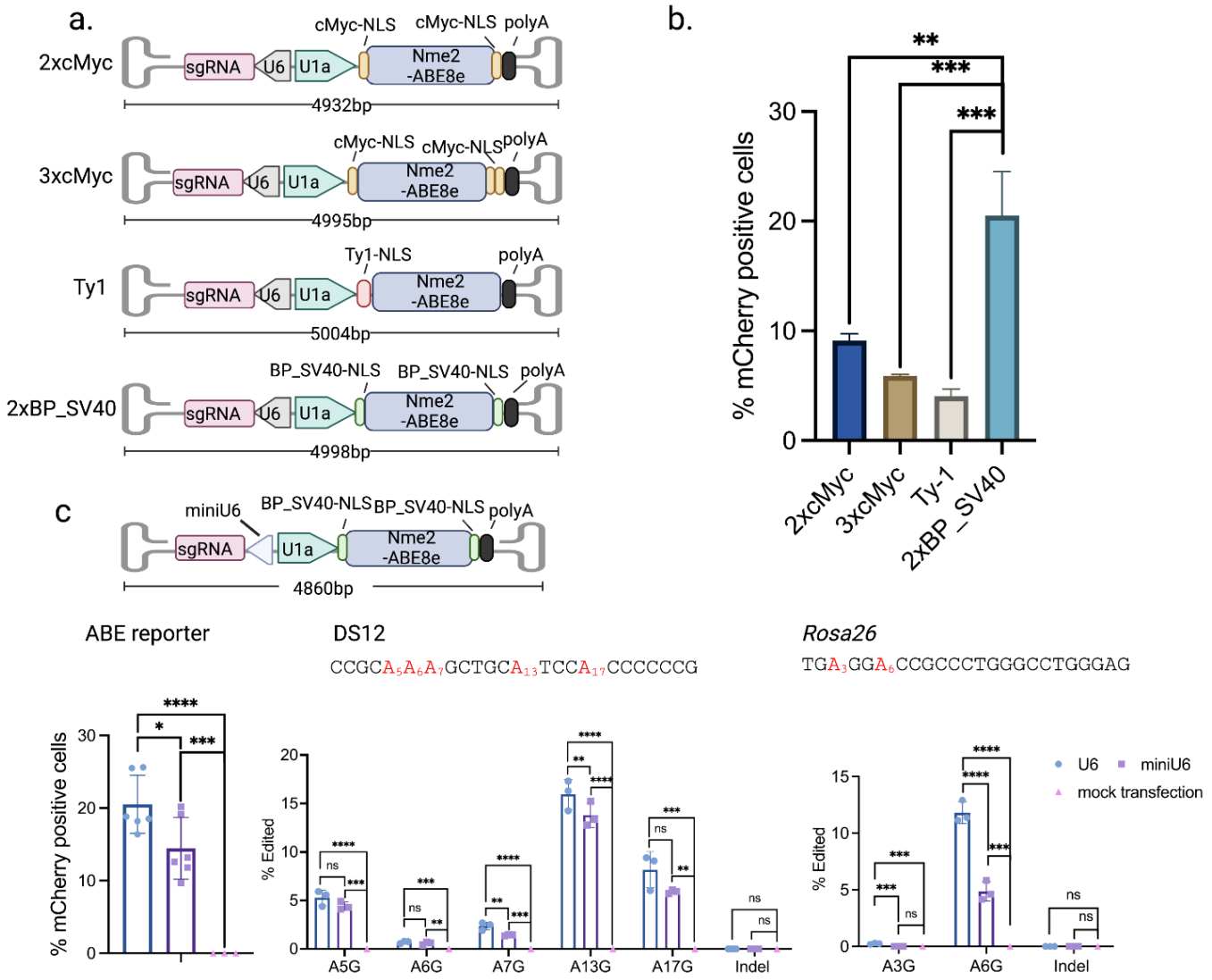

Figure 3

a). Schematic representation of single AAV constructs with different NLS configurations. **b).** Comparison of different NLS configurations by plasmid transfection in the ABE reporter cell line. **c).** Comparison of Nme2-ABE activity when sgRNA expression is driven by the U6 or miniU6 promoters in the 2xBP_SV40 NLS construct targeting the ABE reporter site (left) or endogenous human (middle) and mouse (right) genomic sites by plasmid transfection in cultured cells followed by amplicon deep sequencing (n = 3 biological replicates). Data represent mean ± SD; ns, P > 0.05; *, P < 0.05; **, P < 0.01; ***, P < 0.001; ****, P < 0.0001 (one-way ANOVA).

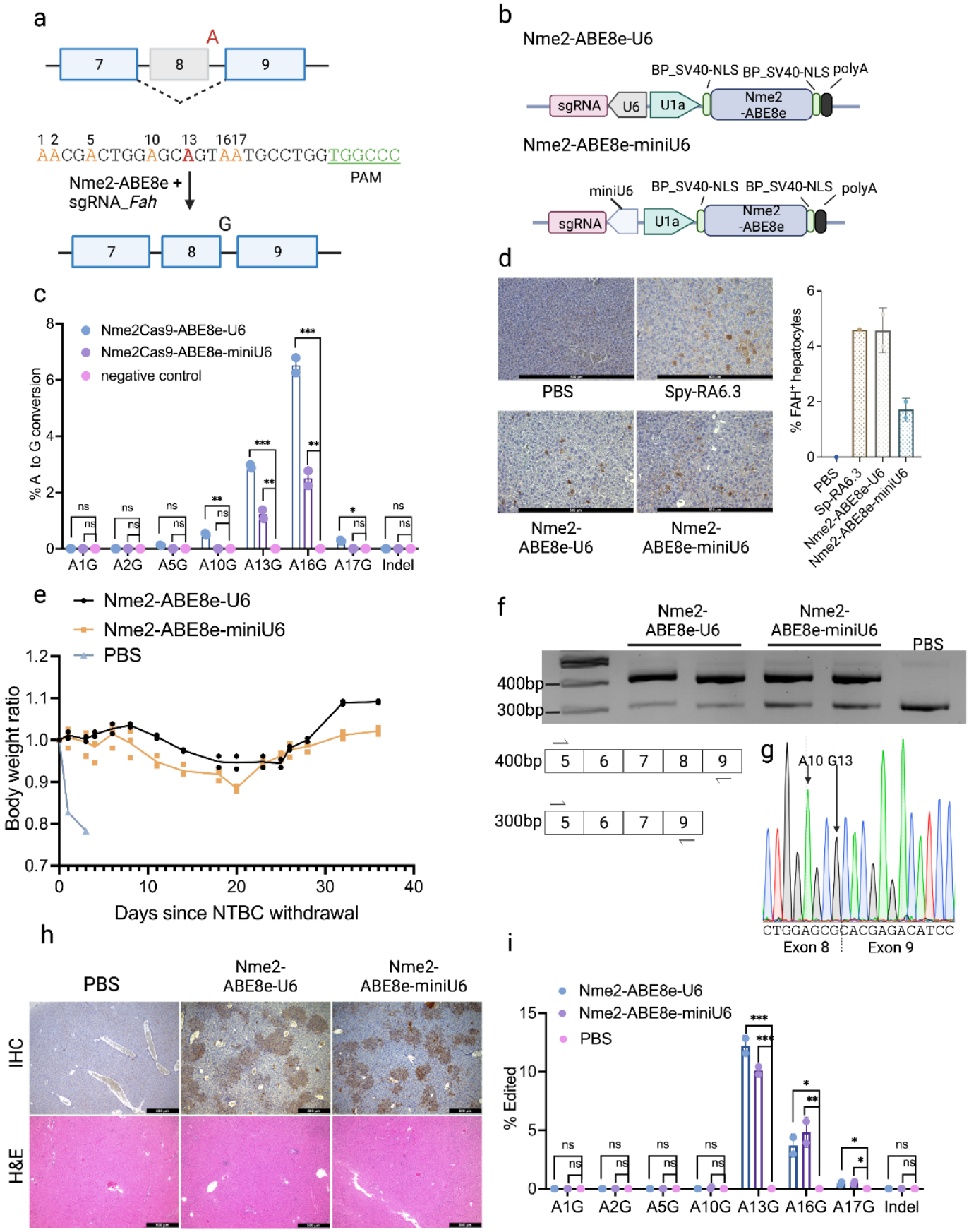
a
A
7
8
9
1 2 5 10 13 1617
AACGACTGGAGCAGTAATGCCTGGTGGCCC
PAM
Nme2-ABE8e +
sgRNA_Fah
G
b
Nme2-ABE8e-U6
BP_SV40-NLS BP_SV40-NLS polyA
sgRNA U6 U1a Nme2 -ABE8e
Nme2-ABE8e-miniU6
miniU6 BP_SV40-NLS BP_SV40-NLS polyA
c
Nme2Cas9-ABE8e-U6
Nme2Cas9-ABE8e-miniU6
negative control
% A to G conversion
A1G A2G A5G A10G A13G A16G A17G Indel
d
PBS
Spy-RA6.3
Nme2-ABE8e-U6
Nme2-ABE8e-miniU6
% FAH+ hepatocytes
e
Nme2-ABE8e-U6
Nme2-ABE8e-miniU6
PBS
Body weight ratio
Days since NTBC withdrawal
f
Nme2-ABE8e-U6
Nme2-ABE8e-miniU6
PBS
400bp
300bp
g
A10 G13
CTGGAGCGCACGAGACATCC
Exon 8
Exon 9
h
PBS
Nme2-ABE8e-U6
Nme2-ABE8e-miniU6
IHC
H&E
i
Nme2-ABE8e-U6
Nme2-ABE8e-miniU6
PBS
% Edited
A1G A2G A5G A10G A13G A16G A17G Indel

Figure 4

a). Illustration of the pathogenic point mutation in the *Fah*$^{PM/PM}$ mouse model that causes exon 8 skipping of the *Fah* gene, and the guide design for Nme2-ABE8e to correct the point mutation. Red and bold, target adenine; orange, other bystander adenines; green and underlined, PAM. **b).** Illustration of constructs of the single-AAV vector plasmids used in *in vivo* studies. **c).** Editing efficiencies at the *Fah* mutant site by AAV plasmid electroporation in MEF cells derived from the *Fah*$^{PM/PM}$ mouse. Data are from amplicon deep sequencing (n = 2 biological replicates). **d).** Anti-FAH immunohistochemistry (IHC) staining showing FAH^{+} hepatocytes, before NTBC withdrawal, in the *Fah*$^{PM/PM}$ mouse hydrodynamically injected with the indicated plasmid. The bar graph quantifies the percentage of FAH^{+} hepatocytes detected by IHC (n = 2 mice per group). Scale bars, 500 μm. **e).** Body weight plot of mice injected with the single-AAV vector plasmid showing gradual weight gain over a month after NTBC withdrawal. **f).** RT–PCR analysis of the plasmid- or PBS-injected mouse livers using primers that span exons 5 and 9. The wild-type amplicon is 405 bp and exon 8 skipped amplicon is 305 bp. **g).** Representative Sanger sequencing trace of the 405 bp RT-PCR band. **h).** Anti-FAH IHC staining showing expansion of FAH^{+} hepatocytes 40 days post NTBC withdrawal. Scale bars, 500 μm. **i).** Quantification of the editing efficiency by amplicon deep sequencing of genomic DNA of the treated mouse livers harvested 40 days post NTBC withdrawal. **d-i**, n = 2 mice per group). Data represent mean ± SD; ns, $P > 0.05$; *, $P < 0.05$; **, $P < 0.01$; ***, $P < 0.001$ (one-way ANOVA).

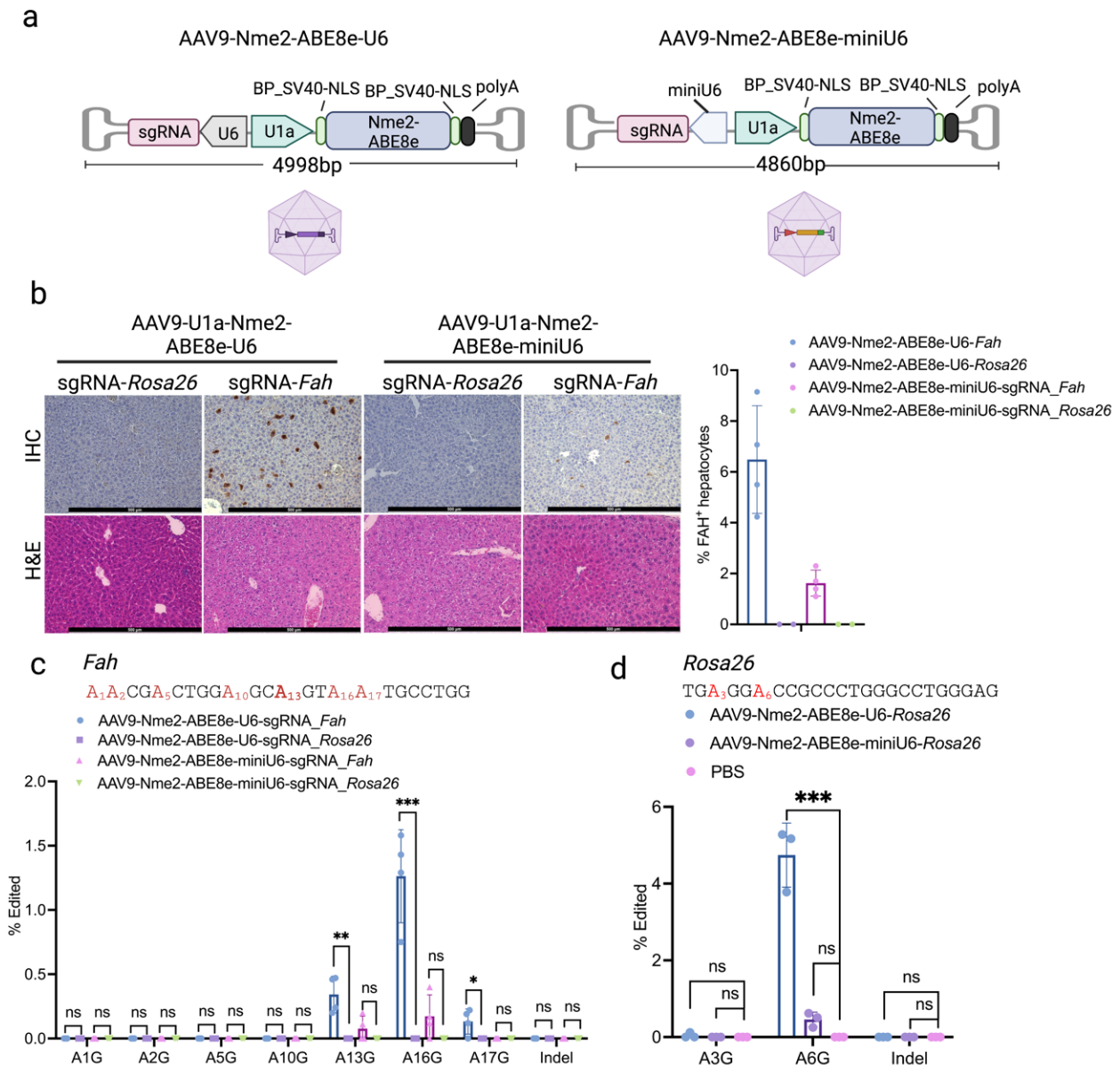

Figure 5

a). Schematic representation of the AAV constructs. **b).** Anti-FAH immunohistochemistry (IHC) staining showing FAH$^+$ hepatocytes, before NTBC withdrawal, in the *Fah*$^{PM/PM}$ mouse injected with AAV9 expressing Nme2-ABE8e with a sgRNA targeting either the *Fah* gene, or the *Rosa26* gene that serves as a negative control. Scale bar, 500 µm. The bar graph quantifies the percentage of FAH$^+$ hepatocytes detected by IHC (n = 4 mice in the *Fah* targeting group, n = 3 mice in the *Rosa26* targeting group). **c, d).** Quantification of the editing efficiency by amplicon deep sequencing of genomic DNA from the AAV9-injected mouse livers harvested before NTBC withdrawal (n = 4 mice in the *Fah* targeting group, n = 3 mice in the *Rosa26* targeting group and the PBS control group). Data represent mean ± SD; ns, $P > 0.05$; *, $P < 0.05$; **, $P < 0.01$; ***, $P < 0.001$ (one-way ANOVA).

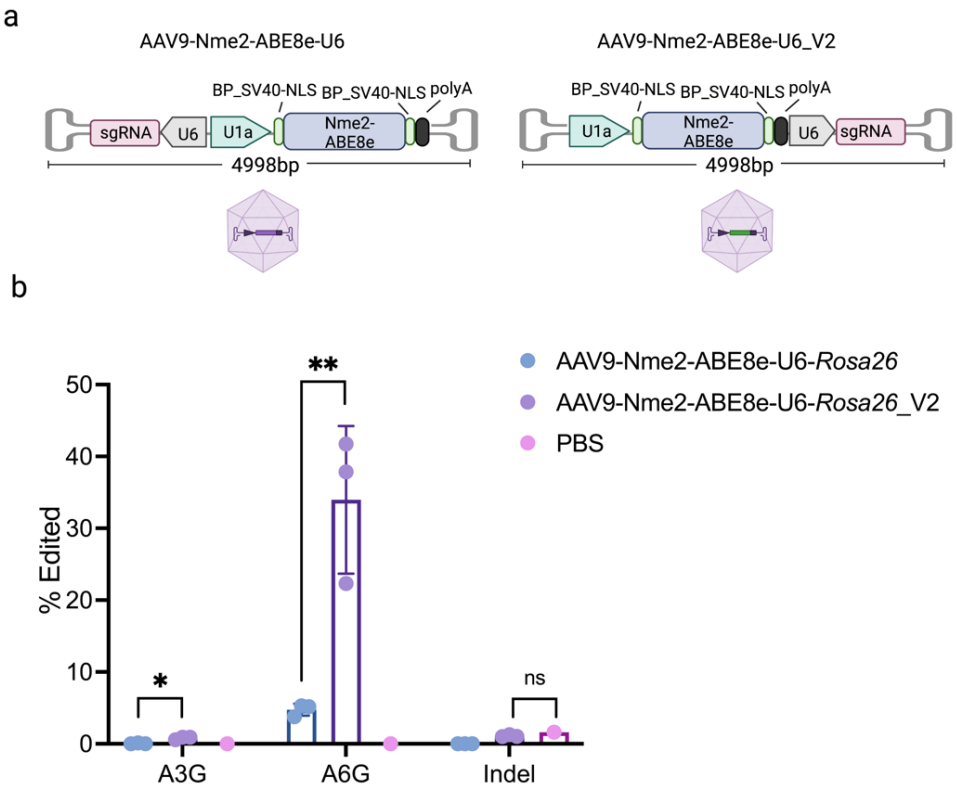

Figure 6

a). Schematic representation of the original (left) and the optimized AAV constructs (AAV9-Nm2-ABE8e-U6_V2, right). **b).** Quantification of the editing efficiency at the *Rosa26* locus by amplicon deep sequencing using mouse livers injected with indicated AAV (n = 3 mice in the AAV injected group, n = 1 mouse in the PBS injected group). Data from the original AAV configuration (**a**, left) is the same as that from the experiment shown in **Figure 5d**. Data represent mean ± SD, ns, P > 0.05; *, P<0.1; **, P < 0.01(one-way ANOVA).

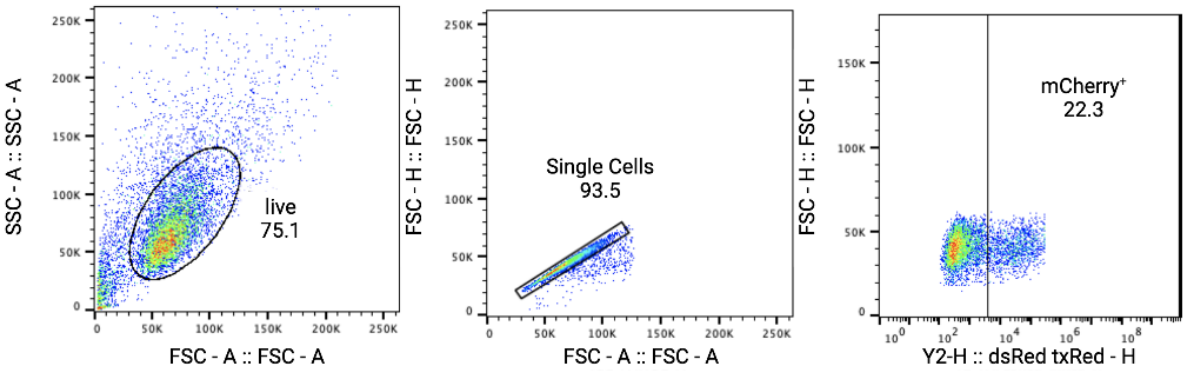

Supplementary Figure 1
Representative flow cytometry gating strategy for the ABE reporter cell line.

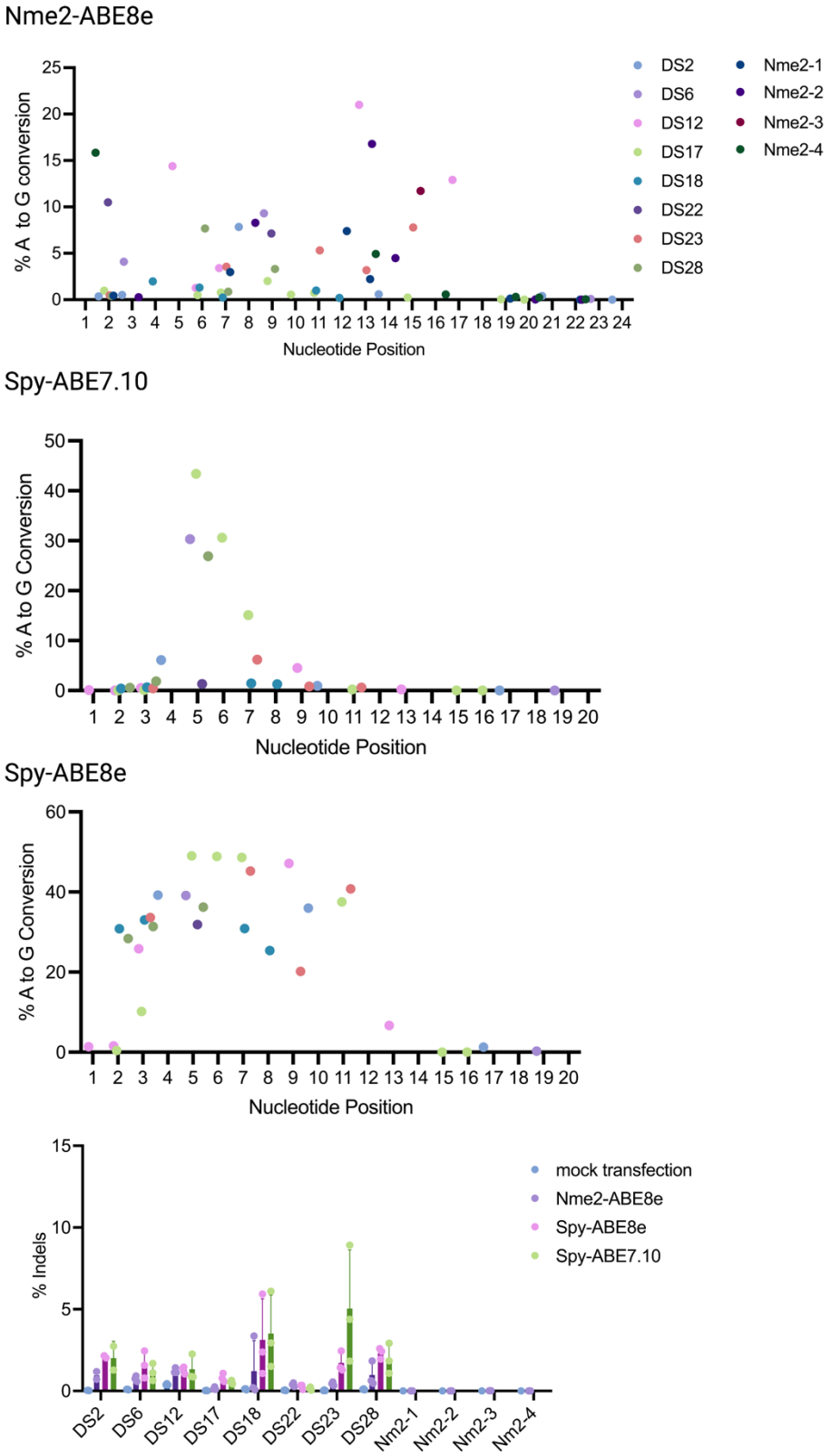

Supplementary Figure 2

Summary of the individual A-to-G conversion efficiency and the indel efficiency (bottom) at 12 target sites for Nme2-ABE8e, which includes 8 dual-target sites (DS 2 - 28) and 4 Nme2Cas9-specific target sites (Nme2 1 - 4), and 8 dual-target sites for Spy-ABE7.10 and Spy-ABE8e. Each data point represents the A-to-G conversion efficiency at the indicated nucleotide position measured by amplicon deep sequencing (n = 3 biological replicates).

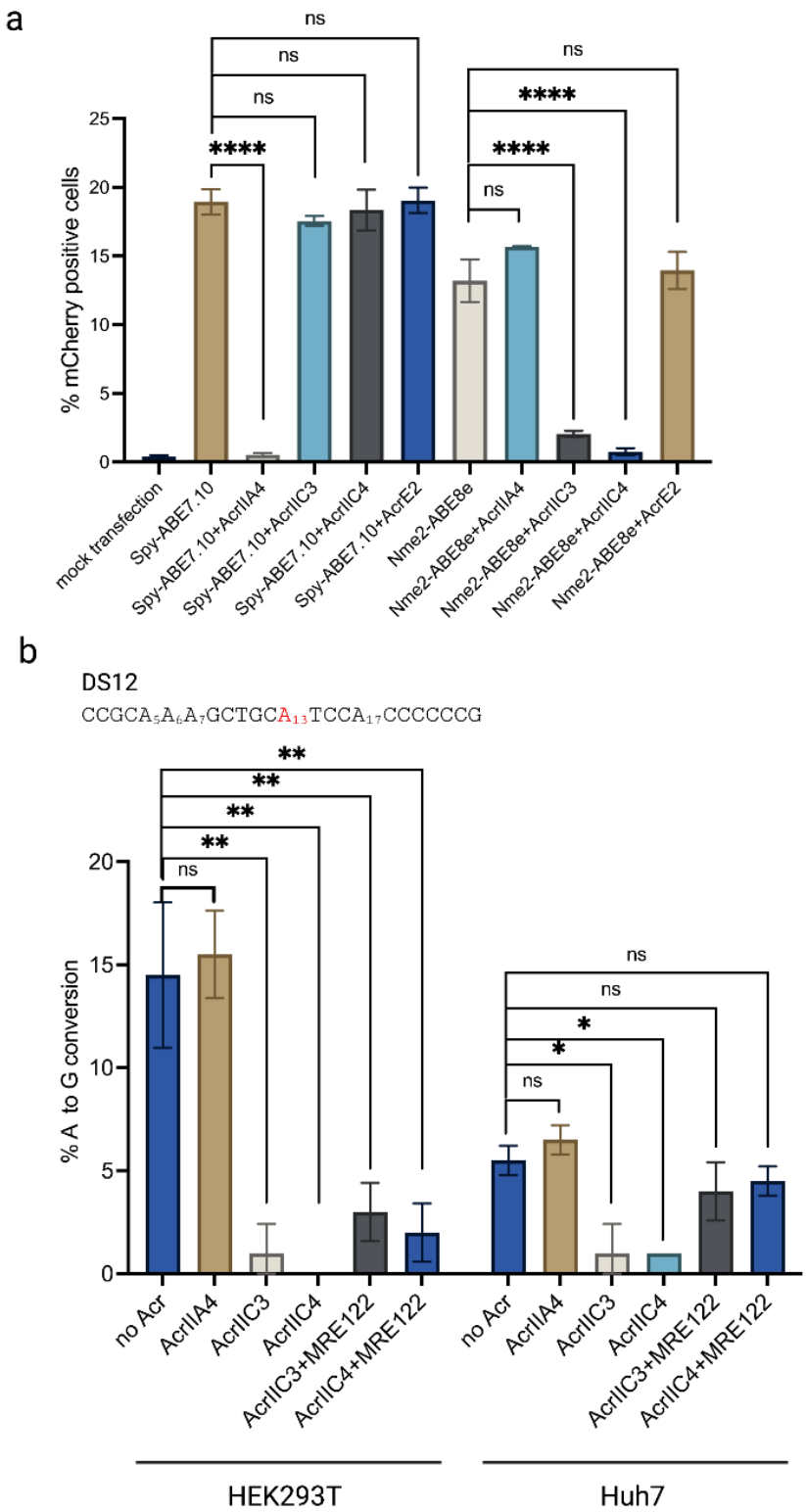

Supplementary Figure 3

a). Anti-CRISPR proteins inhibit the activity of either Spy-ABE7.10 or Nme2-ABE8e in the ABE reporter cell line as a function of their previously defined nuclease specificity (n = 2 biological replicates). **b).** Editing efficiency at the A12 (the highest edited adenine within the target) of the DS12 site by Nme2-ABE8e controlled by microRNA-repressible anti-CRIPSR proteins. Data generated by Sanger sequencing and EditR analysis (n = 2 biological replicates). Data represent mean ± SD; ns, P > 0.05; *, P < 0.05; **, P < 0.01; ****, P < 0.0001 (one-way ANOVA).

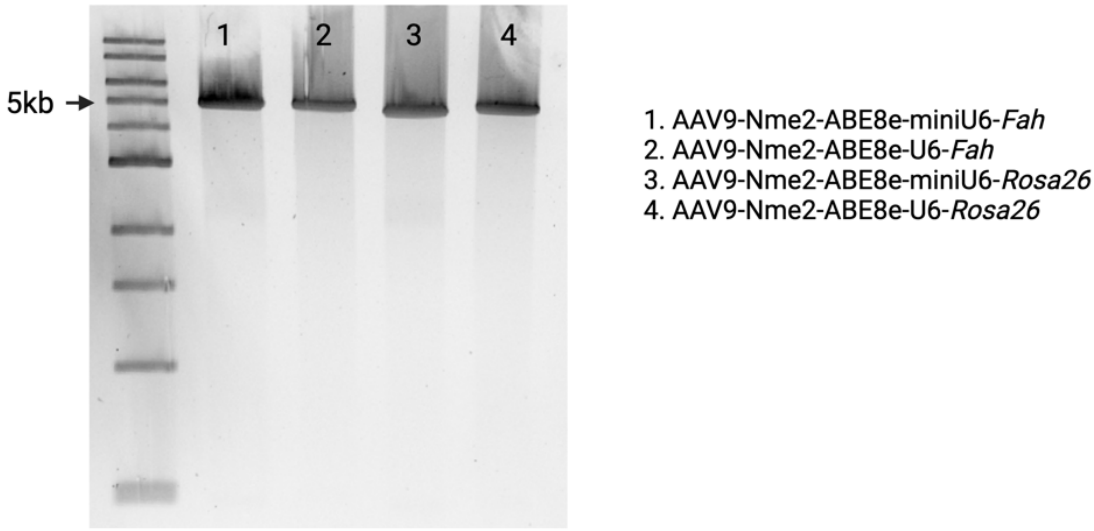

Supplementary Figure 4
Alkaline gel electrophoresis of AAV9 genomic DNA.

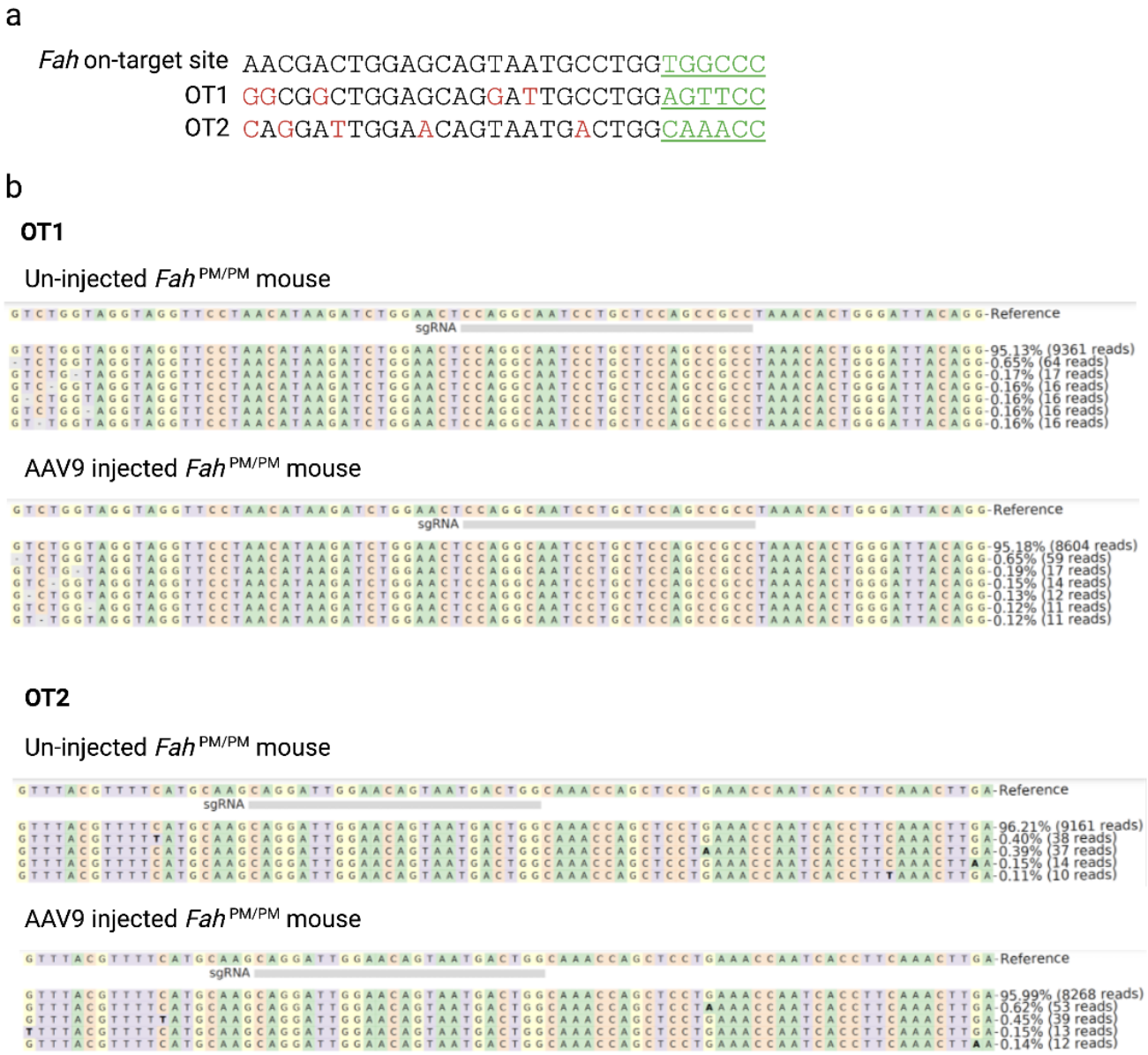

Supplementary Figure 5

a). Sequence of the *Fah* on-target site and two top-rated Cas-OFFinder predicted off-target sites for Nme2-ABE8e. Bases that are different from the on-target site are labeled in red. PAM, green, underlined. **b).** Representative amplicon deep sequencing reads at the predicted off-target sites in mice injected with AAV9 expressing Nme2-ABE8e and sgRNA-*Fah*.

Supplementary note

Nucleotide sequences of plasmids

Nme2-ABE7.10 construct in **Figure 1**

Legend: CMV enhancer, CMV promoter, NLS, **TadA**, linker, TadA7.10, Nme2Cas9-D16A, 3xHA, poly-A signal

GACATTGATTATTGACTAGTTATTAATAGTAATCAATTACGGGGTCATTAGTTCATAGCCCATATATGGAGTTCCGCGTTA
CATAACTTACGGTAAATGGCCCGCCTGGCTGACCGCCCAACGACCCCCGCCCATTGACGTCAATAATGACGTATGTTCCCA
TAGTAACGCCAATAGGGACTTTCCATTGACGTCAATGGGTGGAGTATTTACGGTAAACTGCCCACTTGGCAGTACATCAA
GTGTATCATATGCCAAGTACGCCCCCTATTGACGTCAATGACGGTAAATGGCCCGCCTGGCATTATGCCCAGTACATGACC
TTATGGGACTTTCCTACTTGGCAGTACATCTACGTATTAGTCATCGCTATTACCATGGTGATGCGGTTTTGGCAGTACATCA
ATGGGCGTGGATAGCGGTTTGACTCACGGGGATTTCCAAGTCTCCACCCCATTGACGTCAATGGGAGTTTGTTTTGGCAC
CAAAATCAACGGGACTTTCCAAAATGTCGTAACAACTCCGCCCCATTGACGCAAATGGGCGGTAGGCGTGTACGGTGGG
AGGTCTATATAAGCAGAGCTGGTTTAGTGAACCGTCAGATCCGCTAGAGATCCGCGGCCGCtaatacgactcactatagggcgaa
ttgggtaccgggcccGCCACCATGgctagcCCCGCCGCCAAGCGCGTGAAGCTGGACGGCGGCAGCGGCGGCGGCAGCGGCGG
CGGCAGCGGCCCGGCAGCTAAGAGGGTGAAACTGGATggcggtagcggcggaggcagcggtggcggcagcggccccctcgagccaaaga
agaagcggaaagtc**tctgaagtcgagtttagccacgagtattggatgaggcacgcactgaccctggcaaagcgagcatgggatgaaagagaagtccccgt**
gggcgccgtgctggtgcacaacaatagagtgatcggagagggatggaacaggccaatcggccgccacgaccctaccgcacacgcagagatcatggcactg
aggcagggaggcctggtcatgcagaattaccgcctgatcgatgccaccctgtatgtgacactggagccatgcgtgatgtgcgcaggagcaatgatccacagc
aggatcggaagagtggtgttcggagcacgggacgccaagaccggcgcagcaggctccctgatggatgtgctgcaccaccccggcatgaaccaccgggtgg
agatcacagagggaatcctggcagacgagtgcgccgccctgctgagcgatttctttagaatgcggagacaggagatcaaggcccagaagaaggcacagag
ctccaccgactctggaggatctagcggaggatcctctggaagcgagacaccaggcacaagcgagtccgccacaccagagagctccggcggctcctccggagg
atcctctgaggtggagttttcccacgagtactggatgagacatgccctgaccctggccaagagggcacgcgatgagagggaggtgcctgtgggagccgtgctg
gtgctgaacaatagagtgatcggcgagggctggaacagagccatcggcctgcacgacccaacagcccatgccgaaattatggccctgagacagggcggcctg
gtcatgcagaactacagactgattgacgccaccctgtacgtgacattcgagccttgcgtgatgtgcgccggcgccatgatccactctaggatcggccgcgtggtg
tttggcgtgaggaacgcaaaaaccggcgccgcaggctccctgatggacgtgctgcactaccccggcatgaatcaccgcgtcgaaattaccgagggaatcctgg
cagatgaatgtgccgccctgctgtgctatttctttcggatgcctagacaggtgttcaatgctcagaagaaggcccagagctccaccgactccggaggatctagcg
gaggctcctctggctctgagacacctggcacaagcgagagcgcaacacctgaaagcagcgggggcagcagcgggggtcaatggccgccttcaagcctaac
ccaatcaattacatcctgggactggccatcggaatcgcatccgtgggatgggctatggtggagatcgacgaggaggagaatcctatccggctgatcgatctgg
gcgtgagagtgtttgagagggccgaggtgccaaagaccggcgattctctggctatggcccggagactggcacggagcgtgaggcgcctgacacggagaagg
gcacacaggctgctgagggcacgccggctgctgaagagagagggcgtgctgcaggcagcagacttcgatgagaatggcctgatcaagagcctgccaaacac
cccctggcagctgagagcagccgccctggacaggaagctgacaccactggagtggtctgccgtgctgctgcacctgatcaagcaccgcggctacctgagccag
cggaagaacgagggagagacagcagacaaggagctgggcgccctgctgaagggagtggccaacaatgcccacgccctgcagaccggcgatttcaggacac
ctgccgagctggccctgaataagtttgagaaggagtccggccacatcagaaaccagaggggcgactatagccacaccttctcccgcaaggatctgcaggccg
agctgatcctgctgttcgagaagcagaaggagtttggcaatccacacgtgagcggaggcctgaaggagggaatcgagaccctgctgatgacacagaggcctg
ccctgtccggcgacgcagtgcagaagatgctgggacactgcaccttcgagcctgcagagccaaaggccgccaagaacacctacacagccgagcggtttatct
ggctgacaaagctgaacaatctgagaatcctggagcagggatccgagaggccactgaccgacacagagagggccaccctgatggatgagccttaccggaag
tctaagctgacatatgcccaggccagaaagctgctgggcctggaggacaccgccttctttaagggcctgagatacggcaaggataatgccgaggcctccacac
tgatggagatgaaggcctatcacgccatctctcgcgccctggagaaggagggcctgaaggacaagaagtccccccctgaacctgagctccgagctgcaggatg
agatcggcaccgccttctctctgtttaagaccgacgaggatatcacaggccgcctgaaggacagggtgcagcctgagatcctggaggccctgctgaagcacat
ctctttcgataagtttgtgcagatcagcctgaaggccctgagaaggatcgtgccactgatggagcagggcaagcggtacgacgaggcctgcgccgagatctac
ggcgatcactatggcaagaagaacacagaggagaagatctatctgccccctatccctgccgacgagatcagaaatcctgtggtgctgagggccctgtcccagg
caagaaaagtgatcaacggagtggtgcgccggtacggatctccagcccggatccacatcgagaccgccagagaagtgggcaagagcttcaaggaccggaag
gagatcgagaagagacaggaggagaatcgcaaggatcgggagaaggccgccgccaagtttagggagtacttccctaactttgtgggcgagccaaagtctaa
ggacatcctgaagctgcgcctgtacgagcagcagcacggcaagtgtctgtatagcggcaaggagatcaatctggtgcggctgaacgagaagggctatgtgga
gatcgatcacgccctgcctttctccagaacctgggacgattcttttaacaataaggtgctggtgctgggcagcgagaaccagaataagggcaatcagacaccat
acgagtatttcaatggcaaggacaactccagggagtggcaggagttcaaggcccgcgtggagacctctagatttcccaggagcaagaagcagcggatcctgc
tgcagaagttcgacgaggatggctttaaggagtgcaacctgaatgacaccagatacgtgaaccggttcctgtgccagtttgtggccgatcacatcctgctgacc

ggcaagggcaagagaagggtgttcgcctctaatggccagatcacaaacctgctgaggggattttggggactgaggaaggtgcgggcagagaatgacagaca
ccacgcactggatgcagtggtggtggcatgcagcaccgtggcaatgcagcagaagatcacaagattcgtgaggtataaggagatgaacgcctttgacggcaa
gaccatcgataaggagacaggcaaggtgctgcaccagaagacccacttcccccagccttgggagttctttgcccaggaagtgatgatccgggtgttcggcaag
ccagacggcaagcctgagtttgaggaggccgataccccagagaagctgaggacactgctggcagagaagctgtctagcaggccagaggcagtgcacgagta
cgtgaccccactgttcgtgtccagggcacccaatcggaagatgtctggcgcccacaaggacacactgagaagcgccaagaggtttgtgaagcacaacgagaa
gatctccgtgaagagagtgtggctgaccgagatcaagctggccgatctggagaacatggtgaattacaagaacggcagggagatcgagctgtatgaggccct
gaaggcaaggctggaggcctacggaggaaatgccaagcaggccttcgacccaaaggataaccccttttataagaagggaggacagctggtgaaggccgtgc
gggtggagaagacccaggagagcggcgtgctgctgaataagaagaacgcctacacaatcgccgacaatggcgatatggtgagagtggacgtgttctgtaag
gtggataagaagggcaagaatcagtactttatcgtgcctatctatgcctggcaggtggccgagaacatcctgccagacatcgattgcaagggctacagaatcg
acgatagctatacattctgtttttccctgcacaagtatgacctgatcgccttccagaaggatgagaagtccaaggtggagtttgcctactatatcaattgcgactc
ctctaacggcaggttctacctggcctggcacgataagggcagcaaggagcagcagtttcgcatctccacccagaatctggtgctgatccagaagtatcaggtga
acgagctgggcaaggagatcaggccatgtcggctgaagaagcgcccacccgtgcgggatatcGGCACCGGCGGGtctggaggatctagcggaggatcc
tctggaagcgagacaccaggcacaagcgagtccgccacaccagagagctccggcggctcctccggaggatccGTATACCCATACGATGTTCCTGAC
TATGCGGGCTATCCCTATGACGTCCCGGACTATGCAGGATCGTATCCTTATGACGTTCCAGATTACGCTGGATCCGCCGCT
CCGGCAGCTAAGAAAAAGAAACTGGATTTCGAATCCGGAgaattcctgcagcccgggggatccactagttctagaGGATCCGCCGCTC
CCGCCGCCAAGCGCGTGAAGCTGGACGGCGGCAGCGGCGGCGGCAGCGGCGGCGGCAGCGGCggcggtagcggcggaggca
gcggtggcggcagcggcAAGCGCACCGCCGACAGCCAGCACAGCACCCCCCCCAAGACCAAGCGCAAGGTGGGCGGCAGCGG
CGGCGGCAGCGGCGGCGGCAGCGGCTCCGGACCGGCAGCTAAGAGGGTGAAACTGGATtgaTAAgcggccgccaccgcggtg
gagctccagcttttgttccctttagtgagggttaatGAATTCGAGCCCAAGAAGAAGAGGAAAGTCTAACCGGTCATCATCACCATCAC
CATTGAGTTTAAACCCGCTGATCAGCCTCGACTGTGCCTTCTAGTTGCCAGCCATCTGTTGTTTGCCCCTCCCCCGTGCCTT
CCTTGACCCTGGAAGGTGCCACTCCCACTGTCCTTTCCTAATAAAATGAGAAAATTGCATCGCATTGTCTGAGTAGGTGTC
ATTCTATTCTGGGGGGTGGGGTGGGGCAGGACAGCAAGGGGGAGGATTGGGAAGACAATAGCAGGCATGCTGGGGAT
GCGGTGGGCTCTATGG

Nme2-ABE8e construct in **Figure 1 and Supplementary Figure 3a**

Legend: CMV enhancer, CMV promoter, NLS, TadA8e, linker, Nme2Cas9-D16A, 3xHA, poly-A signal

GACATTGATTATTGACTAGTTATTAATAGTAATCAATTACGGGGTCATTAGTTCATAGCCCATATATGGAGTTCCGCGTTA
CATAACTTACGGTAAATGGCCCGCCTGGCTGACCGCCCAACGACCCCCGCCCATTGACGTCAATAATGACGTATGTTCCCA
TAGTAACGCCAATAGGGACTTTCCATTGACGTCAATGGGTGGAGTATTTACGGTAAACTGCCCACTTGGCAGTACATCAA
GTGTATCATATGCCAAGTACGCCCCCTATTGACGTCAATGACGGTAAATGGCCCGCCTGGCATTATGCCCAGTACATGACC
TTATGGGACTTTCCTACTTGGCAGTACATCTACGTATTAGTCATCGCTATTACCATGGTGATGCGGTTTTGGCAGTACATCA
ATGGGCGTGGATAGCGGTTTGACTCACGGGGATTTCCAAGTCTCCACCCCATTGACGTCAATGGGAGTTTGTTTTGGCAC
CAAAATCAACGGGACTTTCCAAAATGTCGTAACAACTCCGCCCCATTGACGCAAATGGGCGGTAGGCGTGTACGGTGGG
AGGTCTATATAAGCAGAGCTGGTTTAGTGAACCGTCAGATCCGCTAGAGATCCGCGGCCGCtaatacgactcactatagggcgaa
ttgggtaccgggcccGCCACCATGgctagcCCCGCCGCCAAGCGCGTGAAGCTGGACGGCGGCAGCGGCGGCGGCAGCGGCGG
CGGCAGCGGCCCGGCAGCTAAGAGGGTGAAACTGGATggcggtagcggcggaggcagcggtggcggcagcggccccctcgagTctgagg
tggagttttcccacgagtactggatgagacatgccctgaccctggccaagagggcacgcgatgagagggaggtgcctgtgggagccgtgctggtgctgaacaa
tagagtgatcggcgagggctggaacagagccatcggcctgcacgacccaacagcccatgccgaaattatggccctgagacagggcggcctggtcatgcagaa
ctacagactgattgacgccaccctgtacgtgacattcgagccttgcgtgatgtgcgccggcgccatgatccactctaggatcggccgcgtggtgtttggcgtgag
gaacAGCaaaCGGgcgccgcaggctccctgatgAacgtgctgAactaccccggcatgaatcaccgcgtcgaaattaccgagggaatcctggcagatga
atgtgccgccctgctgtgcGACttctACcggatgcctagacaggtgttcaatgctcagaagaaggcccagagctccaTcAactccggaggatctagcggagg
ctcctctggctctgagacacctggcacaagcgagagcgcaacacctgaaagcagcgggggcagcagcgggggggtcaatggccgccttcaagcctaacccaat
caattacatcctgggactggccatcggaatcgcatccgtgggatgggctatggtggagatcgacgaggaggagaatcctatccggctgatcgatctgggcgtg
agagtgtttgagagggccgaggtgccaaagaccggcgattctctggctatggcccggagactggcacggagcgtgaggcgcctgacacggagaagggcaca
caggctgctgagggcacgccggctgctgaagagagagggcgtgctgcaggcagcagacttcgatgagaatggcctgatcaagagcctgccaaacaccccctg
gcagctgagagcagccgccctggacaggaagctgacaccactggagtggtctgccgtgctgctgcacctgatcaagcaccgcggctacctgagccagcggaa
gaacgagggagagacagcagacaaggagctgggcgccctgctgaagggagtggccaacaatgcccacgccctgcagaccggcgatttcaggacacctgccg
agctggccctgaataagtttgagaaggagtccggccacatcagaaaccagaggggcgactatagccacaccttctcccgcaaggatctgcaggccgagctga
tcctgctgttcgagaagcagaaggagtttggcaatccacacgtgagcggaggcctgaaggagggaatcgagaccctgctgatgacacagaggcctgccctgt

ccggcgacgcagtgcagaagatgctgggacactgcaccttcgagcctgcagagccaaaggccgccaagaacacctacacagccgagcggtttatctggctga
caaagctgaacaatctgagaatcctggagcagggatccgagaggccactgaccgacacagagagggccaccctgatggatgagccttaccggaagtctaag
ctgacatatgcccaggccagaaagctgctgggcctggaggacaccgccttctttaagggcctgagatacggcaaggataatgccgaggcctccacactgatgg
agatgaaggcctatcacgccatctctcgcgccctggagaaggagggcctgaaggacaagaagtcccccctgaacctgagctccgagctgcaggatgagatcg
gcaccgccttctctctgtttaagaccgacgaggatatcacaggccgcctgaaggacagggtgcagcctgagatcctggaggccctgctgaagcacatctctttc
gataagtttgtgcagatcagcctgaaggccctgagaaggatcgtgccactgatggagcagggcaagcggtacgacgaggcctgcgccgagatctacggcgat
cactatggcaagaagaacacagaggagaagatctatctgccccctatccctgccgacgagatcagaaatcctgtggtgctgagggccctgtcccaggcaaga
aaagtgatcaacggagtggtgcgccggtacggatctccagcccggatccacatcgagaccgccagagaagtgggcaagagcttcaaggaccggaaggagat
cgagaagagacaggaggagaatcgcaaggatcgggagaaggccgccgccaagtttagggagtacttccctaactttgtgggcgagccaaagtctaaggaca
tcctgaagctgcgcctgtacgagcagcagcacggcaagtgtctgtatagcggcaaggagatcaatctggtgcggctgaacgagaagggctatgtggagatcg
atcacgccctgcctttctccagaacctgggacgattcttttaacaataaggtgctggtgctgggcagcgagaaccagaataagggcaatcagacaccatacga
gtatttcaatggcaaggacaactccagggagtggcaggagttcaaggcccgcgtggagacctctagatttcccaggagcaagaagcagcggatcctgctgca
gaagttcgacgaggatggctttaaggagtgcaacctgaatgacaccagatacgtgaaccggttcctgtgccagtttgtggccgatcacatcctgctgaccggca
agggcaagagaagggtgttcgcctctaatggccagatcacaaacctgctgaggggattttggggactgaggaaggtgcgggcagagaatgacagacaccac
gcactggatgcagtggtggtggcatgcagcaccgtggcaatgcagcagaagatcacaagattcgtgaggtataaggagatgaacgcctttgacggcaagacc
atcgataaggagacaggcaaggtgctgcaccagaagacccacttcccccagccttgggagttctttgcccaggaagtgatgatccgggtgttcggcaagccag
acggcaagcctgagtttgaggaggccgataccccagagaagctgaggacactgctggcagagaagctgtctagcaggccagaggcagtgcacgagtacgtg
accccactgttcgtgtccagggcacccaatcggaagatgtctggcgcccacaaggacacactgagaagcgccaagaggtttgtgaagcacaacgagaagatc
tccgtgaagagagtgtggctgaccgagatcaagctggccgatctggagaacatggtgaattacaagaacggcagggagatcgagctgtatgaggccctgaag
gcaaggctggaggcctacggaggaaatgccaagcaggccttcgacccaaaggataaccccttttataagaagggaggacagctggtgaaggccgtgcgggt
ggagaagacccaggagagcggcgtgctgctgaataagaagaacgcctacacaatcgccgacaatggcgatatggtgagagtggacgtgttctgtaaggtgg
ataagaagggcaagaatcagtactttatcgtgcctatctatgcctggcaggtggccgagaacatcctgccagacatcgattgcaagggctacagaatcgacga
tagctatacattctgtttttccctgcacaagtatgacctgatcgccttccagaaggatgagaagtccaaggtggagtttgcctactatatcaattgcgactcctcta
acggcaggttctacctggcctggcacgataagggcagcaaggagcagcagtttcgcatctccacccagaatctggtgctgatccagaagtatcaggtgaacga
gctgggcaaggagatcaggccatgtcggctgaagaagcgcccacccgtgcggGATATCGGCACCGGCGGGTCTGGAGGATCTAGCGGAGGATCCTCTG
GAAGCGAGACACCAGGCACAAGCGAGTCCGCCACACCAGAGAGCTCCGGCGGCTCCTCCGGAGGATCCGTATACCCATACGATGTTCCTGACTAT
GCGGGCTATCCCTATGACGTCCCGGACTATGCAGGATCGTATCCTTATGACGTTCCAGATTACGCTGGATCCGCCGCTCCG
GCAGCTAAGAAAAAGAAACTGGATTTCGAATCCGGAgaattcctgcagcccgggggatccactagttctagaGGATCCGCCGCTCCCG
CCGCCAAGCGCGTGAAGCTGGACGGCGGCAGCGGCGGCGGCAGCGGCGGCGGCAGCGGCggcggtagcggcggaggcagcg
gtggcggcagcggcAAGCGCACCGCCGACAGCCAGCACAGCACCCCCCCCAAGACCAAGCGCAAGGTGGGCGGCAGCGGCG
GCGGCAGCGGCGGCGGCAGCGGCTCCGGACCGGCAGCTAAGAGGGTGAAACTGGATtgaTAAgcggccgccaccgcggtggag
ctccagcttttgttccctttagtgagggttaatGAATTCGAGCCCAAGAAGAAGAGGAAAGTCTAACCGGTCATCATCACCATCACCAT
TGAGTTTAAACCCGCTGATCAGCCTCGACTGTGCCTTCTAGTTGCCAGCCATCTGTTGTTTGCCCCTCCCCCGTGCCTTCCT
TGACCCTGGAAGGTGCCACTCCCACTGTCCTTTCCTAATAAAATGAGAAAATTGCATCGCATTGTCTGAGTAGGTGTCATT
CTATTCTGGGGGGTGGGGTGGGGCAGGACAGCAAGGGGGAGGATTGGGAAGACAATAGCAGGCATGCTGGGGATGCG
GTGGGCTCTATGG

Spy-ABE7.10 construct in **Figure 1 and Supplementary Figure 3a**

Legend: CMV enhancer, CMV promoter, NLS, **TadA**, linker, TadA7.10, SpyCas9-D10A, 3xHA, poly-A signal

GACATTGATTATTGACTAGTTATTAATAGTAATCAATTACGGGGTCATTAGTTCATAGCCCATATATGGAGTTCCGCGTTA
CATAACTTACGGTAAATGGCCCGCCTGGCTGACCGCCCAACGACCCCCGCCCATTGACGTCAATAATGACGTATGTTCCCA
TAGTAACGCCAATAGGGACTTTCCATTGACGTCAATGGGTGGAGTATTTACGGTAAACTGCCCACTTGGCAGTACATCAA
GTGTATCATATGCCAAGTACGCCCCCTATTGACGTCAATGACGGTAAATGGCCCGCCTGGCATTATGCCCAGTACATGACC
TTATGGGACTTTCCTACTTGGCAGTACATCTACGTATTAGTCATCGCTATTACCATGGTGATGCGGTTTTGGCAGTACATCA
ATGGGCGTGGATAGCGGTTTGACTCACGGGGATTTCCAAGTCTCCACCCCATTGACGTCAATGGGAGTTTGTTTTGGCAC
CAAAATCAACGGGACTTTCCAAAATGTCGTAACAACTCCGCCCCATTGACGCAAATGGGCGGTAGGCGTGTACGGTGGG
AGGTCTATATAAGCAGAGCTGGTTTAGTGAACCGTCAGATCCGCTAGAGATCCGCGGCCGCtaatacgactcactatagggcgaa
ttgggtaccgggcccGCCACCATGgctagcCCCGCCGCCAAGCGCGTGAAGCTGGACGGCGGCAGCGGCGGCGGCAGCGGCGG
CGGCAGCGGCCCGGCAGCTAAGAGGGTGAAACTGGATggcggtagcggcggaggcagcggtggcggcagcggccccctcgagccaaaga

agaagcggaaagtc**tctgaagtcgagtttagccacgagtattggatgaggcacgcactgaccctggcaaagcgagcatgggatgaaagagaagtccccgt**
gggcgccgtgctggtgcacaacaatagagtgatcggagagggatggaacaggccaatcggccgccacgaccctaccgcacacgcagagatcatggcactg
aggcagggaggcctggtcatgcagaattaccgcctgatcgatgccaccctgtatgtgacactggagccatgcgtgatgtgcgcaggagcaatgatccacagc
aggatcggaagagtggtgttcggagcacgggacgccaagaccggcgcagcaggctccctgatggatgtgctgcaccaccccggcatgaaccaccgggtgg
agatcacagagggaatcctggcagacgagtgcgccgccctgctgagcgatttctttagaatgcggagacaggagatcaaggcccagaagaaggcacagag
ctccaccgactctggaggatctagcggaggatcctctggaagcgagacaccaggcacaagcgagtccgccacaccagagagctccggcggctcctccggagg
atcctctgaggtggagttttcccacgagtactggatgagacatgccctgaccctggccaagagggcacgcgatgagagggaggtgcctgtgggagccgtgctg
gtgctgaacaatagagtgatcggcgagggctggaacagagccatcggcctgcacgacccaacagcccatgccgaaattatggccctgagacagggcggcctg
gtcatgcagaactacagactgattgacgccaccctgtacgtgacattcgagccttgcgtgatgtgcgccggcgccatgatccactctaggatcggccgcgtggtg
tttggcgtgaggaacgcaaaaaccggcgccgcaggctccctgatggacgtgctgcactaccccggcatgaatcaccgcgtcgaaattaccgagggaatcctgg
cagatgaatgtgccgccctgctgtgctatttctttcggatgcctagacaggtgttcaatgctcagaagaaggcccagagctccaccgactccggaggatctagcg
gaggctcctctggctctgagacacctggcacaagcgagagcgcaacacctgaaagcagcgggggcagcagcgggggtcaatggccgccttcaagcctaac
ccaatcaattacgatatcGACAAGAAGTACTCCATTGGGCTCGcTATCGGTACCAACAGCGTCGGCTGGGCCGTCATTACGGAC
GAGTACAAGGTGCCGAGCAAAAAATTCAAAGTTCTGGGCAATACCGATCGCCACAGCATAAAGAAGAACCTCATTGGAG
CCCTCCTGTTCGACTCCGGGGAGACGGCCGAAGCCACGCGGCTCAAAAGAACAGCACGGCGCAGATATACCCGCAGAAA
GAATCGGATCTGCTACCTGCAGGAGATCTTTAGTAATGAGATGGCTAAGGTGGATGACTCTTTCTTCCATAGGCTGGAGG
AGTCCTTTTTGGTGGAGGAGGATAAAAAGCACGAGCGCCACCCAATCTTTGGCAATATCGTGGACGAGGTGGCGTACCA
TGAAAAGTACCCAACCATATATCATCTGAGGAAGAAGCTGGTAGACAGTACTGATAAGGCTGACTTGCGGTTGATCTATC
TCGCGCTGGCGCACATGATCAAATTTCGGGGACACTTCCTCATCGAGGGGGACCTGAACCCAGACAACAGCGATGTCGA
CAAACTCTTTATCCAACTGGTTCAGACTTACAATCAGCTTTTCGAGGAGAACCCGATCAACGCATCCGGCGTTGACGCCAA
AGCAATCCTGAGCGCTAGGCTGTCCAAATCCCGGCGGCTCGAAAACCTCATCGCACAGCTCCCTGGGGAGAAGAAGAAC
GGCCTGTTTGGTAATCTTATCGCCCTGTCACTCGGGCTGACCCCCAACTTTAAATCTAACTTCGACCTGGCCGAAGATGCC
AAGCTGCAACTGAGCAAAGACACCTACGATGATGATCTCGACAATCTGCTGGCCCAGATCGGCGACCAGTACGCAGACC
TTTTTTTGGCGGCAAAGAACCTGTCAGACGCCATTCTGCTGAGTGATATTCTGCGAGTGAACACGGAGATCACCAAAGCT
CCGCTGAGCGCTAGTATGATCAAGCGCTATGATGAGCACCACCAAGACTTGACTTTGCTGAAGGCCCTTGTCAGACAGCA
ACTGCCTGAGAAGTACAAGGAAATTTTCTTCGATCAGTCTAAAAATGGCTACGCCGGATACATTGACGGCGGAGCAAGCC
AGGAGGAATTTTACAAATTTATTAAGCCCATCTTGGAAAAAATGGACGGCACCGAGGAGCTGCTGGTAAAGCTGAACAG
AGAAGATCTGTTGCGCAAACAGCGCACTTTCGACAATGGAAGCATCCCCCACCAGATTCACCTGGGCGAACTGCACGCTA
TCCTCAGGCGGCAAGAGGATTTCTACCCCTTTTTGAAAGATAACAGGGAAAAGATTGAGAAAATCCTCACATTTCGGATA
CCCTACTATGTAGGCCCCCTCGCTCGGGGAAATTCCAGATTCGCGTGGATGACTCGCAAATCAGAAGAGACCATCACTCC
CTGGAACTTCGAGGAAGTCGTGGATAAGGGGGCCTCTGCCCAGTCCTTCATCGAAAGGATGACTAACTTTGATAAAAATC
TGCCTAACGAAAAGGTGCTTCCTAAACACTCTCTGCTGTACGAGTACTTCACAGTTTATAACGAGCTCACCAAGGTCAAAT
ACGTCACAGAAGGGATGAGAAAGCCAGCATTCCTGTCTGGAGAGCAGAAGAAAGCTATCGTGGACCTCCTCTTCAAGAC
GAACCGGAAAGTTACCGTGAAACAGCTCAAAGAAGACTATTTCAAAAAGATTGAATGTTTCGACTCTGTTGAAATCAGCG
GAGTGGAGGATCGCTTCAACGCATCCCTGGGAACGTATCACGATCTCCTGAAAATCATTAAAGACAAGGACTTCCTGGAC
AATGAGGAGAACGAGGACATTCTTGAGGACATTGTCCTCACCCTTACGTTGTTTGAAGATAGGGAGATGATTGAAGAAC
GCTTGAAAACTTACGCTCATCTCTTCGACGACAAAGTCATGAAACAGCTCAAGAGACGCCGATATACAGGATGGGGGCG
GCTGTCAAGAAAACTGATCAATGGCATCCGAGACAAGCAGAGTGGAAAGACAATCCTGGATTTTCTTAAGTCCGATGGA
TTTGCCAACCGGAACTTCATGCAGTTGATCCATGATGACTCTCTCACCTTTAAGGAGGACATCCAGAAAGCACAAGTTTCT
GGCCAGGGGGACAGTCTTCACGAGCACATCGCTAATCTTGCAGGTAGCCCAGCTATCAAAAAGGGAATACTGCAGACCG
TTAAGGTCGTGGATGAACTCGTCAAAGTAATGGGAAGGCATAAGCCCGAGAATATCGTTATCGAGATGGCCCGAGAGAA
CCAAACTACCCAGAAGGGACAGAAGAACAGTAGGGAAAGGATGAAGAGGATTGAAGAGGGTATAAAAGAACTGGGGT
CCCAAATCCTTAAGGAACACCCAGTTGAAAACACCCAGCTTCAGAATGAGAAGCTCTACCTGTACTACCTGCAGAACGGC
AGGGACATGTACGTGGATCAGGAACTGGACATCAACCGGTTGTCCGACTACGACGTGGATCATATCGTGCCCCAAAGCTT
TCTCAAAGATGATTCTATTGATAATAAAGTGTTGACAAGATCCGATAAAAATAGAGGGAAGAGTGATAACGTCCCCTCAG
AAGAAGTTGTCAAGAAAATGAAAAATTATTGGCGGCAGCTGCTGAACGCCAAACTGATCACACAACGGAAGTTCGATAA
TCTGACTAAGGCTGAACGAGGTGGCCTGTCTGAGTTGGATAAAGCCGGCTTCATCAAAAGGCAGCTTGTTGAGACACGC
CAGATCACCAAGCACGTGGCCCAAATTCTCGATTCACGCATGAACACCAAGTACGATGAAAATGACAAACTGATTCGAGA
GGTGAAAGTTATTACTCTGAAGTCTAAGCTGGTCTCAGATTTCAGAAAGGACTTTCAGTTTTATAAGGTGAGAGAGATCA

ACAATTACCACCATGCGCATGATGCCTACCTGAATGCAGTGGTAGGCACTGCACTTATCAAAAAATATCCCAAGCTGGAA
TCTGAATTTGTTTACGGAGACTATAAAGTGTACGATGTTAGGAAAATGATCGCAAAGTCTGAGCAGGAAATAGGCAAGG
CCACCGCTAAGTACTTCTTTTACAGCAATATTATGAATTTTTTCAAGACCGAGATTACACTGGCCAATGGAGAGATTCGGA
AGCGACCACTTATCGAAACAAACGGAGAAACAGGAGAAATCGTGTGGGACAAGGGTAGGGATTTCGCGACAGTCCGCA
AGGTCCTGTCCATGCCGCAGGTGAACATCGTTAAAAAGACCGAAGTACAGACCGGAGGCTTCTCCAAGGAAAGTATCCT
CCCGAAAAGGAACAGCGACAAGCTGATCGCACGCAAAAAAGATTGGGACCCCAAGAAATACGGCGGATTCGATTCTCCT
ACAGTCGCTTACAGTGTACTGGTTGTGGCCAAAGTGGAGAAAGGGAAGTCTAAAAAACTCAAAAGCGTCAAGGAACTGC
TGGGCATCACAATCATGGAGCGATCCAGCTTCGAGAAAAACCCCATCGACTTTCTCGAAGCGAAAGGATATAAAGAGGT
CAAAAAAGACCTCATCATTAAGCTGCCCAAGTACTCTCTCTTTGAGCTTGAAAACGGCCGGAAACGAATGCTCGCTAGTG
CGGGCGAGCTGCAGAAAGGTAACGAGCTGGCACTGCCCTCTAAATACGTTAATTTCTTGTATCTGGCCAGCCACTATGAA
AAGCTCAAAGGGTCTCCCGAAGATAATGAGCAGAAGCAGCTGTTCGTGGAACAACACAAACACTACCTTGATGAGATCA
TCGAGCAAATAAGCGAGTTCTCCAAAAGAGTGATCCTCGCCGACGCTAACCTCGATAAGGTGCTTTCTGCTTACAATAAG
CACAGGGATAAGCCCATCAGGGAGCAGGCAGAAAACATTATCCACTTGTTTACTCTGACCAACTTGGGCGCGCCTGCAGC
CTTCAAGTACTTCGACACCACCATAGACAGAAAGCGGTACACCTCTACAAAGGAGGTCCTGGACGCCACACTGATTCATC
AGTCAATTACGGGGCTCTATGAAACAAGAATCGACCTCTCTCAGCTCGGTGGAGACgatatcGGCACCGGCGGGtctggagga
tctagcggaggatcctctggaagcgagacaccaggcacaagcgagtccgccacaccagagagctccggcggctcctccggaggatccGTATACCCATAC
GATGTTCCTGACTATGCGGGCTATCCCTATGACGTCCCGGACTATGCAGGATCGTATCCTTATGACGTTCCAGATTACGCT
GGATCCGCCGCTCCGGCAGCTAAGAAAAAGAAACTGGATTTCGAATCCGGAgaattcctgcagcccgggggatccactagttctagaG
GATCCGCCGCTCCCGCCGCCAAGCGCGTGAAGCTGGACGGCGGCAGCGGCGGCGGCAGCGGCGGCGGCAGCGGCggcg
gtagcggcggaggcagcggtggcggcagcggcAAGCGCACCGCCGACAGCCAGCACAGCACCCCCCCCAAGACCAAGCGCAAGGT
GGGCGGCAGCGGCGGCGGCAGCGGCGGCGGCAGCGGCTCCGGACCGGCAGCTAAGAGGGTGAAACTGGATtgaTAAgc
ggccgccaccgcggtggagctccagcttttgttccctttagtgagggttaatGAATTCGAGCCCAAGAAGAAGAGGAAAGTCTAACCGGTCA
TCATCACCATCACCATTGAGTTTAAACCCGCTGATCAGCCTCGACTGTGCCTTCTAGTTGCCAGCCATCTGTTGTTTGCCCC
TCCCCCGTGCCTTCCTTGACCCTGGAAGGTGCCACTCCCACTGTCCTTTCCTAATAAAATGAGAAAATTGCATCGCATTGTC
TGAGTAGGTGTCATTCTATTCTGGGGGGTGGGGTGGGGCAGGACAGCAAGGGGGAGGATTGGGAAGACAATAGCAGG
CATGCTGGGGATGCGGTGGGCTCTATGG

Spy-ABE8e construct in **Figure 1**

Legend: CMV enhancer, CMV promoter, NLS, TadA8e, linker, SpyCas9-D10A, 3xHA, poly-A signal

GACATTGATTATTGACTAGTTATTAATAGTAATCAATTACGGGGTCATTAGTTCATAGCCCATATATGGAGTTCCGCGTTA
CATAACTTACGGTAAATGGCCCGCCTGGCTGACCGCCCAACGACCCCCGCCCATTGACGTCAATAATGACGTATGTTCCCA
TAGTAACGCCAATAGGGACTTTCCATTGACGTCAATGGGTGGAGTATTTACGGTAAACTGCCCACTTGGCAGTACATCAA
GTGTATCATATGCCAAGTACGCCCCCTATTGACGTCAATGACGGTAAATGGCCCGCCTGGCATTATGCCCAGTACATGACC
TTATGGGACTTTCCTACTTGGCAGTACATCTACGTATTAGTCATCGCTATTACCATGGTGATGCGGTTTTGGCAGTACATCA
ATGGGCGTGGATAGCGGTTTGACTCACGGGGATTTCCAAGTCTCCACCCCATTGACGTCAATGGGAGTTTGTTTTGGCAC
CAAAATCAACGGGACTTTCCAAAATGTCGTAACAACTCCGCCCCATTGACGCAAATGGGCGGTAGGCGTGTACGGTGGG
AGGTCTATATAAGCAGAGCTGGTTTAGTGAACCGTCAGATCCGCTAGAGATCCGCGGCCGCtaatacgactcactatagggcgaa
ttgggtaccgggcccGCCACCATGgctagcCCCGCCGCCAAGCGCGTGAAGCTGGACGGCGGCAGCGGCGGCGGCAGCGGCGG
CGGCAGCGGCCCGGCAGCTAAGAGGGTGAAACTGGATggcggtagcggcggaggcagcggtggcggcagcggccccctcgagTctgagg
tggagttttcccacgagtactggatgagacatgccctgaccctggccaagagggcacgcgatgagagggaggtgcctgtgggagccgtgctggtgctgaacaa
tagagtgatcggcgagggctggaacagagccatcggcctgcacgacccaacagcccatgccgaaattatggccctgagacagggcggcctggtcatgcagaa
ctacagactgattgacgccaccctgtacgtgacattcgagccttgcgtgatgtgcgccggcgccatgatccactctaggatcggccgcgtggtgtttggcgtgag
gaacAGCaaaCGGggcgccgcaggctccctgatgAacgtgctgAactaccccggcatgaatcaccgcgtcgaaattaccgagggaatcctggcagatga
atgtgccgccctgctgtgcGACttctACcggatgcctagacaggtgttcaatgctcagaagaaggcccagagctccaTcAactccggaggatctagcggagg
ctcctctggctctgagacacctggcacaagcgagagcgcaacacctgaaagcagcgggggcagcagcgggggtcaatggccgccttcaagcctaacccaat
caattacgatatcGACAAGAAGTACTCCATTGGGCTCGcTATCGGTACCAACAGCGTCGGCTGGGCCGTCATTACGGACGAGT
ACAAGGTGCCGAGCAAAAAATTCAAAGTTCTGGGCAATACCGATCGCCACAGCATAAAGAAGAACCTCATTGGAGCCCT
CCTGTTCGACTCCGGGGAGACGGCCGAAGCCACGCGGCTCAAAAGAACAGCACGGCGCAGATATACCCGCAGAAAGAA
TCGGATCTGCTACCTGCAGGAGATCTTTAGTAATGAGATGGCTAAGGTGGATGACTCTTTCTTCCATAGGCTGGAGGAGT

CCTTTTTGGTGGAGGAGGATAAAAAGCACGAGCGCCACCCAATCTTTGGCAATATCGTGGACGAGGTGGCGTACCATGA
AAAGTACCCAACCATATATCATCTGAGGAAGAAGCTGGTAGACAGTACTGATAAGGCTGACTTGCGGTTGATCTATCTCG
CGCTGGCGCACATGATCAAATTTCGGGGACACTTCCTCATCGAGGGGGACCTGAACCCAGACAACAGCGATGTCGACAA
ACTCTTTATCCAACTGGTTCAGACTTACAATCAGCTTTTCGAGGAGAACCCGATCAACGCATCCGGCGTTGACGCCAAAGC
AATCCTGAGCGCTAGGCTGTCCAAATCCCGGCGGCTCGAAAACCTCATCGCACAGCTCCCTGGGGAGAAGAAGAACGGC
CTGTTTGGTAATCTTATCGCCCTGTCACTCGGGCTGACCCCCAACTTTAAATCTAACTTCGACCTGGCCGAAGATGCCAAG
CTGCAACTGAGCAAAGACACCTACGATGATGATCTCGACAATCTGCTGGCCCAGATCGGCGACCAGTACGCAGACCTTTT
TTTGGCGGCAAAGAACCTGTCAGACGCCATTCTGCTGAGTGATATTCTGCGAGTGAACACGGAGATCACCAAAGCTCCGC
TGAGCGCTAGTATGATCAAGCGCTATGATGAGCACCACCAAGACTTGACTTTGCTGAAGGCCCTTGTCAGACAGCAACTG
CCTGAGAAGTACAAGGAAATTTTCTTCGATCAGTCTAAAAATGGCTACGCCGGATACATTGACGGCGGAGCAAGCCAGG
AGGAATTTTACAAATTTATTAAGCCCATCTTGGAAAAAATGGACGGCACCGAGGAGCTGCTGGTAAAGCTGAACAGAGA
AGATCTGTTGCGCAAACAGCGCACTTTCGACAATGGAAGCATCCCCCACCAGATTCACCTGGGCGAACTGCACGCTATCC
TCAGGCGGCAAGAGGATTTCTACCCCTTTTTGAAAGATAACAGGGAAAAGATTGAGAAAATCCTCACATTTCGGATACCC
TACTATGTAGGCCCCCTCGCTCGGGGAAATTCCAGATTCGCGTGGATGACTCGCAAATCAGAAGAGACCATCACTCCCTG
GAACTTCGAGGAAGTCGTGGATAAGGGGGCCTCTGCCCAGTCCTTCATCGAAAGGATGACTAACTTTGATAAAAATCTGC
CTAACGAAAAGGTGCTTCCTAAACACTCTCTGCTGTACGAGTACTTCACAGTTTATAACGAGCTCACCAAGGTCAAATACG
TCACAGAAGGGATGAGAAAGCCAGCATTCCTGTCTGGAGAGCAGAAGAAAGCTATCGTGGACCTCCTCTTCAAGACGAA
CCGGAAAGTTACCGTGAAACAGCTCAAAGAAGACTATTTCAAAAAGATTGAATGTTTCGACTCTGTTGAAATCAGCGGAG
TGGAGGATCGCTTCAACGCATCCCTGGGAACGTATCACGATCTCCTGAAAATCATTAAAGACAAGGACTTCCTGGACAAT
GAGGAGAACGAGGACATTCTTGAGGACATTGTCCTCACCCTTACGTTGTTTGAAGATAGGGAGATGATTGAAGAACGCTT
GAAAACTTACGCTCATCTCTTCGACGACAAAGTCATGAAACAGCTCAAGAGACGCCGATATACAGGATGGGGGCGGCTG
TCAAGAAAACTGATCAATGGCATCCGAGACAAGCAGAGTGGAAAGACAATCCTGGATTTTCTTAAGTCCGATGGATTTGC
CAACCGGAACTTCATGCAGTTGATCCATGATGACTCTCTCACCTTTAAGGAGGACATCCAGAAAGCACAAGTTTCTGGCCA
GGGGGACAGTCTTCACGAGCACATCGCTAATCTTGCAGGTAGCCCAGCTATCAAAAAGGGAATACTGCAGACCGTTAAG
GTCGTGGATGAACTCGTCAAAGTAATGGGAAGGCATAAGCCCGAGAATATCGTTATCGAGATGGCCCGAGAGAACCAAA
CTACCCAGAAGGGACAGAAGAACAGTAGGGAAAGGATGAAGAGGATTGAAGAGGGTATAAAAGAACTGGGGTCCCAA
ATCCTTAAGGAACACCCAGTTGAAAACACCCAGCTTCAGAATGAGAAGCTCTACCTGTACTACCTGCAGAACGGCAGGGA
CATGTACGTGGATCAGGAACTGGACATCAACCGGTTGTCCGACTACGACGTGGATCATATCGTGCCCCAAAGCTTTCTCA
AAGATGATTCTATTGATAATAAAGTGTTGACAAGATCCGATAAAAATAGAGGGAAGAGTGATAACGTCCCCTCAGAAGA
AGTTGTCAAGAAAATGAAAAATTATTGGCGGCAGCTGCTGAACGCCAAACTGATCACACAACGGAAGTTCGATAATCTGA
CTAAGGCTGAACGAGGTGGCCTGTCTGAGTTGGATAAAGCCGGCTTCATCAAAAGGCAGCTTGTTGAGACACGCCAGAT
CACCAAGCACGTGGCCCAAATTCTCGATTCACGCATGAACACCAAGTACGATGAAAATGACAAACTGATTCGAGAGGTGA
AAGTTATTACTCTGAAGTCTAAGCTGGTCTCAGATTTCAGAAAGGACTTTCAGTTTTATAAGGTGAGAGAGATCAACAATT
ACCACCATGCGCATGATGCCTACCTGAATGCAGTGGTAGGCACTGCACTTATCAAAAAATATCCCAAGCTGGAATCTGAA
TTTGTTTACGGAGACTATAAAGTGTACGATGTTAGGAAAATGATCGCAAAGTCTGAGCAGGAAATAGGCAAGGCCACCG
CTAAGTACTTCTTTTACAGCAATATTATGAATTTTTTCAAGACCGAGATTACACTGGCCAATGGAGAGATTCGGAAGCGAC
CACTTATCGAAACAAACGGAGAAACAGGAGAAATCGTGTGGGACAAGGGTAGGGATTTCGCGACAGTCCGCAAGGTCC
TGTCCATGCCGCAGGTGAACATCGTTAAAAAGACCGAAGTACAGACCGGAGGCTTCTCCAAGGAAAGTATCCTCCCGAA
AAGGAACAGCGACAAGCTGATCGCACGCAAAAAAGATTGGGACCCCAAGAAATACGGCGGATTCGATTCTCCTACAGTC
GCTTACAGTGTACTGGTTGTGGCCAAAGTGGAGAAAGGGAAGTCTAAAAAACTCAAAAGCGTCAAGGAACTGCTGGGC
ATCACAATCATGGAGCGATCCAGCTTCGAGAAAAACCCCATCGACTTTCTCGAAGCGAAAGGATATAAAGAGGTCAAAA
AAGACCTCATCATTAAGCTGCCCAAGTACTCTCTCTTTGAGCTTGAAAACGGCCGGAAACGAATGCTCGCTAGTGCGGGC
GAGCTGCAGAAAGGTAACGAGCTGGCACTGCCCTCTAAATACGTTAATTTCTTGTATCTGGCCAGCCACTATGAAAAGCT
CAAAGGGTCTCCCGAAGATAATGAGCAGAAGCAGCTGTTCGTGGAACAACACAAACACTACCTTGATGAGATCATCGAG
CAAATAAGCGAGTTCTCCAAAAGAGTGATCCTCGCCGACGCTAACCTCGATAAGGTGCTTTCTGCTTACAATAAGCACAG
GGATAAGCCCATCAGGGAGCAGGCAGAAAACATTATCCACTTGTTTACTCTGACCAACTTGGGCGCGCCTGCAGCCTTCA
AGTACTTCGACACCACCATAGACAGAAAGCGGTACACCTCTACAAAGGAGGTCCTGGACGCCACACTGATTCATCAGTCA
ATTACGGGGCTCTATGAAACAAGAATCGACCTCTCTCAGCTCGGTGGAGACgatatcGGCACCGGCGGGtctggaggatctagc
ggaggatcctctggaagcgagacaccaggcacaagcgagtccgccacaccagagagctccggcggctcctccggaggatccGTATACCCATACGATG

TTCCTGACTATGCGGGCTATCCCTATGACGTCCCGGACTATGCAGGATCGTATCCTTATGACGTTCCAGATTACGCTGGAT
CCGCCGCTCCGGCAGCTAAGAAAAAGAAACTGGATTTCGAATCCGGAgaattcctgcagcccgggggatccactagttctagaGGATC
CGCCGCTCCCGCCGCCAAGCGCGTGAAGCTGGACGGCGGCAGCGGCGGCGGCAGCGGCGGCGGCAGCGGCggcggtagc
ggcggaggcagcggtggcggcagcggcAAGCGCACCGCCGACAGCCAGCACAGCACCCCCCCCAAGACCAAGCGCAAGGTGGGC
GGCAGCGGCGGCGGCAGCGGCGGCGGCAGCGGCTCCGGACCGGCAGCTAAGAGGGTGAAACTGGATtgaTAAgcggccg
ccaccgcggtggagctccagcttttgttccctttagtgagggttaatGAATTCGAGCCCAAGAAGAAGAGGAAAGTCTAACCGGTCATCAT
CACCATCACCATTGAGTTTAAACCCGCTGATCAGCCTCGACTGTGCCTTCTAGTTGCCAGCCATCTGTTGTTTGCCCCTCCC
CCGTGCCTTCCTTGACCCTGGAAGGTGCCACTCCCACTGTCCTTTCCTAATAAAATGAGAAAATTGCATCGCATTGTCTGA
GTAGGTGTCATTCTATTCTGGGGGGTGGGGTGGGGCAGGACAGCAAGGGGGAGGATTGGGAAGACAATAGCAGGCAT
GCTGGGGATGCGGTGGGCTCTATGG

U6-sgRNA construct for Nme2-ABE in **Figure 1**
Legend: U6 promoter, **guide sequence**, guide RNA scaffold, U6 termination signal

GAGGGCCTATTTCCCATGATTCCTTCATATTTGCATATACGATACAAGGCTGTTAGAGAGATAATTGGAATTAATTTGACT
GTAAACACAAAGATATTAGTACAAAATACGTGACGTAGAAAGTAATAATTTCTTGGGTAGTTTGCAGTTTTAAAATTATGT
TTTAAAATGGACTATCATATGCTTACCGTAACTTGAAAGTATTTCGATTTCTTGGCTTTATATATCTTGTGGAAAGGAC**NN**
NNNNNNNNNNNNNNNNNNNNNNGTTGTAGCTCCCTTTCTCATTTCGGAAACGAAATGAGAACCGTTGCTACAATAAG
GCCGTCTGAAAAGATGTGCCGCAACGCTCTGCCCCTTAAAGCTTCTGCTTTAAGGGGCATCGTTTATTTTTTT

U6-sgRNA construct for Spy-ABE in **Figure 1**
Legend: U6 promoter**, guide sequence**, guide RNA scaffold, U6 termination signal
GAGGGCCTATTTCCCATGATTCCTTCATATTTGCATATACGATACAAGGCTGTTAGAGAGATAATTGGAATTAATTTGACT
GTAAACACAAAGATATTAGTACAAAATACGTGACGTAGAAAGTAATAATTTCTTGGGTAGTTTGCAGTTTTAAAATTATGT
TTTAAAATGGACTATCATATGCTTACCGTAACTTGAAAGTATTTCGATTTCTTGGCTTTATATATCTTGTGGAAAGGAC**NN**
NNNNNNNNNNNNNNNNNNNNGTTTTAGAGCTAGAAATAGCAAGTTAAAATAAGGCTAGTCCGTTATCAACTTGAAAAAG
TGGCACCGAGTCGGTGCTTTTTTT

Single-AAV vector with 2xcMyc NLS in **Figure 3a**
Legend: ITR, U1a promoter, cMyc NLS, TadA8e, linker, Nme2Cas9-D16A, short poly-A signal, U6 promoter,
guide sequence, guide RNA scaffold, U6 termination signal
Cctgcaggcagctgcgcgctcgctcgctcactgaggccgcccgggcaaagcccgggcgtcgggcgacctttggtcgcccggcctcagtgagcgagcgagcgc
gcagagagggagtggccaactccatcactaggggttcctgcggcctctagaGTTTAAACAAAAAAA
TAAACGATGCCCCTTAAAGCAGAAGCTTTAAGGGGCAGAGCGTTGCGGCACATCTTTTCAGACGGCCTTATTGTAGCAAC
GTTTCGGGAGCTACAAC**NNNNNNNNNNNNNNNNNNNNNNNN**GGTGTTTCGTCCTTTCCACAAGATATATAAAGCCA
AGAAATCGAAATACTTTCAAGTTACGGTAAGCATATGATAGTCCATTTTAAAACATAATTTTAAAACTGCAAACTACCCAA
GAAATTATTACTTTCTACGTCACGTATTTTGTACTAATATCTTTGTGTTTACAGTCAAATTAATTCTAATTATCTCTCTAACA
GCCTTGTATCGTATATGCAAATATGAAGGAATCATGGGAAATAGGCCCTCTCTAGaatggaggcggtactatgtagatgagaattca
ggagcaaactgggaaaagcaactgcttccaaatatttgtgatttttacagtgtagttttggaaaaactcttagcctaccaattcttctaagtgttttaaaatgtggg
agccagtacacatgaagttatagagtgttttaatgaggcttaaatatttaccgtaactatgaaatgctacgcatatcatgctgttcaggctccgtggccacgcaa
ctcatactACCGGTGCCACCATGCCCGCCGCCAAGCGCGTGAAGCTGGACGGCGGCAGCGGCGGCGGCTctgaggtggagttttc
ccacgagtactggatgagacatgccctgaccctggccaagagggcacgcgatgagagggaggtgcctgtgggagccgtgctggtgctgaacaatagagtgat
cggcgagggctggaacagagccatcggcctgcacgacccaacagcccatgccgaaattatggccctgagacagggcggcctggtcatgcagaactacagact
gattgacgccaccctgtacgtgacattcgagccttgcgtgatgtgcgccggcgccatgatccactctaggatcggccgcgtggtgtttggcgtgaggaacAGCa
aaCGGggcgccgcaggctccctgatgAacgtgctgAactaccccggcatgaatcaccgcgtcgaaattaccgagggaatcctggcagatgaatgtgccgcc
ctgctgtgcGACttctACcggatgcctagacaggtgttcaatgctcagaagaaggcccagagctccaTcAactccggaggatctagcggaggctcctctggc
tctgagacacctggcacaagcgagagcgcaacacctgaaagcagcgggggcagcagcgggggggtcaatggccgccttcaagcctaacccaatcaattacat
cctgggactggccatcggaatcgcatccgtgggatgggctatggtggagatcgacgaggaggagaatcctatccggctgatcgatctgggcgtgagagtgtttg
agagggccgaggtgccaaagaccggcgattctctggctatggcccggagactggcacggagcgtgaggcgcctgacacggagaagggcacacaggctgctg

agggcacgccggctgctgaagagagagggcgtgctgcaggcagcagacttcgatgagaatggcctgatcaagagcctgccaaacacccctggcagctgag
agcagccgccctggacaggaagctgacaccactggagtggtctgccgtgctgctgcacctgatcaagcaccgcggctacctgagccagcggaagaacgaggg
agagacagcagacaaggagctgggcgccctgctgaagggagtggccaacaatgcccacgccctgcagaccggcgatttcaggacacctgccgagctggccc
tgaataagtttgagaaggagtccggccacatcagaaaccagaggggcgactatagccacaccttctcccgcaaggatctgcaggccgagctgatcctgctgtt
cgagaagcagaaggagtttggcaatccacacgtgagcggaggcctgaaggagggaatcgagaccctgctgatgacacagaggcctgccctgtccggcgacg
cagtgcagaagatgctgggacactgcaccttcgagcctgcagagccaaaggccgccaagaacacctacacagccgagcggtttatctggctgacaaagctga
acaatctgagaatcctggagcagggatccgagaggccactgaccgacacagagagggccaccctgatggatgagccttaccggaagtctaagctgacatatg
cccaggccagaaagctgctgggcctggaggacaccgccttctttaagggcctgagatacggcaaggataatgccgaggcctccacactgatggagatgaagg
cctatcacgccatctctcgcgccctggagaaggagggcctgaaggacaagaagtcccccctgaacctgagctccgagctgcaggatgagatcggcaccgcctt
ctctctgtttaagaccgacgaggatatcacaggccgcctgaaggacagggtgcagcctgagatcctggaggccctgctgaagcacatctctttcgataagtttgt
gcagatcagcctgaaggccctgagaaggatcgtgccactgatggagcagggcaagcggtacgacgaggcctgcgccgagatctacggcgatcactatggca
agaagaacacagaggagaagatctatctgccccctatccctgccgacgagatcagaaatcctgtggtgctgagggccctgtcccaggcaagaaaagtgatca
acggagtggtgcgccggtacggatctccagcccggatccacatcgagaccgccagagaagtgggcaagagcttcaaggaccggaaggagatcgagaagag
acaggaggagaatcgcaaggatcgggagaaggccgccgccaagtttagggagtacttccctaactttgtgggcgagccaaagtctaaggacatcctgaagct
gcgcctgtacgagcagcagcacggcaagtgtctgtatagcggcaaggagatcaatctggtgcggctgaacgagaagggctatgtggagatcgatcacgccct
gcctttctccagaacctgggacgattcttttaacaataaggtgctggtgctgggcagcgagaaccagaataagggcaatcagacaccatacgagtatttcaatg
gcaaggacaactccagggagtggcaggagttcaaggcccgcgtggagacctctagatttcccaggagcaagaagcagcggatcctgctgcagaagttcgacg
aggatggctttaaggagtgcaacctgaatgacaccagatacgtgaaccggttcctgtgccagtttgtggccgatcacatcctgctgaccggcaagggcaagag
aagggtgttcgcctctaatggccagatcacaaacctgctgaggggattttggggactgaggaaggtgcgggcagagaatgacagacaccacgcactggatgc
agtggtggtggcatgcagcaccgtggcaatgcagcagaagatcacaagattcgtgaggtataaggagatgaacgcctttgacggcaagaccatcgataagga
gacaggcaaggtgctgcaccagaagacccacttcccccagccttgggagttctttgcccaggaagtgatgatccgggtgttcggcaagccagacggcaagcct
gagtttgaggaggccgataccccagagaagctgaggacactgctggcagagaagctgtctagcaggccagaggcagtgcacgagtacgtgaccccactgttc
gtgtccagggcacccaatcggaagatgtctggcgcccacaaggacacactgagaagcgccaagaggtttgtgaagcacaacgagaagatctccgtgaagag
agtgtggctgaccgagatcaagctggccgatctggagaacatggtgaattacaagaacggcagggagatcgagctgtatgaggccctgaaggcaaggctgg
aggcctacggaggaaatgccaagcaggccttcgacccaaaggataaccccttttataagaagggaggacagctggtgaaggccgtgcgggtggagaagacc
caggagagcggcgtgctgctgaataagaagaacgcctacacaatcgccgacaatggcgatatggtgagagtggacgtgttctgtaaggtggataagaagggc
aagaatcagtactttatcgtgcctatctatgcctggcaggtggccgagaacatcctgccagacatcgattgcaagggctacagaatcgacgatagctatacatt
ctgtttttccctgcacaagtatgacctgatcgccttccagaaggatgagaagtccaaggtggagtttgcctactatatcaattgcgactcctctaacggcaggttc
tacctggcctggcacgataagggcagcaaggagcagcagtttcgcatctccacccagaatctggtgctgatccagaagtatcaggtgaacgagctgggcaag
gagatcaggccATGTCGGCTGAAGAAGCGCCCacccgtgcggGAGGATCCCGCCGCCAAGCGCGTGAAGCTGGACTAAAATAA
AAGATCTTTATTTTCATTAGATCTGTGTGTTGGTTTTTTGTGTAAGCgcggccgcaggaacccctagtgatggagttggccactccctctct
gcgcgctcgctcgctcactgaggccgggcgaccaaaggtcgcccgacgcccgggctttgcccgggcggcctcagtgagcgagcgagcgcgcagctgcctgca
gg

Single-AAV vector with 3xcMyc NLS in **Figure 3a**

Legend: ITR, U1a promoter, cMyc NLS, TadA8e, linker, Nme2Cas9-D16A, short poly-A signal, U6 promoter, **guide sequence**, guide RNA scaffold, U6 termination signal

Cctgcaggcagctgcgcgctcgctcgctcactgaggccgcccgggcaaagcccgggcgtcgggcgacctttggtcgcccggcctcagtgagcgagcgagcgc
gcagagagggagtggccaactccatcactaggggttcctgcggcctctagaGTTTAAACAAAAAAA
TAAACGATGCCCCTTAAAGCAGAAGCTTTAAGGGGCAGAGCGTTGCGGCACATCTTTTCAGACGGCCTTATTGTAGCAAC
GTTTCGGGAGCTACAAC**NNNNNNNNNNNNNNNNNNNNNNNNN**GGTGTTTCGTCCTTTCCACAAGATATATAAAGCCA
AGAAATCGAAATACTTTCAAGTTACGGTAAGCATATGATAGTCCATTTTAAAACATAATTTTAAAACTGCAAACTACCCAA
GAAATTATTACTTTCTACGTCACGTATTTTGTACTAATATCTTTGTGTTTACAGTCAAATTAATTCTAATTATCTCTCTAACA
GCCTTGTATCGTATATGCAAATATGAAGGAATCATGGGAAATAGGCCCTCTCTAGaatggaggcggtactatgtagatgagaattca
ggagcaaactgggaaaagcaactgcttccaaatatttgtgatttttacagtgtagttttggaaaaactcttagcctaccaattcttctaagtgttttaaaatgtggg
agccagtacacatgaagttatagagtgttttaatgaggcttaaatatttaccgtaactatgaaatgctacgcatatcatgctgttcaggctccgtggccacgcaa
ctcatactACCGGTGCCACCATGCCCGCCGCCAAGCGCGTGAAGCTGGACGGCGGCAGCGGCGGCGGCTctgaggtggagttttc
ccacgagtactggatgagacatgccctgaccctggccaagagggcacgcgatgagagggaggtgcctgtgggagccgtgctggtgctgaacaatagagtgat
cggcgagggctggaacagagccatcggcctgcacgacccaacagcccatgccgaaattatggccctgagacagggcggcctggtcatgcagaactacagact

gattgacgccaccctgtacgtgacattcgagccttgcgtgatgtgcgccggcgccatgatccactctaggatcggccgcgtggtgtttggcgtgaggaacAGCa
aaCGGggcgccgcaggctccctgatgAacgtgctgAactaccccggcatgaatcaccgcgtcgaaattaccgagggaatcctggcagatgaatgtgccgcc
ctgctgtgcGACttctACcggatgcctagacaggtgttcaatgctcagaagaaggcccagagctccaTcAactccggaggatctagcggaggctcctctggc
tctgagacacctggcacaagcgagagcgcaacacctgaaagcagcgggggcagcagcgggggggtcaatggccgccttcaagcctaacccaatcaattacat
cctgggactggccatcggaatcgcatccgtgggatgggctatggtggagatcgacgaggaggagaatcctatccggctgatcgatctgggcgtgagagtgtttg
agagggccgaggtgccaaagaccggcgattctctggctatggcccggagactggcacggagcgtgaggcgcctgacacggagaagggcacacaggctgctg
agggcacgccggctgctgaagagagagggcgtgctgcaggcagcagacttcgatgagaatggcctgatcaagagcctgccaaacaccccctggcagctgag
agcagccgccctggacaggaagctgacaccactggagtggtctgccgtgctgctgcacctgatcaagcaccgcggctacctgagccagcggaagaacgaggg
agagacagcagacaaggagctgggcgccctgctgaagggagtggccaacaatgcccacgccctgcagaccggcgatttcaggacacctgccgagctggccc
tgaataagtttgagaaggagtccggccacatcagaaaccagaggggcgactatagccacaccttctcccgcaaggatctgcaggccgagctgatcctgctgtt
cgagaagcagaaggagtttggcaatccacacgtgagcggaggcctgaaggagggaatcgagaccctgctgatgacacagaggcctgccctgtccggcgacg
cagtgcagaagatgctgggacactgcaccttcgagcctgcagagccaaaggccgccaagaacacctacacagccgagcggtttatctggctgacaaagctga
acaatctgagaatcctggagcagggatccgagaggccactgaccgacacagagagggccaccctgatggatgagccttaccggaagtctaagctgacatatg
cccaggccagaaagctgctgggcctggaggacaccgccttctttaagggcctgagatacggcaaggataatgccgaggcctccacactgatggagatgaagg
cctatcacgccatctctcgcgccctggagaaggagggcctgaaggacaagaagtcccccctgaacctgagctccgagctgcaggatgagatcggcaccgcctt
ctctctgtttaagaccgacgaggatatcacaggccgcctgaaggacagggtgcagcctgagatcctggaggccctgctgaagcacatctctttcgataagtttgt
gcagatcagcctgaaggccctgagaaggatcgtgccactgatggagcagggcaagcggtacgacgaggcctgcgccgagatctacggcgatcactatggca
agaagaacacagaggagaagatctatctgccccctatccctgccgacgagatcagaaatcctgtggtgctgagggccctgtcccaggcaagaaaagtgatca
acggagtggtgcgccggtacggatctccagcccggatccacatcgagaccgccagagaagtgggcaagagcttcaaggaccggaaggagatcgagaagag
acaggaggagaatcgcaaggatcgggagaaggccgccgccaagtttagggagtacttccctaactttgtgggcgagccaaagtctaaggacatcctgaagct
gcgcctgtacgagcagcagcacggcaagtgtctgtatagcggcaaggagatcaatctggtgcggctgaacgagaagggctatgtggagatcgatcacgccct
gcctttctccagaacctgggacgattcttttaacaataaggtgctggtgctgggcagcgagaaccagaataagggcaatcagacaccatacgagtatttcaatg
gcaaggacaactccagggagtggcaggagttcaaggcccgcgtggagacctctagatttcccaggagcaagaagcagcggatcctgctgcagaagttcgacg
aggatggctttaaggagtgcaacctgaatgacaccagatacgtgaaccggttcctgtgccagtttgtggccgatcacatcctgctgaccggcaagggcaagag
aagggtgttcgcctctaatggccagatcacaaacctgctgaggggattttggggactgaggaaggtgcgggcagagaatgacagacaccacgcactggatgc
agtggtggtggcatgcagcaccgtggcaatgcagcagaagatcacaagattcgtgaggtataaggagatgaacgcctttgacggcaagaccatcgataagga
gacaggcaaggtgctgcaccagaagacccacttcccccagccttgggagttctttgcccaggaagtgatgatccgggtgttcggcaagccagacggcaagcct
gagtttgaggaggccgataccccagagaagctgaggacactgctggcagagaagctgtctagcaggccagaggcagtgcacgagtacgtgaccccactgttc
gtgtccagggcacccaatcggaagatgtctggcgcccacaaggacacactgagaagcgccaagaggtttgtgaagcacaacgagaagatctccgtgaagag
agtgtggctgaccgagatcaagctggccgatctggagaacatggtgaattacaagaacggcagggagatcgagctgtatgaggccctgaaggcaaggctgg
aggcctacggaggaaatgccaagcaggccttcgacccaaaggataaccccttttataagaagggaggacagctggtgaaggccgtgcgggtggagaagacc
caggagagcggcgtgctgctgaataagaagaacgcctacacaatcgccgacaatggcgatatggtgagagtggacgtgttctgtaaggtggataagaagggc
aagaatcagtactttatcgtgcctatctatgcctggcaggtggccgagaacatcctgccagacatcgattgcaagggctacagaatcgacgatagctatacatt
ctgtttttccctgcacaagtatgacctgatcgccttccagaaggatgagaagtccaaggtggagtttgcctactatatcaattgcgactcctctaacggcaggttc
tacctggcctggcacgataagggcagcaaggagcagcagtttcgcatctccacccagaatctggtgctgatccagaagtatcaggtgaacgagctgggcaag
gagatcaggccATGTCGGCTGAAGAAGCGCCCacccgtgcggGAGGATCCGGCAGCTAAGAGGGTGAAACTGGATGGCGGCA
GCGGCGGCGGCAGCGGCGGCGGCAGCGGCCCCGCCGCCAAGCGCGTGAAGCTGGACTAAAATAAAAGATCTTTATTTTC
ATTAGATCTGTGTGTTGGTTTTTTGTGTAAGCgcggccgcaggaacccctagtgatggagttggccactccctctctgcgcgctcgctcgctcact
gaggccgggcgaccaaaggtcgcccgacgcccgggctttgcccgggcggcctcagtgagcgagcgagcgcgcagctgcctgcagg

Single-AAV vector with Ty1 NLS in **Figure 3a**

Legend: ITR, U1a promoter, Ty1 NLS, TadA8e, linker, Nme2Cas9-D16A, short poly-A signal, U6 promoter, **guide sequence**, guide RNA scaffold, U6 termination signal

Cctgcaggcagctgcgcgctcgctcgctcactgaggccgcccgggcaaagcccgggcgtcgggcgacctttggtcgcccggcctcagtgagcgagcgagcgc
gcagagagggagtggccaactccatcactaggggttcctgcggcctctagaGTTTAAACAAAAAAA
TAAACGATGCCCCTTAAAGCAGAAGCTTTAAGGGGCAGAGCGTTGCGGCACATCTTTTCAGACGGCCTTATTGTAGCAAC
GTTTCGGGAGCTACAACNNNNNNNNNNNNNNNNNNNNNNNNGGTGTTTCGTCCTTTCCACAAGATATATAAAGCCA
AGAAATCGAAATACTTTCAAGTTACGGTAAGCATATGATAGTCCATTTTAAAACATAATTTTAAAACTGCAAACTACCCAA
GAAATTATTACTTTCTACGTCACGTATTTTGTACTAATATCTTTGTGTTTACAGTCAAATTAATTCTAATTATCTCTCTAACA

GCCTTGTATCGTATATGCAAATATGAAGGAATCATGGGAAATAGGCCCTCTCTAGaatggaggcggtactatgtagatgagaattca
ggagcaaactgggaaaagcaactgcttccaaatatttgtgatttttacagtgtagttttggaaaaactcttagcctaccaattcttctaagtgttttaaaatgtggg
agccagtacacatgaagttatagagtgttttaatgaggcttaaatatttaccgtaactatgaaatgctacgcatatcatgctgttcaggctccgtggccacgcaa
ctcatactACCGGTGCCACCATGAACTCAAAGAAAAGGTCACTGGAGGACAACGAAACGGAAATCAAAGTCTCCAGAGACA
CCTGGAACACTAAGAACATGCGGTCCCTGGAACCGCCACGAAGCAAGAAACGGATACATGGCGGTAGCGGCGGAGGCA
GCGGTGGCGGCAGCGGCTctgaggtggagttttcccacgagtactggatgagacatgccctgaccctggccaagagggcacgcgatgagagggagg
tgcctgtgggagccgtgctggtgctgaacaatagagtgatcggcgagggctggaacagagccatcggcctgcacgacccaacagcccatgccgaaattatgg
ccctgagacagggcggcctggtcatgcagaactacagactgattgacgccaccctgtacgtgacattcgagccttgcgtgatgtgcgccggcgccatgatccac
tctaggatcggccgcgtggtgtttggcgtgaggaacAGCaaaCGGggcgccgcaggctccctgatgAacgtgctgAactaccccggcatgaatcaccgcgt
cgaaattaccgagggaatcctggcagatgaatgtgccgccctgctgtgcGACttctACcggatgcctagacaggtgttcaatgctcagaagaaggcccagag
ctccaTcAactccggaggatctagcggaggctcctctggctctgagacacctggcacaagcgagagcgcaacacctgaaagcagcgggggcagcagcgggg
ggtcaatggccgccttcaagcctaacccaatcaattacatcctgggactggccatcggaatcgcatccgtgggatgggctatggtggagatcgacgaggagga
gaatcctatccggctgatcgatctgggcgtgagagtgtttgagagggccgaggtgccaaagaccggcgattctctggctatggcccggagactggcacggagc
gtgaggcgcctgacacggagaagggcacacaggctgctgagggcacgccggctgctgaagagagagggcgtgctgcaggcagcagacttcgatgagaatg
gcctgatcaagagcctgccaaacacccccctggcagctgagagcagccgccctggacaggaagctgacaccactggagtggtctgccgtgctgctgcacctgat
caagcaccgcggctacctgagccagcggaagaacgagggagagacagcagacaaggagctgggcgccctgctgaagggagtggccaacaatgcccacgcc
ctgcagaccggcgatttcaggacacctgccgagctggccctgaataagtttgagaaggagtccggccacatcagaaaccagaggggcgactatagccacacc
ttctcccgcaaggatctgcaggccgagctgatcctgctgttcgagaagcagaaggagtttggcaatccacacgtgagcggaggcctgaaggagggaatcgag
accctgctgatgacacagaggcctgccctgtccggcgacgcagtgcagaagatgctgggacactgcaccttcgagcctgcagagccaaaggccgccaagaac
acctacacagccgagcggtttatctggctgacaaagctgaacaatctgagaatcctggagcagggatccgagaggccactgaccgacacagagagggccacc
ctgatggatgagccttaccggaagtctaagctgacatatgcccaggccagaaagctgctgggcctggaggacaccgccttctttaagggcctgagatacggca
aggataatgccgaggcctccacactgatggagatgaaggcctatcacgccatctctcgcgccctggagaaggagggcctgaaggacaagaagtcccccctga
acctgagctccgagctgcaggatgagatcggcaccgccttctctctgtttaagaccgacgaggatatcacaggccgcctgaaggacagggtgcagcctgagat
cctggaggccctgctgaagcacatctctttcgataagtttgtgcagatcagcctgaaggccctgagaaggatcgtgccactgatggagcagggcaagcggtac
gacgaggcctgcgccgagatctacggcgatcactatggcaagaagaacacagaggagaagatctatctgccccctatccctgccgacgagatcagaaatcct
gtggtgctgagggccctgtcccaggcaagaaaagtgatcaacggagtggtgcgccggtacggatctccagcccggatccacatcgagaccgccagagaagtg
ggcaagagcttcaaggaccggaaggagatcgagaagagacaggaggagaatcgcaaggatcgggagaaggccgccgccaagtttagggagtacttcccta
actttgtgggcgagccaaagtctaaggacatcctgaagctgcgcctgtacgagcagcagcacggcaagtgtctgtatagcggcaaggagatcaatctggtgcg
gctgaacgagaagggctatgtggagatcgatcacgccctgcctttctccagaacctgggacgattcttttaacaataaggtgctggtgctgggcagcgagaacc
agaataagggcaatcagacaccatacgagtatttcaatggcaaggacaactccagggagtggcaggagttcaaggcccgcgtggagacctctagatttccca
ggagcaagaagcagcggatcctgctgcagaagttcgacgaggatggctttaaggagtgcaacctgaatgacaccagatacgtgaaccggttcctgtgccagtt
tgtggccgatcacatcctgctgaccggcaagggcaagagaagggtgttcgcctctaatggccagatcacaaacctgctgaggggattttggggactgaggaag
gtgcgggcagagaatgacagacaccacgcactggatgcagtggtggtggcatgcagcaccgtggcaatgcagcagaagatcacaagattcgtgaggataa
ggagatgaacgcctttgacggcaagaccatcgataaggagacaggcaaggtgctgcaccagaagacccacttcccccagccttgggagttctttgcccagga
agtgatgatccgggtgttcggcaagccagacggcaagcctgagtttgaggaggccgataccccagagaagctgaggacactgctggcagagaagctgtctag
caggccagaggcagtgcacgagtacgtgaccccactgttcgtgtccagggcacccaatcggaagatgtctggcgcccacaaggacacactgagaagcgccaa
gaggtttgtgaagcacaacgagaagatctccgtgaagagagtgtggctgaccgagatcaagctggccgatctggagaacatggtgaattacaagaacggcag
ggagatcgagctgtatgaggccctgaaggcaaggctggaggcctacggaggaaatgccaagcaggccttcgacccaaaggataaccccttttataagaaggg
aggacagctggtgaaggccgtgcgggtggagaagacccaggagagcggcgtgctgctgaataagaagaacgcctacacaatcgccgacaatggcgatatgg
tgagagtggacgtgttctgtaaggtggataagaagggcaagaatcagtactttatcgtgcctatctatgcctggcaggtggccgagaacatcctgccagacatc
gattgcaagggctacagaatcgacgatagctatacattctgtttttccctgcacaagtatgacctgatcgccttccagaaggatgagaagtccaaggtggagttt
gcctactatatcaattgcgactcctctaacggcaggttctacctggcctggcacgataagggcagcaaggagcagcagtttcgcatctccacccagaatctggt
gctgatccagaagtatcaggtgaacgagctgggcaaggagatcaggccATGTCGGCTGAAGAAGCGCCCacccgtgcggTAAAATAAAAGAT
CTTTATTTTCATTAGATCTGTGTGTTGGTTTTTTGTGTAAGCgcggccgcaggaacccctagtgatggagttggccactccctctctgcgcgct
cgctcgctcactgaggccgggcgaccaaaggtcgcccgacgcccgggctttgcccgggcggcctcagtgagcgagcgagcgcgcagctgcctgcagg

Single-AAV vector with 2xBP_SV40 NLS in **Figure 2d, 3a, and Supplementary Figure 3b**
Legend: ITR, U1a promoter, BP_SV40 NLS, TadA8e, linker, Nme2Cas9-D16A, short poly-A signal, U6 promoter, **guide sequence**, guide RNA scaffold, U6 termination signal

Cctgcaggcagctgcgcgctcgctcgctcactgaggccgcccgggcaaagcccgggcgtcgggcgacctttggtcgcccggcctcagtgagcgagcgagcgc
gcagagagggagtggccaactccatcactaggggttcctgcggcctctagaGTTTAAACAAAAAAA
TAAACGATGCCCCTTAAAGCAGAAGCTTTAAGGGGCAGAGCGTTGCGGCACATCTTTTCAGACGGCCTTATTGTAGCAAC
GTTTCGGGAGCTACAAC**NNNNNNNNNNNNNNNNNNNNNNNNNNNN**GGTGTTTCGTCCTTTCCACAAGATATATAAAGCCA
AGAAATCGAAATACTTTCAAGTTACGGTAAGCATATGATAGTCCATTTTAAAACATAATTTTAAAACTGCAAACTACCCAA
GAAATTATTACTTTCTACGTCACGTATTTTGTACTAATATCTTTGTGTTTACAGTCAAATTAATTCTAATTATCTCTCTAACA
GCCTTGTATCGTATATGCAAATATGAAGGAATCATGGGAAATAGGCCCTCTCTAGaatggaggcggtactatgtagatgagaattca
ggagcaaactgggaaaagcaactgcttccaaatatttgtgatttttacagtgtagttttggaaaaactcttagcctaccaattcttctaagtgttttaaaatgtggg
agccagtacacatgaagttatagagtgttttaatgaggcttaaatatttaccgtaactatgaaatgctacgcatatcatgctgttcaggctccgtggccacgcaa
ctcatactACCGGTGCCACCATGaaaagaaccgccgacggcagcgaattcgagcccaagaagaagaggaaagtcGGCGGTAGCGGCGGAG
GCAGCGGTGGCGGCAGCGGCTctgaggtggagttttcccacgagtactggatgagacatgccctgaccctggccaagagggcacgcgatgagagg
gaggtgcctgtgggagccgtgctggtgctgaacaatagagtgatcggcgagggctggaacagagccatcggcctgcacgacccaacagcccatgccgaaatt
atggccctgagacagggcggcctggtcatgcagaactacagactgattgacgccaccctgtacgtgacattcgagccttgcgtgatgtgcgccggcgccatgat
ccactctaggatcggccgcgtggtgtttggcgtgaggaacAGCaaaCGGggcgccgcaggctccctgatgAacgtgctgAactaccccggcatgaatcacc
gcgtcgaaattaccgagggaatcctggcagatgaatgtgccgccctgctgtgcGACttctACcggatgcctagacaggtgttcaatgctcagaagaaggccc
agagctccaTcAactccggaggatctagcggaggctcctctggctctgagacacctggcacaagcgagagcgcaacacctgaaagcagcgggggcagcagc
ggggggtcaatggccgccttcaagcctaacccaatcaattacatcctgggactggccatcggaatcgcatccgtgggatgggctatggtggagatcgacgagg
aggagaatcctatccggctgatcgatctgggcgtgagagtgtttgagagggccgaggtgccaaagaccggcgattctctggctatggcccggagactggcacg
gagcgtgaggcgcctgacacggagaagggcacacaggctgctgagggcacgccggctgctgaagagagagggcgtgctgcaggcagcagacttcgatgag
aatggcctgatcaagagcctgccaaacacccccctggcagctgagagcagccgccctggacaggaagctgacaccactggagtggtctgccgtgctgctgcacc
tgatcaagcaccgcggctacctgagccagcggaagaacgagggagagacagcagacaaggagctgggcgccctgctgaagggagtggccaacaatgccca
cgccctgcagaccggcgatttcaggacacctgccgagctggccctgaataagtttgagaaggagtccggccacatcagaaaccagaggggcgactatagcca
caccttctcccgcaaggatctgcaggccgagctgatcctgctgttcgagaagcagaaggagtttggcaatccacacgtgagcggaggcctgaaggagggaatc
gagaccctgctgatgacacagaggcctgccctgtccggcgacgcagtgcagaagatgctgggacactgcaccttcgagcctgcagagccaaaggccgccaag
aacacctacacagccgagcggtttatctggctgacaaagctgaacaatctgagaatcctggagcagggatccgagaggccactgaccgacacagagagggc
caccctgatggatgagccttaccggaagtctaagctgacatatgcccaggccagaaagctgctgggcctggaggacaccgccttctttaagggcctgagatac
ggcaaggataatgccgaggcctccacactgatggagatgaaggcctatcacgccatctctcgcgccctggagaaggagggcctgaaggacaagaagtcccccc
ctgaacctgagctccgagctgcaggatgagatcggcaccgccttctctctgtttaagaccgacgaggatatcacaggccgcctgaaggacagggtgcagcctg
agatcctggaggccctgctgaagcacatctctttcgataagtttgtgcagatcagcctgaaggccctgagaaggatcgtgccactgatggagcagggcaagcg
gtacgacgaggcctgcgccgagatctacggcgatcactatggcaagaagaacacagaggagaagatctatctgccccctatccctgccgacgagatcagaaa
tcctgtggtgctgagggccctgtcccaggcaagaaaagtgatcaacggagtggtgcgccggtacggatctccagcccggatccacatcgagaccgccagaga
agtgggcaagagcttcaaggaccggaaggagatcgagaagagacaggaggagaatcgcaaggatcgggagaaggccgccgccaagtttagggagtacttc
cctaactttgtgggcgagccaaagtctaaggacatcctgaagctgcgcctgtacgagcagcagcacggcaagtgtctgtatagcggcaaggagatcaatctgg
tgcggctgaacgagaagggctatgtggagatcgatcacgccctgcctttctccagaacctgggacgattcttttaacaataaggtgctggtgctgggcagcgag
aaccagaataagggcaatcagacaccatacgagtatttcaatggcaaggacaactccagggagtggcaggagttcaaggcccgcgtggagacctctagattt
cccaggagcaagaagcagcggatcctgctgcagaagttcgacgaggatggctttaaggagtgcaacctgaatgacaccagatacgtgaaccggttcctgtgc
cagtttgtggccgatcacatcctgctgaccggcaagggcaagagaagggtgttcgcctctaatggccagatcacaaacctgctgaggggattttggggactga
ggaaggtgcgggcagagaatgacagacaccacgcactggatgcagtggtggtggcatgcagcaccgtggcaatgcagcagaagatcacaagattcgtgagg
tataaggagatgaacgcctttgacggcaagaccatcgataaggagacaggcaaggtgctgcaccagaagacccacttcccccagccttgggagttctttgccc
aggaagtgatgatccgggtgttcggcaagccagacggcaagcctgagtttgaggaggccgataccccagagaagctgaggacactgctggcagagaagctg
tctagcaggccagaggcagtgcacgagtacgtgaccccactgttcgtgtccagggcacccaatcggaagatgtctggcgcccacaaggacacactgagaagc
gccaagaggtttgtgaagcacaacgagaagatctccgtgaagagagtgtggctgaccgagatcaagctggccgatctggagaacatggtgaattacaagaac
ggcagggagatcgagctgtatgaggccctgaaggcaaggctggaggcctacggaggaaatgccaagcaggccttcgacccaaaggataaccccttttataag
aagggaggacagctggtgaaggccgtgcgggtggagaagacccaggagagcggcgtgctgctgaataagaagaacgcctacacaatcgccgacaatggcg
atatggtgagagtggacgtgttctgtaaggtggataagaagggcaagaatcagtactttatcgtgcctatctatgcctggcaggtggccgagaacatcctgcca
gacatcgattgcaagggctacagaatcgacgatagctatacattctgtttttccctgcacaagtatgacctgatcgccttccagaaggatgagaagtccaaggtg
gagtttgcctactatatcaattgcgactcctctaacggcaggttctacctggcctggcacgataagggcagcaaggagcagcagtttcgcatctccacccagaat
ctggtgctgatccagaagtatcaggtgaacgagctgggcaaggagatcaggccATGTCGGCTGAAGAAGCGCCCacccgtgcggGAGGATaaa
agaaccgccgacggcagcgaattcgagcccaagaagaagaggaaagtctaaAATAAAAGATCTTTATTTTCATTAGATCTGTGTGTTGGTT

TTTTGTGTAAGCgcggccgcaggaacccctagtgatggagttggccactccctctctgcgcgctcgctcgctcactgaggccgggcgaccaaaggtcgccc
gacgcccgggctttgcccgggcggcctcagtgagcgagcgagcgcgcagctgcctgcagg

Single-AAV vector with miniU6 promoter in **Figure 3c**
Legend: ITR, U1a promoter, BP_SV40 NLS, TadA8e, linker, Nme2Cas9-D16A, short poly-A signal, miniU6 promoter, **guide sequence**, guide RNA scaffold, U6 termination signal
Cctgcaggcagctgcgcgctcgctcgctcactgaggccgcccgggcaaagcccgggcgtcgggcgacctttggtcgcccggcctcagtgagcgagcgagcgc
gcagagagggagtggccaactccatcactaggggttcctgcggcctctagaGTTTAAACAAAAAAA
TAAACGATGCCCCTTAAAGCAGAAGCTTTAAGGGGCAGAGCGTTGCGGCACATCTTTTCAGACGGCCTTATTGTAGCAAC
GTTTCGGGAGCTACAACNNNNNNNNNNNNNNNNNNNNNNNNGGTGTTTCGTCCTTTCCACAAGATATATAAAGCCA
AGAAATCGAAATACTTTCAAGTTACGGTAAGCTATCGTATATGCAAATATGAAGGAATCATGGGAAATAGGCCCTCTCTA
Gaatggaggcggtactatgtagatgagaattcaggagcaaactgggaaaagcaactgcttccaaatatttgtgatttttacagtgtagttttggaaaaactctt
agcctaccaattcttctaagtgttttaaaatgtgggagccagtacacatgaagttatagagtgttttaatgaggcttaaatatttaccgtaactatgaaatgctac
gcatatcatgctgttcaggctccgtggccacgcaactcatactACCGGTGCCACCATGaaaagaaccgccgacggcagcgaattcgagcccaagaaga
agaggaaagtcGGCGGTAGCGGCGGAGGCAGCGGTGGCGGCAGCGGCTctgaggtggagttttcccacgagtactggatgagacatgccc
tgaccctggccaagagggcacgcgatgagagggaggtgcctgtgggagccgtgctggtgctgaacaatagagtgatcggcgagggctggaacagagccatc
ggcctgcacgacccaacagcccatgccgaaattatggccctgagacagggcggcctggtcatgcagaactacagactgattgacgccaccctgtacgtgacat
tcgagccttgcgtgatgtgcgccggcgccatgatccactctaggatcggccgcgtggtgtttggcgtgaggaacAGCaaaCGGggcgccgcaggctccctga
tgAacgtgctgAactaccccggcatgaatcaccgcgtcgaaattaccgagggaatcctggcagatgaatgtgccgccctgctgtgcGACttctACcggatgc
ctagacaggtgttcaatgctcagaagaaggcccagagctccaTcAactccggaggatctagcggaggctcctctggctctgagacacctggcacaagcgaga
gcgcaacacctgaaagcagcgggggcagcagcgggggggtcaatggccgccttcaagcctaacccaatcaattacatcctgggactggccatcggaatcgcat
ccgtgggatgggctatggtggagatcgacgaggaggagaatcctatccggctgatcgatctgggcgtgagagtgtttgagagggccgaggtgccaaagaccg
gcgattctctggctatggcccggagactggcacggagcgtgaggcgcctgacacggagaagggcacacaggctgctgagggcacgccggctgctgaagaga
gagggcgtgctgcaggcagcagacttcgatgagaatggcctgatcaagagcctgccaaacacccccctggcagctgagagcagccgccctggacaggaagct
gacaccactggagtggtctgccgtgctgctgcacctgatcaagcaccgcggctacctgagccagcggaagaacgagggagagacagcagacaaggagctgg
gcgccctgctgaagggagtggccaacaatgcccacgccctgcagaccggcgatttcaggacacctgccgagctggccctgaataagtttgagaaggagtccg
gccacatcagaaaccagaggggcgactatagccacaccttctcccgcaaggatctgcaggccgagctgatcctgctgttcgagaagcagaaggagtttggca
atccacacgtgagcggaggcctgaaggagggaatcgagaccctgctgatgacacagaggcctgccctgtccggcgacgcagtgcagaagatgctgggacact
gcaccttcgagcctgcagagccaaaggccgccaagaacacctacacagccgagcggtttatctggctgacaaagctgaacaatctgagaatcctggagcagg
gatccgagaggccactgaccgacacagagagggccaccctgatggatgagccttaccggaagtctaagctgacatatgcccaggccagaaagctgctgggcc
tggaggacaccgccttctttaagggcctgagatacggcaaggataatgccgaggcctccacactgatggagatgaaggcctatcacgccatctctcgcgccctg
gagaaggagggcctgaaggacaagaagtcccccctgaacctgagctccgagctgcaggatgagatcggcaccgccttctctctgtttaagaccgacgaggat
atcacaggccgcctgaaggacagggtgcagcctgagatcctggaggccctgctgaagcacatctctttcgataagtttgtgcagatcagcctgaaggccctgag
aaggatcgtgccactgatggagcagggcaagcggtacgacgaggcctgcgccgagatctacggcgatcactatggcaagaagaacacagaggagaagatct
atctgccccctatccctgccgacgagatcagaaatcctgtggtgctgagggccctgtcccaggcaagaaaagtgatcaacggagtggtgcgccggtacggatct
ccagcccggatccacatcgagaccgccagagaagtgggcaagagcttcaaggaccggaaggagatcgagaagagacaggaggagaatcgcaaggatcgg
gagaaggccgccgccaagtttagggagtacttccctaactttgtgggcgagccaaagtctaaggacatcctgaagctgcgcctgtacgagcagcagcacggca
agtgtctgtatagcggcaaggagatcaatctggtgcggctgaacgagaagggctatgtggagatcgatcacgccctgcctttctccagaacctgggacgattct
tttaacaataaggtgctggtgctgggcagcgagaaccagaataagggcaatcagacaccatacgagtatttcaatggcaaggacaactccagggagtggcag
gagttcaaggcccgcgtggagacctctagatttcccaggagcaagaagcagcggatcctgctgcagaagttcgacgaggatggctttaaggagtgcaacctga
atgacaccagatacgtgaaccggttcctgtgccagtttgtggccgatcacatcctgctgaccggcaagggcaagagaagggtgttcgcctctaatggccagatc
acaaacctgctgaggggattttggggactgaggaaggtgcgggcagagaatgacagacaccacgcactggatgcagtggtggtggcatgcagcaccgtggc
aatgcagcagaagatcacaagattcgtgaggtataaggagatgaacgcctttgacggcaagaccatcgataaggagacaggcaaggtgctgcaccagaaga
cccacttcccccagccttgggagttctttgcccaggaagtgatgatccgggtgttcggcaagccagacggcaagcctgagtttgaggaggccgataccccagag
aagctgaggacactgctggcagagaagctgtctagcaggccagaggcagtgcacgagtacgtgaccccactgttcgtgtccagggcacccaatcggaagatg
tctggcgcccacaaggacacactgagaagcgccaagaggtttgtgaagcacaacgagaagatctccgtgaagagagtgtggctgaccgagatcaagctggc
cgatctggagaacatggtgaattacaagaacggcagggagatcgagctgtatgaggccctgaaggcaaggctggaggcctacggaggaaatgccaagcagg
ccttcgacccaaaggataaccccttttataagaagggaggacagctggtgaaggccgtgcgggtggagaagacccaggagagcggcgtgctgctgaataag
aagaacgcctacacaatcgccgacaatggcgatatggtgagagtggacgtgttctgtaaggtggataagaagggcaagaatcagtactttatcgtgcctatct

atgcctggcaggtggccgagaacatcctgccagacatcgattgcaagggctacagaatcgacgatagctatacattctgtttttccctgcacaagtatgacctga
tcgccttccagaaggatgagaagtccaaggtggagtttgcctactatatcaattgcgactcctctaacggcaggttctacctggcctggcacgataagggcagc
aaggagcagcagtttcgcatctccacccagaatctggtgctgatccagaagtatcaggtgaacgagctgggcaaggagatcaggccATGTCGGCTGAA
GAAGCGCCCacccgtgcggGAGGATaaaagaaccgccgacggcagcgaattcgagcccaagaagaagaggaaagtctaaAATAAAAGATCTT
TATTTTCATTAGATCTGTGTGTTGGTTTTTTGTGTAAGCgcggccgcaggaacccctagtgatggagttggccactccctctctgcgcgctcgct
cgctcactgaggccgggcgaccaaaggtcgcccgacgcccgggctttgcccgggcggcctcagtgagcgagcgagcgcgcagctgcctgcagg

AAV-Nm2-ABE8e-U6_V2 in **Figure 6**

Legend: ITR, U1a promoter, BP_SV40 NLS, TadA8e, linker, Nme2Cas9-D16A, short poly-A signal, U6 promoter, **guide sequence**, guide RNA scaffold, U6 termination signal

Cctgcaggcagctgcgcgctcgctcgctcactgaggccgcccgggcaaagcccgggcgtcgggcgacctttggtcgcccggcctcagtgagcgagcgagcgc
gcagagagggagtggccaactccatcactaggggttcctgcggcctctagagtttatggaggcggtactatgtagatgagaattcaggagcaaactgggaaaa
gcaactgcttccaaatatttgtgatttttacagtgtagttttggaaaaactcttagcctaccaattcttctaagtgttttaaaatgtgggagccagtacacatgaag
ttatagagtgttttaatgaggcttaaatatttaccgtaactatgaaatgctacgcatatcatgctgttcaggctccgtggccacgcaactcatactaccggtgcca
ccatgaaaagaaccgccgacggcagcgaattcgagcccaagaagaagaggaaagtcggcggtagcggcggaggcagcggtggcggcagcggcTctgagg
tggagttttcccacgagtactggatgagacatgccctgaccctggccaagagggcacgcgatgagagggaggtgcctgtgggagccgtgctggtgctgaacaa
tagagtgatcggcgagggctggaacagagccatcggcctgcacgacccaacagcccatgccgaaattatggccctgagacagggcggcctggtcatgcagaa
ctacagactgattgacgccaccctgtacgtgacattcgagccttgcgtgatgtgcgccggcgccatgatccactctaggatcggccgcgtggtgtttggcgtgag
gaacagcaaacggggcgccgcaggctccctgatgaacgtgctgaactaccccggcatgaatcaccgcgtcgaaattaccgagggaatcctggcagatgaatg
tgccgccctgctgtgcgacttctaccggatgcctagacaggtgttcaatgctcagaagaaggcccagagctccatcaactccggaggatctagcggaggctcct
ctggctctgagacacctggcacaagcgagagcgcaacacctgaaagcagcgggggcagcagcgggggggtcaatggccgccttcaagcctaacccaatcaatt
acatcctgggactggccatcggaatcgcatccgtgggatgggctatggtggagatcgacgaggaggagaatcctatccggctgatcgatctgggcgtgagagt
gtttgagagggccgaggtgccaaagaccggcgattctctggctatggcccggagactggcacggagcgtgaggcgcctgacacggagaagggcacacaggc
tgctgagggcacgccggctgctgaagagagagggcgtgctgcaggcagcagacttcgatgagaatggcctgatcaagagcctgccaaacacccccctggcagc
tgagagcagccgccctggacaggaagctgacaccactggagtggtctgccgtgctgctgcacctgatcaagcaccgcggctacctgagccagcggaagaacg
agggagagacagcagacaaggagctgggcgccctgctgaagggagtggccaacaatgcccacgccctgcagaccggcgatttcaggacacctgccgagctg
gccctgaataagtttgagaaggagtccggccacatcagaaaccagaggggcgactatagccacaccttctcccgcaaggatctgcaggccgagctgatcctgc
tgttcgagaagcagaaggagtttggcaatccacacgtgagcggaggcctgaaggagggaatcgagaccctgctgatgacacagaggcctgccctgtccggcg
acgcagtgcagaagatgctgggacactgcaccttcgagcctgcagagccaaaggccgccaagaacacctacacagccgagcggtttatctggctgacaaagc
tgaacaatctgagaatcctggagcagggatccgagaggccactgaccgacacagagagggccaccctgatggatgagccttaccggaagtctaagctgacat
atgcccaggccagaaagctgctgggcctggaggacaccgccttctttaagggcctgagatacggcaaggataatgccgaggcctccacactgatggagatga
aggcctatcacgccatctctcgcgccctggagaaggagggcctgaaggacaagaagtcccccctgaacctgagctccgagctgcaggatgagatcggcaccg
ccttctctctgtttaagaccgacgaggatatcacaggccgcctgaaggacagggtgcagcctgagatcctggaggccctgctgaagcacatctctttcgataagt
ttgtgcagatcagcctgaaggccctgagaaggatcgtgccactgatggagcagggcaagcggtacgacgaggcctgcgccgagatctacggcgatcactatg
gcaagaagaacacagaggagaagatctatctgccccctatccctgccgacgagatcagaaatcctgtggtgctgagggccctgtcccaggcaagaaaagtga
tcaacggagtggtgcgccggtacggatctccagcccggatccacatcgagaccgccagagaagtgggcaagagcttcaaggaccggaaggagatcgagaag
agacaggaggagaatcgcaaggatcgggagaaggccgccgccaagtttagggagtacttccctaactttgtgggcgagccaaagtctaaggacatcctgaag
ctgcgcctgtacgagcagcagcacggcaagtgtctgtatagcggcaaggagatcaatctggtgcggctgaacgagaagggctatgtggagatcgatcacgcc
ctgcctttctccagaacctgggacgattcttttaacaataaggtgctggtgctgggcagcgagaaccagaataagggcaatcagacaccatacgagtatttcaa
tggcaaggacaactccagggagtggcaggagttcaaggcccgcgtggagacctctagatttcccaggagcaagaagcagcggatcctgctgcagaagttcga
cgaggatggctttaaggagtgcaacctgaatgacaccagatacgtgaaccggttcctgtgccagtttgtggccgatcacatcctgctgaccggcaagggcaag
agaagggtgttcgcctctaatggccagatcacaaacctgctgaggggattttggggactgaggaaggtgcgggcagagaatgacagacaccacgcactggat
gcagtggtggtggcatgcagcaccgtggcaatgcagcagaagatcacaagattcgtgaggtataaggagatgaacgcctttgacggcaagaccatcgataag
gagacaggcaaggtgctgcaccagaagacccacttcccccagccttgggagttctttgcccaggaagtgatgatccgggtgttcggcaagccagacggcaagc
ctgagtttgaggaggccgataccccagagaagctgaggacactgctggcagagaagctgtctagcaggccagaggcagtgcacgagtacgtgaccccactgt
tcgtgtccagggcacccaatcggaagatgtctggcgcccacaaggacacactgagaagcgccaagaggtttgtgaagcacaacgagaagatctccgtgaaga
gagtgtggctgaccgagatcaagctggccgatctggagaacatggtgaattacaagaacggcagggagatcgagctgtatgaggccctgaaggcaaggctg
gaggcctacggaggaaatgccaagcaggccttcgacccaaaggataaccccttttataagaagggaggacagctggtgaaggccgtgcgggtggagaagac
ccaggagagcggcgtgctgctgaataagaagaacgcctacacaatcgccgacaatggcgatatggtgagagtggacgtgttctgtaaggtggataagaaggg

caagaatcagtactttatcgtgcctatctatgcctggcaggtggccgagaacatcctgccagacatcgattgcaagggctacagaatcgacgatagctatacat
tctgtttttccctgcacaagtatgacctgatcgccttccagaaggatgagaagtccaaggtggagtttgcctactatatcaattgcgactcctctaacggcaggtt
ctacctggcctggcacgataagggcagcaaggagcagcagtttcgcatctccacccagaatctggtgctgatccagaagtatcaggtgaacgagctgggcaag
gagatcaggccatgtcggctgaagaagcgcccacccgtgcggGAGGATaaaagaaccgccgacggcagcgaattcgagcccaagaagaagaggaaagt
ctaaAATAAAAGATCTTTATTTTCATTAGATCTGTGTGTTGGTTTTTTGTGTaagcgctctagagagggcctatttcccatgattccttcata
tttgcatatacgatacaaggctgttagagagataattagaattaatttgactgtaaacacaaagatattagtacaaaatacgtgacgtagaaagtaataatttct
tgggtagtttgcagttttaaaattatgttttaaaatggactatcatatgcttaccgtaacttgaaagtatttcgatttcttggctttatatatcttgtggaaaggacg
aaacacc**NNNNNNNNNNNNNNNNNNNNNNNNN**gttgtagctcccgaaacgttgctacaataaggccgtctgaaaagatgtgccgcaacgctc
tgccccttaaagcttctgctttaaggggcatcgtttattttttttgtttaaacgcaggaacccctagtgatggagttggccactccctctctgcgcgctcgctcgctca
ctgaggccgggcgaccaaaggtcgcccgacgcccgggctttgcccgggcggcctcagtgagcgagcgagcgcgcagctgcctgcagg

AcrIIA4 plasmid in **Supplementary Figure 3**
Legend: CMV IE94 promoter, AcrIIA4, SV40 polyA signal,
GACCATAGCCAATTCAATATGGCGTATATGGACTCATGCCAATTCAATATGGTGGATCTGGACCTGTGCCAATTCAATATG
GCGTATATGGACTCGTGCCAATTCAATATGGTGGATCTGGACCCCAGCCAATTCAATATGGCGGACTTGGCACCATGCCA
ATTCAATATGGCGGACTTGGCACTGTGCCAACTGGGGAGGGGTCTACTTGGCACGGTGCCAAGTTTGAGGAGGGGTCTT
GGCCCTGTGCCAAGTCCGCCATATTGAATTGGCATGGTGCCAATAATGGCGGCCATATTGGCTATATGCCAGGATCAATA
TATAGGCAATATCCAATATGGCCCTATGCCAATATGGCTATTGGCCAGGTTCAATACTATGTATTGGCCCTATGCCATATA
GTATTCCATATATGGGTTTTCCTATTGACGTAGATAGCCCCTCCCAATGGGCGGTCCCATATACCATATATGGGGCTTCCT
AATACCGCCCATAGCCACTCCCCCATTGACGTCAATGGTCTCTATATATGGTCTTTCCTATTGACGTCATATGGGCGGTCCT
ATTGACGTATATGGCGCCTCCCCCATTGACGTCAATTACGGTAAATGGCCCGCCTGGCTCAATGCCCATTGACGTCAATAG
GACCACCCACCATTGACGTCAATGGGATGGCTCATTGCCCATTCATATCCGTTCTCACGCCCCCTATTGACGTCAATGACG
GTAAATGGCCCACTTGGCAGTACATCAATATCTATTAATAGTAACTTGGCAAGTACATTACTATTGGAAGGACGCCAGGG
TACATTGGCAGTACTCCCATTGACGTCAATGGCGGTAAATGGCCCGCGATGGCTGCCAAGTACATCCCCATTGACGTCAA
TGGGGAGGGGCAATGACGCAAATGGGCGTTCCATTGACGTAAATGGGCGGTAGGCGTGCCTAATGGGAGGTCTATATA
AGCAATGCTCGTTTAGGGAACATGAACATTAACGACCTCATACGAGAGATTAAGAACAAAGATTACACCGTCAAACTGTC
AGGAACTGATAGTAACTCAATCACCCAGCTTATTATCAGGGTAAACAATGATGGGAATGAATATGTGATATCTGAGAGCG
AAAACGAGTCTATCGTCGAGAAATTCATTTCCGCTTTTAAGAACGGGTGGAATCAGGAATATGAGGATGAAGAAGAATTT
TACAATGACATGCAGACGATCACGTTGAAAAGTGAACTGAACTAACTCGAGCCTCTAGAACTATAGTGAGTCGTATTACG
TAGATCCAGACATGATAAGATACATTGATGAGTTTGGACAAACCACAACTAGAATGCAGTGAAAAAAATGCTTTATTTGT
GAAATTTGTGATGCTATTGCTTTATTTGTAACCATTATAAGCTGCAATAAACAAGTT

AcrIIC4-MRE122 plasmid in **Supplementary Figure 3b**
Legend: ITR, CMV enhancer, CB promoter, SV40 interon, AcrIIC4, FLAG, SV40 NLS, 3 x MRE122, BGh polyA, U6 promoter, **guide sequence**, guide RNA scaffold, U6 termination signal
ctgcgcgctcgctcgctcactgaggccgcccgggcaaagcccgggcgtcgggcgacctttggtcgcccggcctcagtgagcgagcgagcgcgcagagaggga
gtgtagccatgctctaggaagatcaattcggtacaattcagctagcGTTTAAACAAAAAAATAAACGATGCCCCTTAAAGCAGAAGCTTTA
AGGGGCAGAGCGTTGCGGCACATCTTTTCAGACGGCCTTATTGTAGCAACGTTTCGGGAGCTACAAC**NNNNNNNNNNNN**
NNNNNNNNNNggtgtttcgtcctttccacaagatatataaagccaagaaatcgaaatactttcaagttacggtaagcatatgatagtccattttaaaaca
taattttaaaactgcaaactacccaagaaattattactttctacgtcacgtattttgtactaatatctttgtgtttacagtcaaattaattctaattatctctctaaca
gccttgtatcgtatatgcaaatatgaaggaatcatgggaaataggccctccgcgtcgacattgattattgactctggtcgttacataacttacggtaaatggccc
gcctggctgaccgcccaacgaccccgcccattgacgtcaataatgacgtatgttcccatagtaacgccaatagggactttccattgacgtcaatgggtggagtat
ttacggtaaactgcccacttggcagtacatcaagtgtatcatatgccaagtacgccccctattgacgtcaatgacggtaaatggcccgcctggcattatgcccag
tacatgaccttatgggactttcctacttggcagtacatctactcgaggccacgttctgcttcactctccccatctcccccccctccccacccccaattttgtatttatt
tatttttaattattttgtgcagcgatgggggcgggggggggggggggggcgcgcgccaggcggggcggggcggggcgaggggcggggcggggcgagg
cggagaggtgcggcggcagccaatcagagcggcgcgctccgaaagtttccttttatggcgaggcggcggcggcggccctataaaaagcgaagcgcgcg
gcgggcgggagcgggatcagccaccgcggtggcggcctagagtcgacgaggaactgaaaaaccagaaagttaactggtaagtttagtctttttgtcttttattt
caggtcccggatccggtggtggtgcaaatcaaagaactgctcctcagtggatgttgcctttacttctaggcctgtacggaagtgttacttctgctctaaaagctgc
ggaattgtacccgcggccgatccaCCGGTgccgccaccATGAAGATCACCAGCAGCAACTTCGCGACCATTGCGACCAGCGAGAACT

TTGCGAAGCTGAGCGTGCTGCCGAAAAACCACCGTGAGCCGATCAAGGGTCTGTTCAAAAGCGCGGTTGAACAGTTTAG
CAGCGCGCGTGACTTCTTTAAGAACGAGAACTACAGCAAAGAGCTGGCGGAAAAGTTCAACAAAGAAGCGGTGAACGA
GGCGGTTGAAAAGCTGCAAAAAGCGATCGATCTGGCGGAAAAACAGGGCATTCAATTTggcggggattataaggatgatgatgat
aagggctccCCTAAGAAGAAGAGAAAGGTGTGATAAAGCGGCCATCAAGCTtGACAAACACCATTGTCACACTCCAACAAAC
ACCATTGTCACACTCCAACAAACACCATTGTCACACTCCACCATAgAGCTcgctgatcagcctcgactgtgccttctagttgccagccatct
gttgtttgcccctcccccgtgccttccttgaccctggaaggtgccactcccactgtcctttcctaataaaatgaggaaattgcatcgcattgtctgagtaggtgtcat
tctattctggggggtggggtggggcaggacagcaagggggaggattgggaagacaattaggtagataagtagcatggcgggttaatcattaactacaaggaa
cccctagtgatggagttggccactccctctctgcgcgctcgctcgctcactgaggccgggcgaccaaaggtcgcccgacgcccgggctttgcccgggcggcctc
agtgagcgagcgagcgcgcag